STERICALLY DEMANDING ORGANOMETALLIC COMPLEXES CONTAINING MULTIPLE CLUSTERS OR POLYPHENYLATED LIGANDS

By

LISA CHEN-FANG CHAO, B. Sc.

A Thesis

Submitted to the School of Graduate Studies

in Partial Fulfilment of the Requirements

for the Degree

Doctor of Philosophy

McMaster University

STERICALLY DEMANDING ORGANOMETALLIC COMPLEXES

DOCTOR OF PHILOSOPHY (1995) McMASTER UNIVERSITY

(Chemistry) Hamilton, Ontario

TITLE: Sterically Demanding Organometallic Complexes Containing Multiple Clusters or Polyphenylated Ligands

AUTHOR: Lisa Chen-Fang Chao, B. Sc. (University of British Columbia, B.C.)

SUPERVISOR: Professor M. J. McGlinchey

NUMBER OF PAGES: xvi, 161

ABSTRACT

Sterically demanding organometallic complexes, in which bulky clusters or large polyphenylated groups are incorporated, possess interesting structural character as well as molecular dynamics.

Trichloroacetate esters, p-$C_6H_4(O_2C\text{-}CCl_3)_2$ and $C(CH_2\text{-}O_2C\text{-}CCl_3)_4$, can be utilized as templates in building multi-cobalt cluster systems such as p-$C_6H_4(O_2C\text{-}CCo_3(CO)_9)_2$ and $C[CH_2\text{-}O_2C\text{-}CCo_3(CO)_9]_3(CH_2\text{-}O_2C\text{-}CCl_3)$. The crystal structure of $C(CH_2\text{-}O_2C\text{-}CCl_3)_4$ has been obtained and a molecular modelling study was performed on the tetra-cluster $C[CH_2\text{-}O_2C\text{-}CCo_3(CO)_9]_4$.

The 1,1,1-trichloroacetylacetonate complexes of Co(II), Co(III), or Al(III) can also be used as templates in the preparation of multi-cluster molecules by reaction with $Co_2(CO)_8$. The uncomplexed cluster ligand, $CH_3C(O)CHC(OH)CCo_3(CO)_9$, was structurally characterized. Its direction of enolization was studied by EHMO (Extended Hückel Molecular Orbital) calculations. The tendency to enolize is also found in (benzoylacetone)$Cr(CO)_3$ which was characterized by x-ray crystallography.

The Diels-Alder reaction of tetraphenylcyclopentadienone (tetracyclone) with triphenylcyclopropene yields a ketone adduct, C_7Ph_7HCO, with an *endo* hydrogen at the methine carbon; thermal elimination of CO produces heptaphenylcycloheptatriene, C_7Ph_7H, a sterically crowded polyaryl system. This initially formed conformer with a pseudo-equatorial phenyl substituent at the sp^3 position is sterically hindered and undergoes a

conformational flip which allows the phenyl group to occupy the favored pseudo-axial site. However, the remaining phenyls are sterically encumbered and slowed rotation of these rings can be monitored by ^{1}H and ^{13}C NMR spectroscopy. The intermediacy of the conformer is shown by the formation of isomers of $C_7(p\text{-tolyl})_2Ph_5H$, arising via a series of [1,5] hydrogen shifts that are possible only for this conformer. Similarly, use of 2,5-dimethyl-3,4-diphenyl-cyclopentadienone yields $C_7Me_2Ph_5H$ in which [1,5] hydrogen shifts also occur.

The heptaphenyltropylium ion, $C_7Ph_7^+Br^-$ or $C_7Ph_7^+BF_4^-$, has a planar central seven membered ring. The $C_7Ph_7^-K^+$ anion, which is prepared from $C_7Ph_7^+Br^-$ and potassium metal, reacts with Me_3SnCl and $SiMe_2HCl$ to form σ-bonded derivatives, $C_7Ph_7\text{-}SnMe_3$ and $C_7Ph_7\text{-}SiMe_2H$.

The reaction of $Cr(CO)_6$ with C_7Ph_7H, or $C_7Me_2Ph_5H$, leads to incorporation of a $Cr(CO)_3$ group on a peripheral phenyl ring rather than on the seven-membered ring. However, the tricyclic ketone, C_7Ph_7HCO, which is the precursor to C_7Ph_7H, reacts with $Mo(CO)_6$ to give the π-allyl complex, $(\eta^5\text{-}C_5Ph_4OH)Mo(CO)_2(\eta^3\text{-}C_3Ph_3H_2)$, in which the triphenylcyclopropene ring has been opened as seen in its x-ray crystal structure.

ACKNOWLEDGEMENTS

I wish to express my sincere gratitude to my supervisor Dr. M. J. McGlinchey for the guidance that he provided throughout the course of this work. His good humour, enthusiasm, and patience were greatly appreciated. I have learned a great deal and am grateful for the opportunity to have worked in his lab.

I would also like to thank my supervisory committee, Dr. A. Bain and Dr. H. D. H. Stöver for their time and input into my Ph.D. research. Special thanks go to Dr. Hari Gupta who helped me in the synthesis of several of the cycloheptatriene molecules.

I also appreciate the assistance from Dr. Don Hughes and Mr. Brian Sayer in the NMR facility. I thank Dr. Jim Britten for helping me obtain several crystal structures, and for answering the many questions I always had on crystal structure solving. I thank Dr. Richard Smith, Faj Ramelan, and Leah Allen in the mass spectrometry facility.

The funding from the Department of Chemistry and McMaster University is gratefully acknowledged. Also, thanks to Carol Dada and the departmental office staff for the help provided in the successful completion of this work.

To everyone with whom I worked with in ABB 357, Patty, Kris, Lijuan, Andreas, Luc, Suzie, Pippa, Ralph, Jamie, and Mark, thank you for your friendship and chemical expertise. I particularly want to thank Patty, Kris, and

Andreas for showing me the ropes when I first arrived in 1990. I also want to thank Suzie for running the selective inversion experiments. As well, I am glad to have had the opportunity to become friends with Lijuan and, in later years, Pippa. Of course, I can't possibly forget to mention the partners in crime, Ralph and Jamie! Thanks Ralph for all the tips on using the fancy Windows programs and for those wonderful pasta dinners. Thanks Jamie for all the flattery, really!

I must also mention other chemists that I have gotten to know and who have made the time at McMaster a very memorable one. I thank Gerri and Marlene MaEachern for their friendship. As well, thanks to the two Mike's (Roth and St. Pierre) for the good times when playing poker and billiards.

Moving to Ontario has been an experience for me, I have made some good friends who have supported me throughout my work: Shelley Tom, who was there for me from the very beginning, thanks for exploring Hamilton with me; Stephanie and Michael Ng, thanks for the times at Fat Tuesday; the gang, Phil Wong, Tony Lee, Anna Lin, and Anna Chan, thanks for keeping me sane by dragging me off to Toronto when I really needed to; and the Ng and Wong families, your hospitality was much appreciated.

Lastly, many thanks to my parents, my sister, Dorothy, and my brother, Stephen, for their love and support throughout my thesis work.

TABLE OF CONTENTS

LIST OF TABLES

LIST OF SCHEMES

LIST OF FIGURES

PREFACE

The preparation of sterically hindered organometallic complexes has been the subject of considerable research interest. These studies have led to advances in stereochemical theory and the understanding of chiral conformations in these molecules. Steric hindrance in a complex can arise from large organometallic fragments such as metal clusters, as well as from bulky organic ligands such as polyaryls. The first part of the thesis will discuss the preparation of sterically-demanding systems containing bulky alkylidynetricobalt nonacarbonyl clusters. Not only are these complexes aesthetically pleasing, but also they may have potential commercial applications as chiral-selective catalysts. The second portion of this thesis will cover sterically crowded complexes in which the hindrance arises from the organic ligand, i.e., a polyphenylated ring. These molecules are synthetically challenging and possess interesting molecular dynamics. Steric crowding can result in slowed rotation of substituent groups or slowed rotation of organometallic tripodal groups.

CHAPTER ONE

INTRODUCTION TO ORGANO-TRANSITION METAL CLUSTERS

Organotransition metal clusters are of particular interest because of their potential use as catalysts that can be designed to meet specifications. A cluster has been defined by Cotton and Wilkinson as a group of two or more metal atoms in which there are substantial and direct bonds between the metal atoms [1]. Cluster complexes can be viewed as a microsurface made up of selected metal atoms in a fixed geometric array upon which chemical reactions can occur. Organo-transition metal cluster chemistry can provide a link between the relatively well-understood chemistry of homogeneous mononuclear catalysts and that of the less clearly defined solid surface of heterogeneous catalysts [2].

1.1 Catalytic Applications of Organo-Transition Metal Clusters

The industrial output of chemicals via heterogeneous catalysts currently greatly outweighs the production via homogeneous catalysts [2]. Heterogeneous catalysts are insoluble in the reaction medium, their active sites are located on a solid surface. These catalysts are favored by industry because of the relative ease of separation of the products, as well as their robustness. The industrial production of fuel from synthesis gas ($CO + H_2$), known as the Fischer-Tropsch process, is an example of a heterogeneous catalyzed reaction Scheme 1).

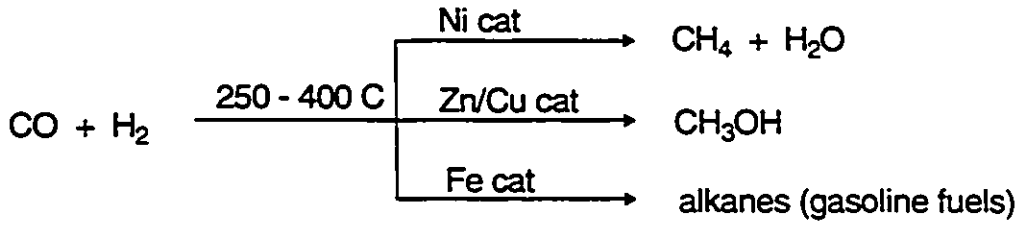

Scheme 1 : The Fischer-Tropsch process.

Homogeneous catalysts, on the other hand, are soluble in their reaction medium; their active sites are the metal atoms of a molecular complex. The Ziegler-Natta polymerization of ethene shown in Scheme 2, illustrates the use of these catalysts. Cocatalysts of aluminum alkyls (e.g., Et_2AlCl) and titanium compounds (e.g., $TiCl_4$) lead to the rapid polymerization of ethene under relatively mild conditions (50°/10 atm) [3]. The crystalline and low-branching high density polyethene (HDPE) product is used in the making of bottles, drums, films, pipes, and cable insulation [4].

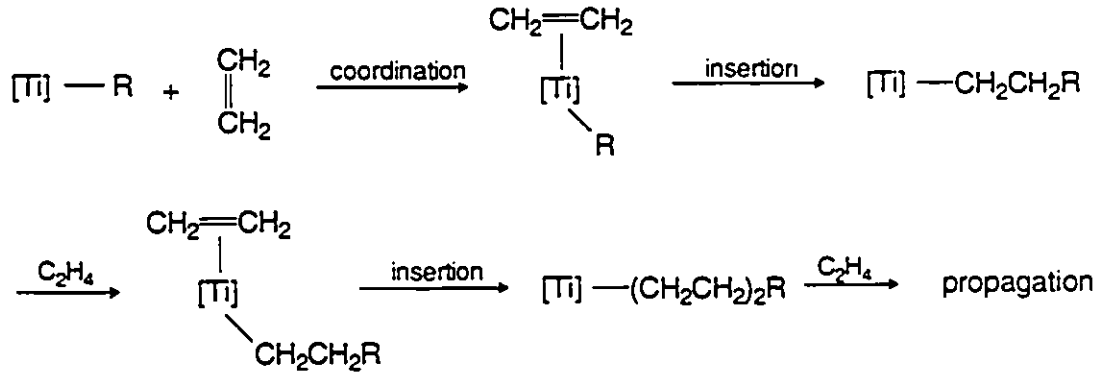

Scheme 2: The Ziegler-Natta polymerization of ethene.

There is a growing shift toward the use of homogeneous catalysis because of several advantages that it has over heterogeneous catalysis [2]. The higher selectivity and lower energy requirements (temperature, pressure) make homogeneous catalysts more economically favorable. A molecular catalyst is also easier to modify than a surface catalyst of variable composition, and lastly, a soluble species can be more easily studied by infrared or Nuclear Magnetic Resonance (NMR) spectroscopic techniques.

Can a compromise between homogeneous and heterogeneous catalysts be found? A favorable catalyst would be one in which the surface remained ideal at all times, any modifications made simple, and the reaction could easily be followed. Metal clusters can provide such surfaces. Each cluster is a microsurface upon which a specific reaction can occur.

Catalytic studies have already been carried out by using cobalt carbonyl clusters. The hydroformylation of 1- and 2-pentene (Scheme 3) has been catalyzed by $Co_3(CO)_9C$-Ph and $Co_4(CO)_8(\mu_2\text{-}CO)_2(\mu_4\text{-}PPh)_2$ to yield aldehydes in high yield (based on pentene consumption) with a fairly high normal-to-branched selectivity [5].

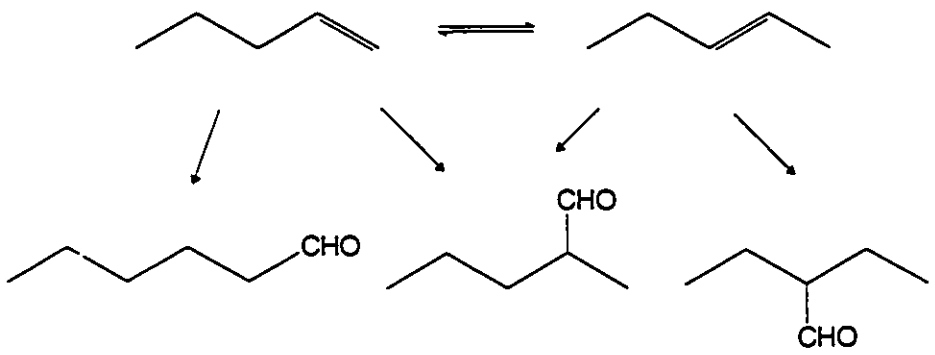

Scheme 3: Hydroformylation of 1- and 2-pentene by cobalt carbonyl clusters.

Hydroformylation reactions can also be carried out using (μ_3-CCH_3)-$Co_3(CO)_7$-dppm, **1**, as the catalyst. The dppm (diphenylphosphinomethane) bridging group stabilizes the cluster and activates it for catalysis [6].

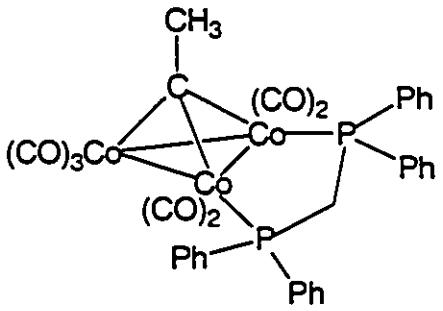

1

Other reactions have also been studied; the hydrogenation of acetylene has been catalyzed by the $Co_2(CO)_6(HC{\equiv}CH)$ cluster (Scheme 4) [7].

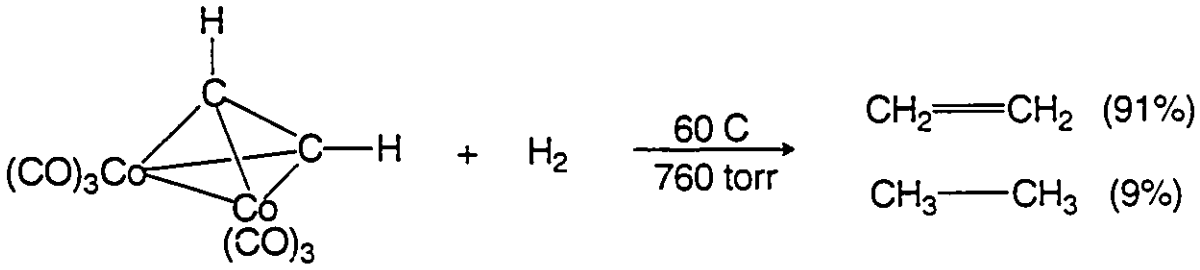

Scheme 4: The hydrogenation of acetylene using $Co_2(CO)_6(HC{\equiv}CH)$ catalyst.

1.2 Synthetic Routes to Organo-Transition Metal Clusters

1.2.1 Preparation of Alkylidyne Tricobalt Nonacarbonyl Clusters

The syntheses of clusters are no longer the serendipitous ways of the past. Today there are well-known and established methods for synthesizing transition metal clusters.

By adding a metal-metal bond across a metal-carbon multiple bond, trimetallic clusters, which contain a triply-bridging carbynyl moiety, can be made. Stone has brilliantly used this reaction in his study of trimetallic mixed metal clusters as typified by Scheme 5 [8,9].

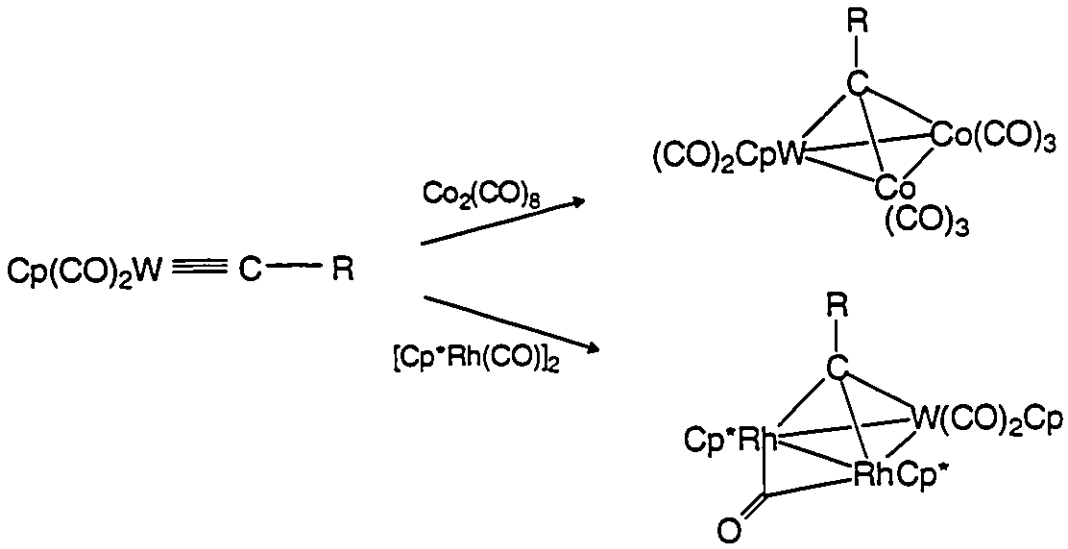

Scheme 5: Trimetallic mixed metal cluster syntheses

Bimetallic clusters can be used as starting materials themselves to make trimetallic clusters. The first example of the class of alkylidynetricobalt

nonacarbonyl complexes, $Co_3(CO)_9C$-R, was derived from the bimetallic cluster, acetylene dicobalt hexacarbonyl in 1958 (Scheme 6) [10].

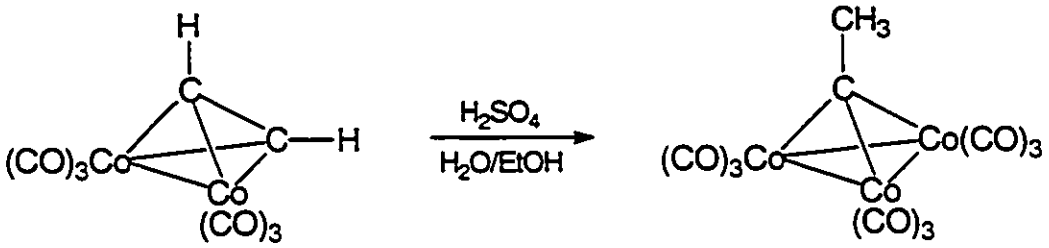

Scheme 6: The first synthesis of the class of clusters, $Co_3(CO)_9C$-R.

Provided there was at least one terminally bonded hydrogen, i.e., $Co_2(CO)_6(RC{\equiv}CH)$, a variety of clusters of the type $Co_3(CO)_9C$-CH_2R could be made. Unfortunately, this conversion is limited to producing complexes with a CH_2 group attached to the apical carbon atom [11].

The first member of the alkylidynetricobalt nonacarbonyl clusters to be characterized was $Co_3(CO)_9C$-CH_3 by Sutton and Dahl as shown in Figure 1 [12]. This established the presence of a tetrahedral CCo_3 cluster core, the basic structure of the clusters discussed in this thesis. One view of the bonding in such systems treats the apical carbon as being coordinated symmetrically via σ-bonds to three cobalt atoms. Each cobalt has an eighteen-electron closed shell configuration by bonding to two other cobalt atoms, the apical carbon atom, and three terminal carbon monoxide ligands. The Co-Co bond distance (average 2.47Å) is noticeably longer than the Co-C bond distance (average 1.90Å). The arrangement of the terminal carbonyl ligands is of special interest. Six of the

nine carbonyl ligands are disposed upwards in the general direction of the apical carbon atom and its substituent. As a result, any reactions at the apical carbon atom or at its substituent may be subjected to substantial steric hindrance [11].

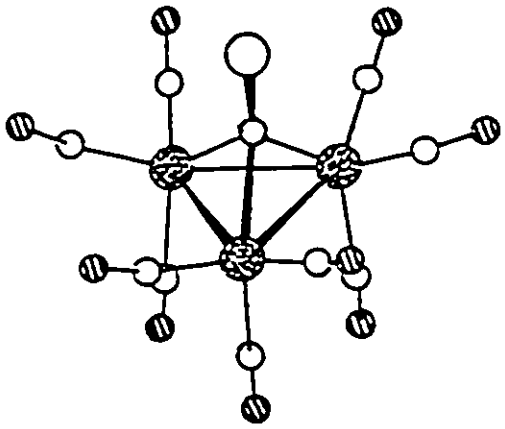

Figure 1: X-ray crystal structure of $Co_3(CO)_9C\text{-}CH_3$.

A more general preparative route to functionally substituted tricobalt cluster complexes that was later developed was the reaction of α, α, α-trihalomethyl compounds with $Co_2(CO)_8$ as shown in Scheme 7 [13,14].

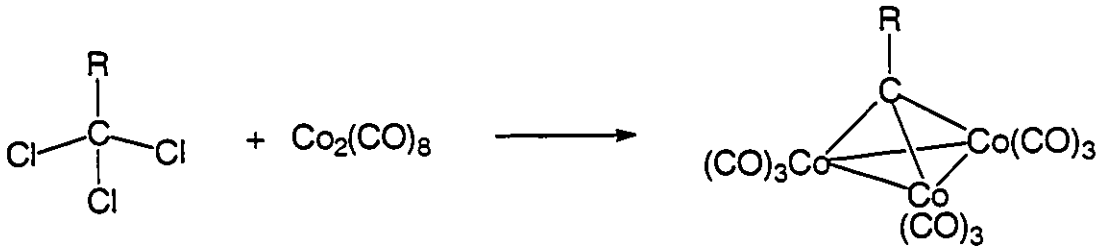

Scheme 7: The trichloroalkane and dicobalt octacarbonyl route to clusters.

The three chlorine atoms are each replaced by $Co(CO)_3$ moieties resulting in a tetrahedral cluster. This procedure may be used to prepare a great variety of alkylidynetricobalt nonacarbonyl complexes where R = halogen, alkyl, or aryl. Introducing a reactive organic functional group, such as an ester, at the apical carbon atom can also be done [15]. A selection of examples is presented in Table 1.

Starting Halide	Product	Percent Yield
CCl_4	$Co_3(CO)_9C$ - Cl	46
CH_3CCl_3	$Co_3(CO)_9C$ - CH_3	43
$C_6H_5CCl_3$	$Co_3(CO)_9C$ - C_6H_5	29
$(CH_3)_3SiCCl_3$	$Co_3(CO)_9C$ - $Si(CH_3)_3$	41
$CH_3CH_2O_2CCCl_3$	$Co_3(CO)_9C$ - $CO_2CH_2CH_3$	53

Table 1: $Co_3(CO)_9C$-R clusters from the $RCCl_3/Co_2(CO)_8$ reaction [15].

Some dihalomethyl compounds also may be used as starting materials. $PhCHCl_2$ and CH_3OCHCl_2 react with $Co_2(CO)_8$ to give Ph-$CCo_3(CO)_9$ and CH_3O-$CCo_3(CO)_9$, respectively. A multi-cluster system, **2**, was synthesized by Seyferth via the reaction of hexachlorocyclopropane and dicobalt octacarbonyl in tetrahydrofuran [16]. The apical carbon of a carbynyl tricobalt cluster is bonded to an alkynyl dicobalt cluster. Another carbynyl tricobalt cluster is linked to this dicobalt cluster via an acetylene bond.

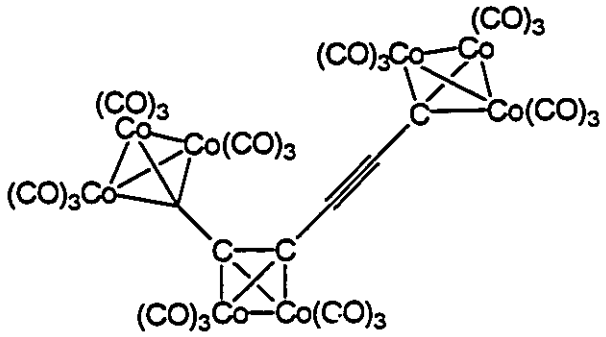

2

1.2.2 Apical Group Manipulation

The tetrahedral clusters can themselves be further manipulated to produce a variety of interesting new clusters. The group bonded to the apical carbon atom can be converted to different functional groups. Apical group manipulations have been extensively studied for the alkylidynetricobalt nonacarbonyl clusters, $Co_3(CO)_9C$-R. Thus, one can begin with an ester which via the free acid and its various derivatives, can be converted to many other organic functional groups. The basic hydrolysis of $Co_3(CO)_9C$-$CO_2CH_2CH_3$ by Na_2CO_3 results in the destruction of the complex [17]. However, these systems are not destroyed by Lewis acids or protonic acids, and this leads to some very useful reactions. Hammett *et al.* had made some observations on solutions of carboxylic acids in concentrated sulfuric acid [18]. In the majority of cases, dissolution of a carboxylic acid in concentrated sulfuric acid yields the monoprotonated species. However, some highly hindered carboxylic acids will react further to give the much less hindered acylium ion as shown in Scheme 8.

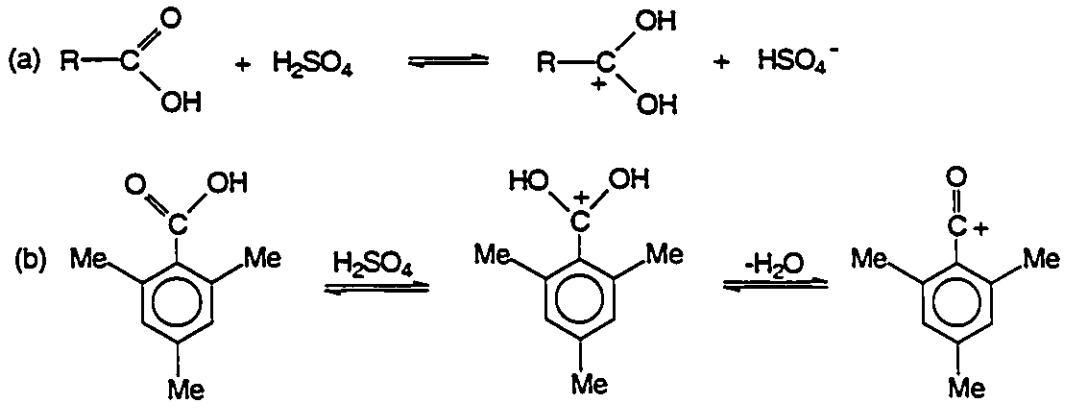

Scheme 8: Mechanism for the acid hydrolysis of a sterically hindered carboxylic acid.

When a sulfuric acid solution containing such an acylium ion is poured onto ice, the carboxylic acid is formed; when it is treated with an alcohol, the ester is formed. This hydrolysis has also been applied to the esters of cobalt clusters. When a cluster possessing an ester functionality at the apical position is dissolved in concentrated sulfuric acid, a yellow-brown solution is formed. Quenching the reaction with water results in a cluster with a carboxylic acid functionality in place of the ester. When the intermediate is allowed to react with an alcohol, the ester of the alcohol is obtained. The intermediate is proposed to be the tricobaltcarbon decacarbonyl cation, $[Co_3(CO)_9C\text{-}CO]^+$, **3**.

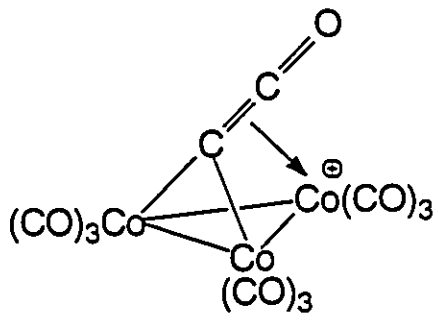

3

Unfortunately, sulfuric acid is not a convenient solvent to study the

chemistry of **3**, since it is not compatible with many nucleophiles with which one might want it to react. Seyferth and co-workers found that the reaction of esters with 65% aqueous hexafluorophosphoric acid and propionic anhydride results in a black, microcrystalline salt, $[Co_3(CO)_9CCO]^+PF_6^-$ which could react directly with a wide variety of nucleophiles as surveyed in Scheme 9. This then results

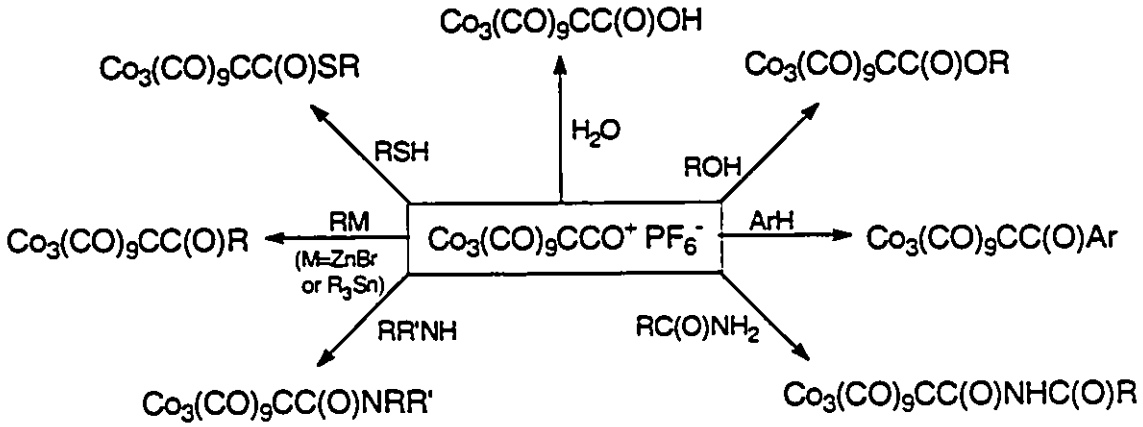

Scheme 9: General reactions of $[Co_3(CO)_9CCO]^+PF_6^-$ [17].

in the acylation of alcohols, phenols, thiols, ammonia, amines, and even tripeptides (Scheme 10).

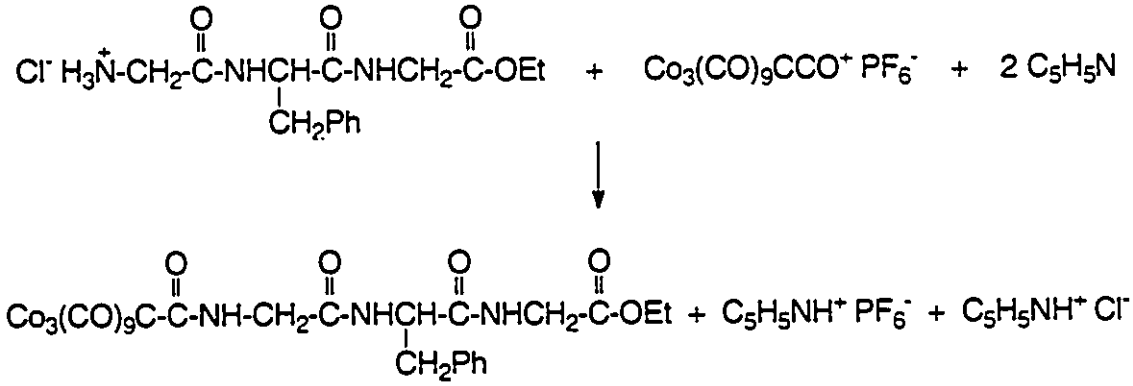

Scheme 10: The acylation of a tripeptide hydrochloride [17].

Another route to the intermediate cationic cluster was also discovered by Seyferth and co-workers [19,20]. When $Co_3(CO)_9C$-Cl and a two- to three-fold excess of $AlCl_3$ are mixed in dichloromethane a yellow-brown reaction mixture is also produced. Such solutions are stable at room temperature for several days under nitrogen. The acylium salt, $[Co_3(CO)_9CCO]^+AlCl_4^-$, appears to form initially. Treatment of this yellow-brown solution with any of the nucleophiles known to react with $[Co_3(CO)_9CCO]^+PF_6^-$ results in the formation of the expected acylated product. Several examples are presented in Table 2.

Nucleophile	R in $Co_3(CO)_9C$ - R	Percent Yield
CH_3OH	CO_2CH_3	83
C_6H_5OH	$CO_2C_6H_5$	66
CH_2=$CHCH_2OH$	CO_2CH_2CH=CH_2	66
$(CH_3CH_2)_2NH$	$C(O)N(CH_2CH_3)_2$	75
Cp - Fe - Cp	C(O) - C_5H_4 - Fe - Cp	41

Table 2: Synthetic applications of the $[Co_3(CO)_9CCO]^+AlCl_4^-$ reagent [19,20]

Acylations of alcohols, phenol, thiols, and amines have been accomplished in good yield and in what appear to be nearly instantaneous reactions. The reaction does not need external carbon monoxide; the reaction proceeds similarly under a nitrogen atmosphere. The CO function at the apical carbon atom is proposed to come from carbon monoxide ligands on cobalt in $Co_3(CO)_9C$-Cl. The proposed mechanism of the reaction involves the initial

formation of the $Co_3(CO)_9CCl\text{-}AlCl_3$ complex in which substantial polarization of the C-Cl bond has occurred. A second molecule of $AlCl_3$ complexes to a terminal carbonyl ligand providing the activation for CO migration from cobalt to the electron-deficient apical carbon atom. This is not unreasonable since aluminum alkyls have been reported to promote a terminal to bridging carbon monoxide ligand shift in a binuclear ruthenium complex [21]. The cobalt to carbon CO transfer would leave coordinatively unsaturated cobalt atoms in cluster acylium ions which would then require efficent transfer of CO from other molecules in order to obtain the $[Co_3(CO)_9CCO]^+$ species in high yield.

These acyl derivatives could in some cases undergo thermal decarbonylation to give the corresponding alkyl or aryl cobalt complexes [22,23]. Studies from this laboratory have shown that it is not the ketonic carbonyl which is lost during the reaction [24]. In fact, the carbon monoxide originally lost is a cobalt carbonyl and its place is taken by the carbon monoxide moiety from the ketonic position (Scheme 11).

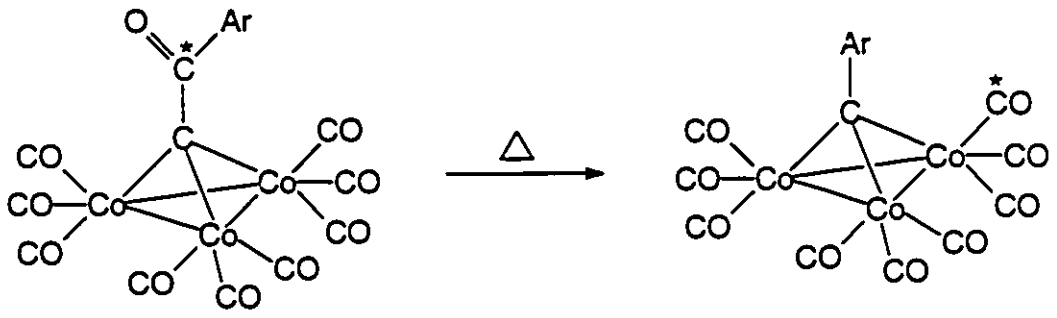

Scheme 11: Thermal decarbonylation of an aroyl cluster.

Perhaps the loss of a cobalt carbonyl is followed by the interaction of the acyl group with the vacant coordination site. A developing electron deficiency at the carbonyl carbon atom is alleviated by the migration of the functional group to this site as shown in Scheme 12.

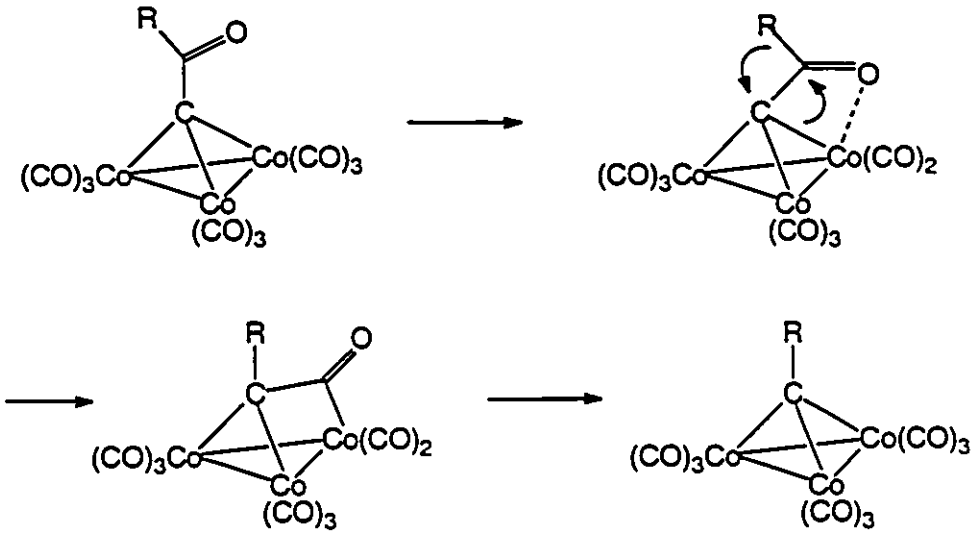

Scheme 12: Proposed mechanism of the decarbonylation of aroyl clusters.

1.3 Multiple Cluster Systems

Numerous routes for synthesizing organo-transition metal clusters have been developed. However, little work has been done on the synthesis of high-nuclearity complexes containing two or more organo-transition metal clusters. A few examples have recently appeared in literature illustrating the formation of remarkable oligo-cluster systems by combining both coordination chemistry and organometallic cluster chemistry [35,36,38,39]. Cluster-

substituted carboxylate ligands are used in preparing these large assemblies. In principle, joining a cluster to a ligand functionality allows the construction of clusters on clusters based on the established coordination geometries of a cationic metal core.

1.3.1 The Carboxylate Ligand

The coordination complexes that are important in the construction of oligo-cluster complexes are the metal carboxylates. The carboxylate ligand ($RCOO^-$) may bond in several different ways as depicted in Figure 2. The most common are the unidentate, symmetrical chelate, and *syn-syn* bridging modes.

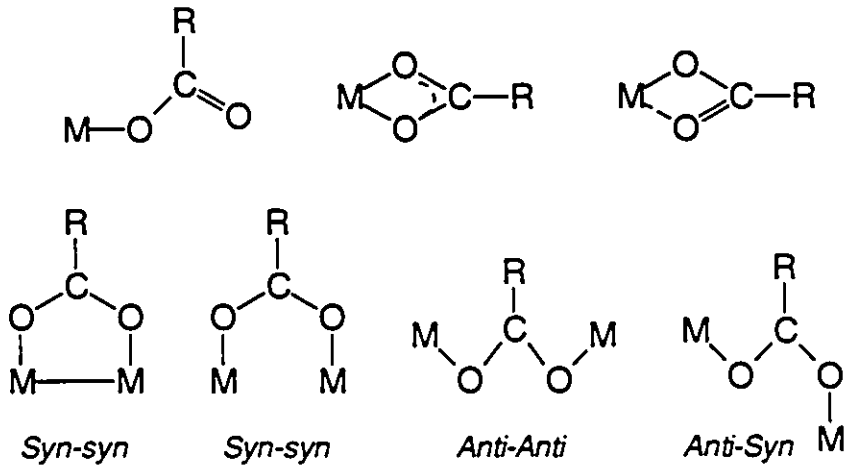

Figure 2: The different bonding modes of the carboxylate ligand [25].

The acetate ligand, $MeCOO^-$, has been the most extensively studied carboxylate [26]. It is found in its *syn-syn* bridging mode in many multi-nuclear

complexes. The complexes of the general formula, $M_4O[O_2CMe]_6$, **4**, where M = Be, Zn, or Co contain a μ^4-tetrahedral oxygen in the centre of a tetrahedron of metal atoms. The six acetates bridge the edges of the metal tetrahedron [27].

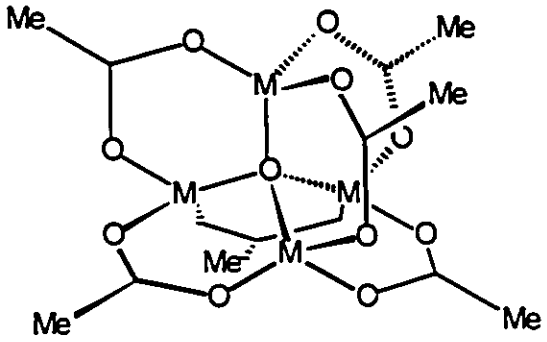

4

Bridging acetates are also found in complexes of the general formula, $[M_3O(O_2CMe)_6L_3]^+$, **5**, where M = V, Cr, Mn, Fe, Ru, Co, Rh, Ir, and Pt and L = H_2O, MeOH, or pyr [28]. The complex contains an oxygen-centred triangle. At the corner of each triangle is an octahedral metal centre. The M_3O unit usually adopts a planar geometry.

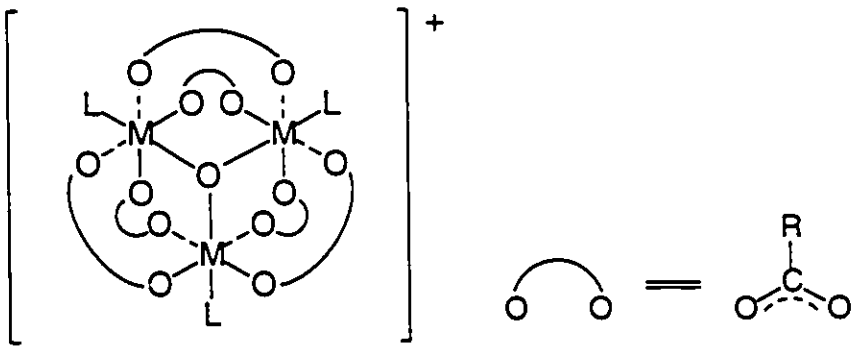

5

A variety of molecules of the type, $[M_3O(O_2CMe)_6L_3]^+$, **5**, have been

examined with respect to their redox properties. For example, $[Ru_3O(O_2CMe)_6L_3]^+$, which can be obtained on refluxing $RuCl_{3(aq)}$ with sodium acetate in acetic acid, yields mixed oxidation state systems [29]. As well, the carboxylates in this complex can act as hydrogenation catalysts in DMF and in the presence of phosphines. The $[Co_3O(O_2CMe)_5(OH)(py)_3]^+$ can oxidize, with oxygen, aromatic and other organic compounds [30].

A third group of compounds containing multi-bridging acetates are the $M_2(O_2CMe)_4L_2$ complexes, **6**, where the M = Cr, Mo, Ru, Os, and Rh [31]. The four acetate groups bridge a metal-metal multiple bond. Very often two axial ligands such as H_2O or ROH will also coordinate. The $Cr_2(O_2CMe)_4(H_2O)_2$ complex has been prepared and the strength of the Cr-Cr quadruple bond was shown to be inversely related to the strength of the axial ligand bond and to a much lesser extent, sensitive to the basicity of the $RCOO^-$ group [32]. The $Rh_2(O_2CMe)_4$ complex is obtained on heating sodium acetate with $RhCl_3 \cdot H_2O$ in methanol. Again, the end positions are occupied by donor ligands; with adducts of oxygen donors they are green or blue; but with π-acids such as PPh_3 they are red [33].

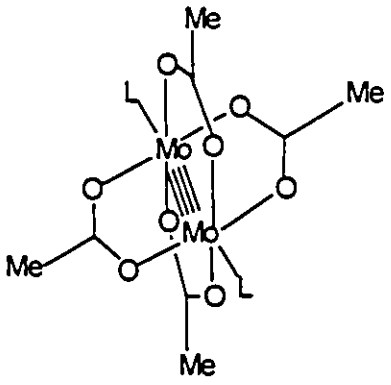

6

This chemistry of complexes containing the carboxylate ligand, $RCOO^-$ where R is an organic substituent, has already been studied extensively. Examples where this substituent is an organo-transition metal cluster have only recently been examined. Introducing a cluster with a ligand functionality to various metal salts, results in the formation of analogous multi-nuclear compounds. These novel compounds are known as inorganometallic compounds [34].

1.3.2. The Cluster Carboxylate Ligand

The carboxylate cluster ligand consists of a $Co_3(CO)_9C$ coupled to a carboxylate functionality (COO^-). The direct electronic interaction between these two fragments creates a ligand that coordinates easily to a metal core resulting in a high-nuclearity complex.

The facile low-temperature formation of $OZn_4[O_2CCCo_3(CO)_9]_6$, 7, from $Co_3(CO)_9C$-COOH and $ZnEt_2$ was reported by Fehlner *et al.* [35].

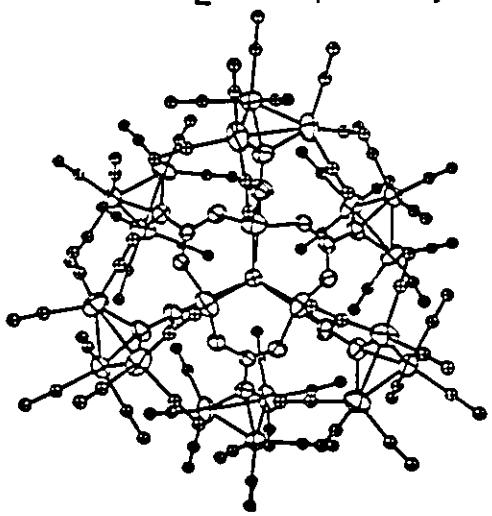

Figure 3: X-ray crystal structure of 7 with view down the pseudo 3-fold axis.

The crystal structure is shown in Figure 3. Complex **7** is a pseudo-spherical particle with a diameter of 15-16 Å. The tetrahedral OZn_4 core has each of its six edges bridged by a (carboxymethylidyne)tricobalt nonacarbonyl group. Hence, all four zinc atoms are tetrahedrally coordinated to four oxygen atoms. The central OZn_4 core determines the octahedral spatial distribution of the transition metal clusters.

The analogous $OCo_4[O_2CCCo_3(CO)_9]_6$, **8**, was reported independently by Schore and co-workers. The serendipitous synthesis of **8** involved simply the addition of the solution obtained from the reaction of $AlCl_3$ and $Co_3(CO)_9C$-Cl in CH_2Cl_2 to ice water (Figure 4) [36]. The complex is similar in structure to **7**, six carboxylate cluster ligands edge-bridging a cobalt tetrahedron with an oxygen atom in the centre.

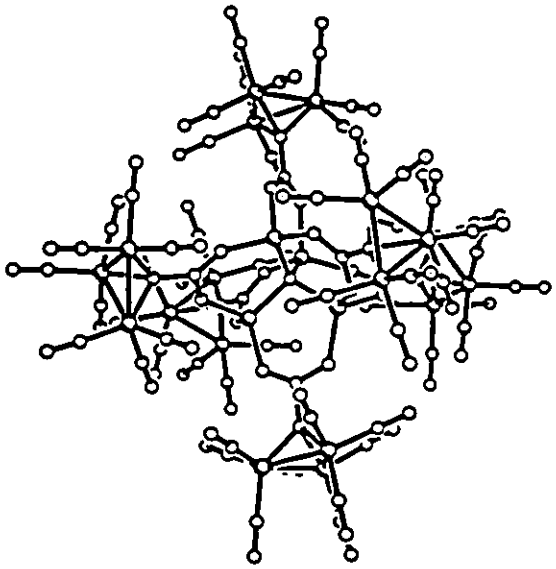

Figure 4: X-ray crystal structure of 8.

The $M_4O[Co_3(CO)_9CCO_2]_6$ complexes discussed are metal cluster analogues of the classical $M_4O[RCO_2]_6$ "basic" metal carboxylates mentioned in

1.3.1.. Because the R groups in **7** and **8** are not simple methyl groups but are themselves clusters, these products are known as inorganometallic compounds.

In the carboxylate cluster ligand, the direct electronic interaction between $Co_3(CO)_9C$ and the carboxylate functionality (COO^-) affects the kinetics and mechanisms of coordination and may therefore be the reason for the facile formation of complexes **7** and **8**. Two ligand precursors, $Co_3(CO)_9\{\mu^3\text{-}C[1,4\text{-}C_6H_4(CH_2)_2COOH]\}$, **9**, and $Co_3(CO)_9\{\mu^3\text{-}CCOOH\}$, **10**, were compared in a study of carboxylate clusters as substituents [37]. For **9**, the cluster fragment is electronically isolated from the ligand functionality. The ligand, **10**, on the other hand, has good electronic communication between the cluster and ligand functionality. Molecule **10** can spontaneously convert to $OCo_4[O_2CCCo_3(CO)_9]_6$, **8**, in solution. The ligand, **9**, which is stable in solution, can be treated with one half mole of diethylzinc yielding $Zn[Co_3(CO)_9CC_6H_4(CH_2)_2CO_2]_2$, which is analogous to the product from either acetic acid or $C_6H_5(CH_2)_2COOH$ with the same reaction stoichiometry. Thus, in the absence of conjugation between the metal cluster and the acid functionality, the cluster acid, **9**, behaves as a simple carboxylic acid. In contrast, the reaction of **10** with $ZnEt_2$ in any mole ratio results in $OZn_4[O_2CCCo_3(CO)_9]_6$, **7**, in high yield. Therefore, the different chemistry of **10** can be attributed to the direct electronic interaction of the tricobalt cluster to the carboxylate fragment.

Metal-metal quadruply bonded compounds have also been used as cores for coordinating cluster carboxylate ligands [38]. Again, these complexes are analogous to the metal carboxylates of the type, $M_2(O_2CCH_3)_4$. Coordination results in a complex with a square planar array of transition metal

clusters. The $Mo_2(O_2CCH_3)_4$ reacts with the cluster acid, $Co_3(CO)_9C$-COOH, **10**, to form three high nuclearity clusters of clusters.

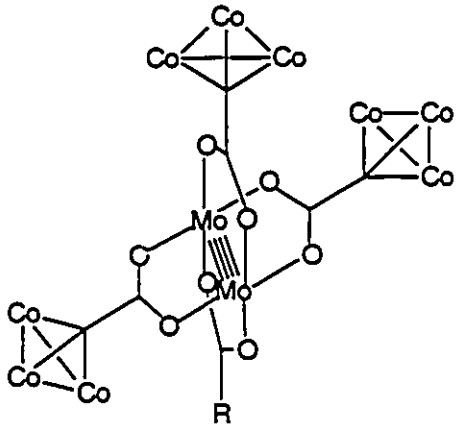

11: R=CH_3 **12**: R=$CCo_3(CO)_9$

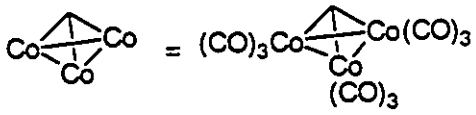

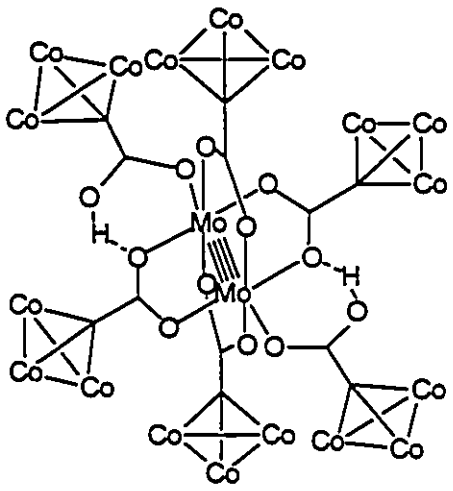

13

One tri- and two different tetracluster-substituted species were isolated having the general formula, $Mo_2\{\mu_2\text{-}[(CO)_9Co_3C\text{-}CO_2]\}_m(CH_3CO_2)_{4\text{-}m}[(CO)_9CO_3C\text{-}CO_2H]_n$ where m = 3, n = 0, **11**; m = 4, n = 0, **12**; m = 4, n = 2, **13**. These species have a similar structure to the parent $Mo_2(O_2CCH_3)_4$ complex. The substantial electronic interaction between the $Co_3(CO)_9C$ fragment and the (COO^-) group presumably makes $[Co_3(CO)_9C\text{-}CO_2]^-$ a much better ligand than acetate.

Metal cluster substituents possess a relatively fragile framework and therefore require careful reaction conditions. This drawback was an advantage in the preparation of the $OCo_4[O_2CCCo_3(CO)_9]_6$, **8**, in which the cobalt atoms

of the OCo_4 core arise from the decomposition of the cluster acid, **10**. Thus, **10** serves not only to bridge the metal centres but acts as a source for the core framework. Another example reported by Fehlner *et al.* again possesses several carboxylate cluster ligands [39]. The ligand plays a structural role in the stabilization of an unusual complex containing formal Cd(I). The complex $[\mu_3\text{-}Co(CO)_3]Cd\{\mu\text{-}[(CO)_9Co_3C\text{-}CO_2]\}_3(THF)_3$, **14**, is prepared from the slow addition of $CdMe_2$ to $Co_3(CO)_9C\text{-}COOH$, **10**, in THF at room temperature.

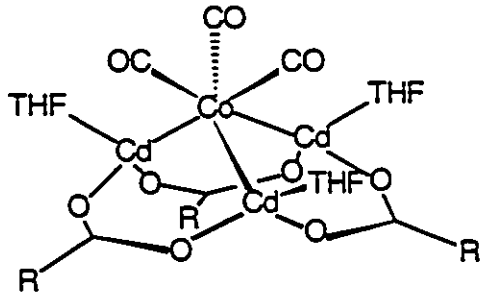

14

The compound consists of an equilateral triangle of Cd atoms capped by a $Co(CO)_3$ fragment with the Cd-Cd edges bridged by $[Co_3(CO)_9C\text{-}CO_2)]^-$ ligands. Each Cd atom is also coordinated to a molecule of THF. The cluster acid, **10**, again serves as the source for the ligand that bridges the Cd-Cd edges as well as a thermal source of the $Co(CO)_3$ metal fragment that caps the Cd_3 triangle.

1.4 Statement of the Problem

In recent years, the attachment of metal carbonyl fragments to surfaces has been the subject of considerable activity [40]. An oligo-cluster

complex could effectively serve as a multi-catalytic site upon which a reaction or numerous reactions, concurrently or sequentially, could be facilitated. Can a methodical procedure for synthesizing these high-nuclearity cluster systems be found? By beginning with various organic or inorganic precursors of specific size or shape, one could "coat" their surfaces with organo-transition metal clusters. The methylidynetricobalt nonacarbonyl cluster was selected for the purposes of this investigation.

CHAPTER TWO

ORGANIC TEMPLATES BEARING MULTIPLE CLUSTER FRAGMENTS

While most of the work done by Fehlner [35,38,39] and Schore [36] depended on the self-assembly of large cluster systems, one might choose to investigate a systematic route to high-nuclearity complexes. One can readily envisage coating a molecule of a selected shape and size with a layer of organo-transition metal cluster fragments. Thus, one might choose to build prolate, oblate, disk-like, or spherical molecules based upon an appropriate organic template. (Scheme 13).

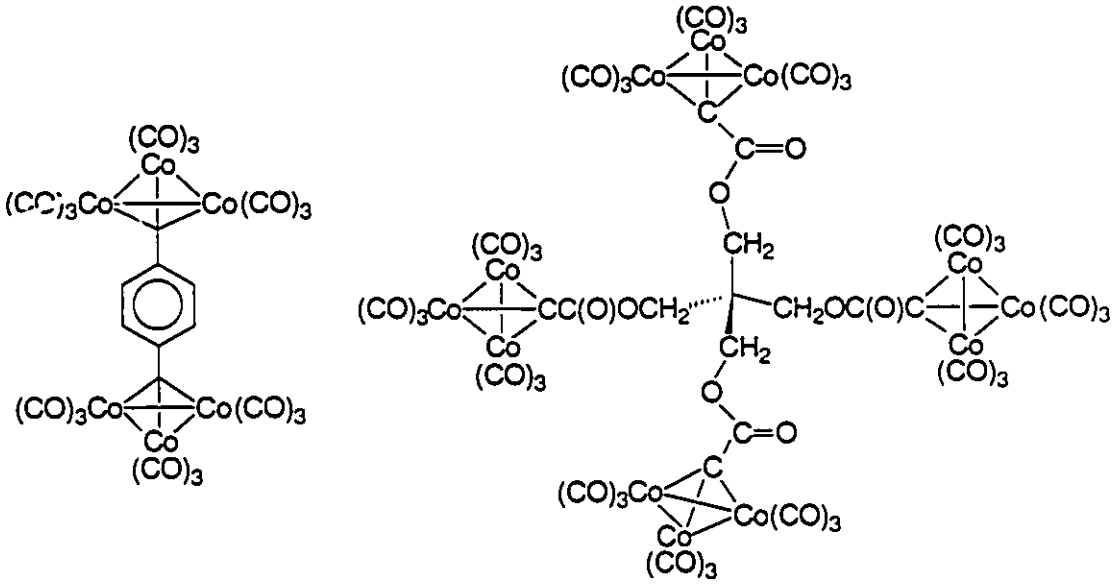

(a) disk-like

(b) spherical

Scheme 13: Different possible shapes for cluster complex systems.

An -OH functionality of an organic precursor can be readily converted to the $-O_2CCCo_3(CO)_9$ fragment via the various synthetic techniques mentioned in Chapter 1.2. Thus molecules possessing several hydroxy groups such as hydroquinone could lead to oligo-cluster complexes that are disk shaped (13a). Pentaerythritol could result in a spherical cluster system (13b).

2.1 Preparation of p-$C_6H_4[OC(O)CCo_3(CO)_9]_2$

Hydroquinone, p-$C_6H_4[OH]_2$, possesses two -OH groups that were initially converted to $-O_2CCCl_3$ groups by treatment with trichloroacetylchloride, CCl_3-CO-Cl. The trichloromethyl groups in p-$C_6H_4[OC(O)CCl_3]_2$ were then replaced by alkylidynetricobalt nonacarbonyl clusters by reaction with dicobalt octacarbonyl, $Co_2(CO)_8$ (Scheme 14). Each chlorine atom is replaced by a $Co(CO)_3$ moiety, resulting in a tetrahedral cluster both at the 1 and 4 position of the phenyl ring.

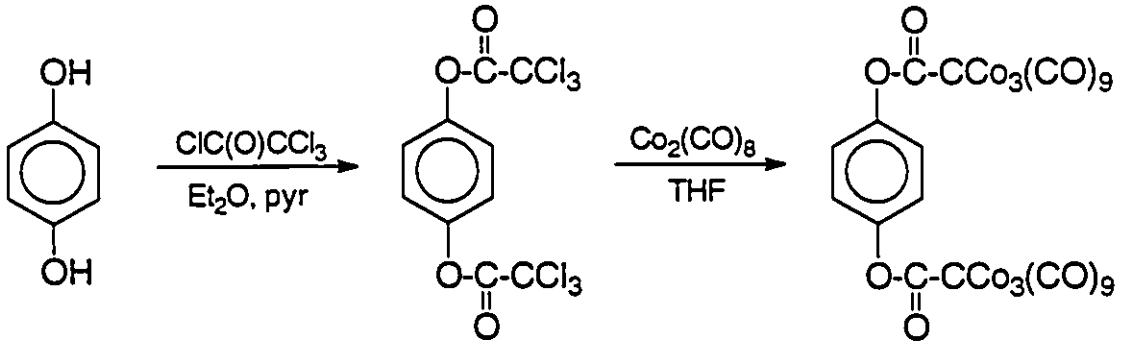

15

Scheme 14: The preparation of p-$C_6H_4[OC(O)CCo_3(CO)_9]_2$, 15.

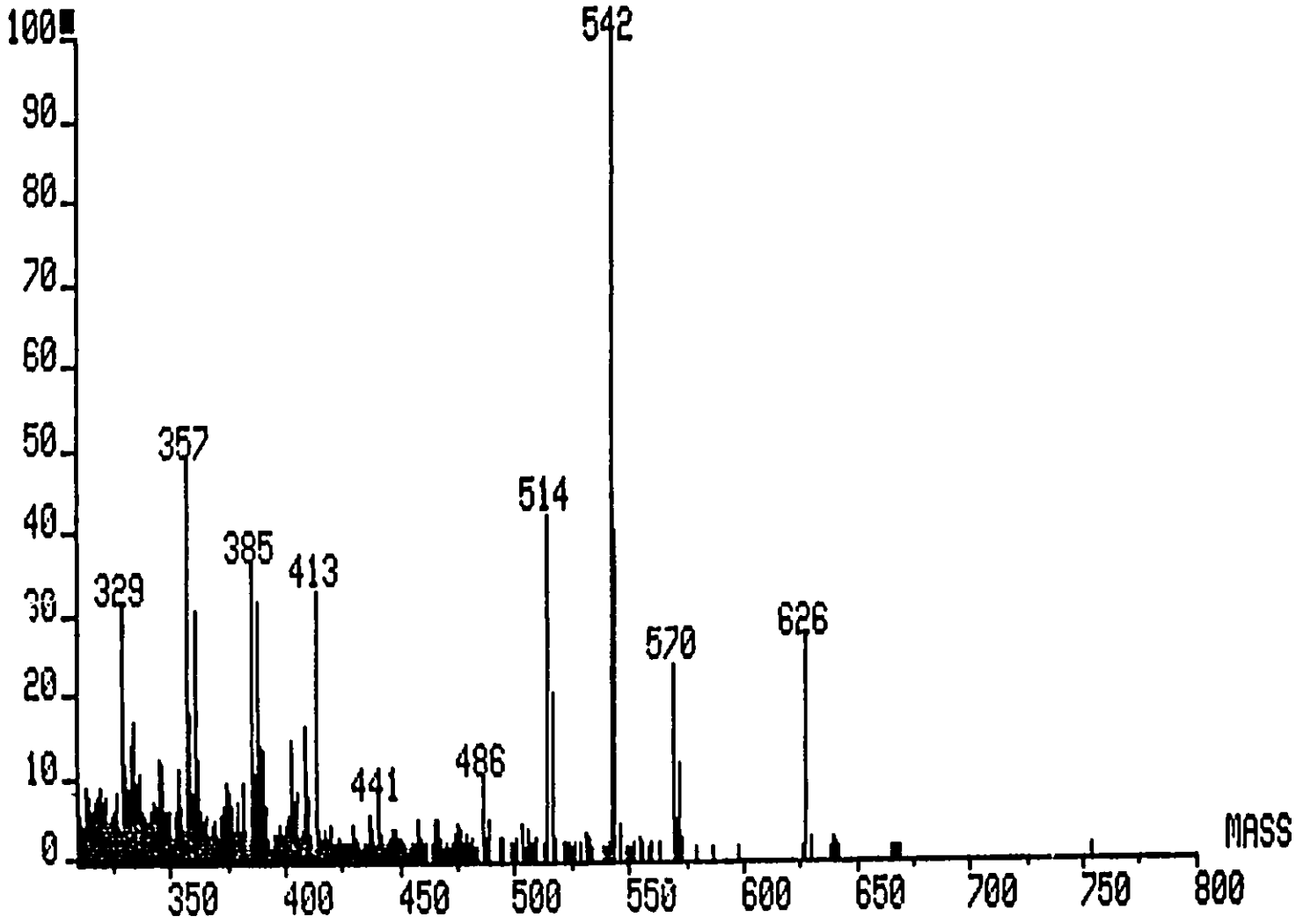

Figure 5: The [FAB]$^+$ mass spectrum of p-$C_6H_4[OC(O)CCo_3(CO)_9]_2$, **15.**

The purple product, which was a mixture of the mono- and bis-substituted cluster, was separated by flash chromatography. The $[FAB]^+$ mass spectrum (MS) of *p*-$C_6H_4[OC(O)CCo_3(CO)_9]_2$, **15**, in Figure 5, shows the successive loss of metal carbonyl groups. The loss of all 18 metal carbonyl groups results in the base peak at m/z 542. The spectrum also shows the loss of a 19th carbonyl ligand. As discussed in Chapter **1.2.2**, apical carbonyl groups are known to migrate to a vacant metal carbonyl position. Thus, the ester carbonyl's migration to a vacant cobalt carbonyl position followed by its loss during the MS analysis, would explain this 19th carbonyl. In addition, the parent ion peak minus a $[-O_2CCCo_3(CO)_9]$ fragment results in a peak at 486. As is commonly the case with metal carbonyl complexes, the parent ion peak is not seen.

Therefore, by taking a rather simple organic template such as hydroquinone, a disk-like molecule coated with organo-tricobalt clusters can be prepared.

2.2 Preparation of $C[CH_2OC(O)CCo_3(CO)_9]_3[CH_2OC(O)CCl_3]$

To prepare an oligo-cluster based upon an organic tetrahedral precursor, pentaerythritol, *i.e*, tetra(hydroxymethyl)methane, was utilized. This alcohol was treated with CCl_3-CO-Cl to yield the tetrakis-trichloroacetate ester $C(CH_2\text{-}O_2C\text{-}CCl_3)_4$, **16**. Reaction of **16** with excess $Co_2(CO)_8$ led to a complex mixture of products several of which were separable on a column by flash chromatographic techniques (Scheme 15). The highest molecular weight product corresponded to $C[CH_2\text{-}O_2C\text{-}CCo_3(CO)_9]_3(CH_2\text{-}O_2C\text{-}CCl_3)$, **17**, the tris-cluster complex.

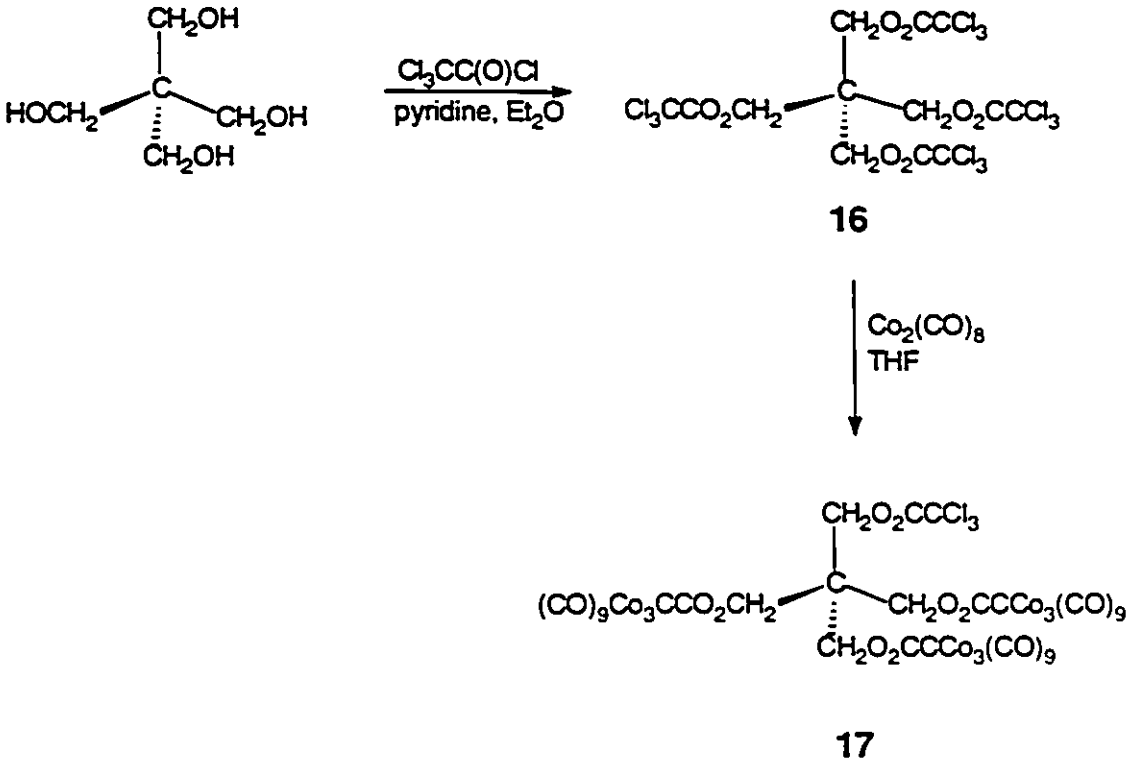

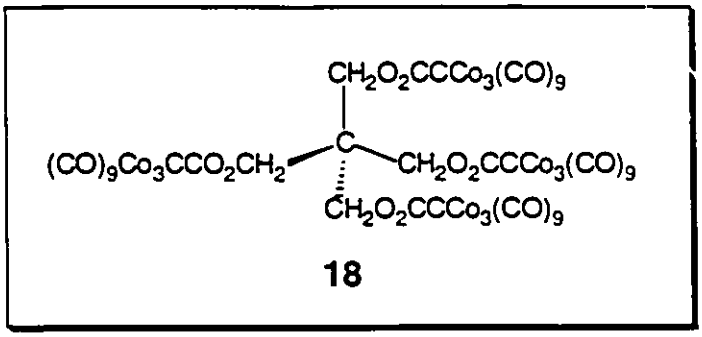

Scheme 15: The preparation of $C[CH_2\text{-}O_2C\text{-}CCo_3(CO)_9]_3(CH_2\text{-}O_2C\text{-}CCl_3)$, 17.

One is tempted to ascribe the failure to isolate the tetra-cluster $C[CH_2\text{-}O_2C\text{-}CCo_3(CO)_9]_4$, **18**, to problems of steric crowding. In order to model this 12-cobalt molecule, it was decided first of all to obtain the x-ray crystal structure of the 12-chloro complex **16** and then to use a molecular modelling program to replace the CCl_3 units by $CCo_3(CO)_9$ moieties.

Molecules in which a tetrahedral atom bears four identical bulky groups have been extensively studied by Mislow [41]. For example, in tetrakis(trimethylsilyl)silane $Si(SiMe_3)_4$, the steric crowding causes each methyl group to mesh tightly with those in the remaining trimethylsilyl groups. $Si(SiMe_3)_4$ does not adopt T_d symmetry; instead the twisting of the four groups lowers the symmetry to that of the rotational sub-group *T*, in which the C_3 axes are retained but the mirror planes are lost.

The tetra-ester, **16**, crystallizes in the triclinic space group *P1* with 2 molecules per unit cell. As shown in Figure 6, the molecular structure reveals that the tetrahedral symmetry of **16** is indeed broken, but in a different fashion to that found for $Si(SiMe_3)_4$. The trichloroacetate chains fold so as to produce a flattened tetrahedron; they are oriented in pairwise fashion so as to give a molecule of approximate D_{2d} symmetry in which the C_3 axes are lost but two mirror planes and the S_4 axis are retained. The crystallographic collection parameters, atom coordinates and selected bond length and angle data for **16** are listed in the Appendix .

Now, using the modelling program ALCHEMY [42], the four trichloromethyl units in **16** were replaced by $CCo_3(CO)_9$ fragments. These latter groups were constructed by using parameters taken from the x-ray crystal structure of $CH_3CCo_3(CO)_9$ [43]. The computer-derived model of the molecule

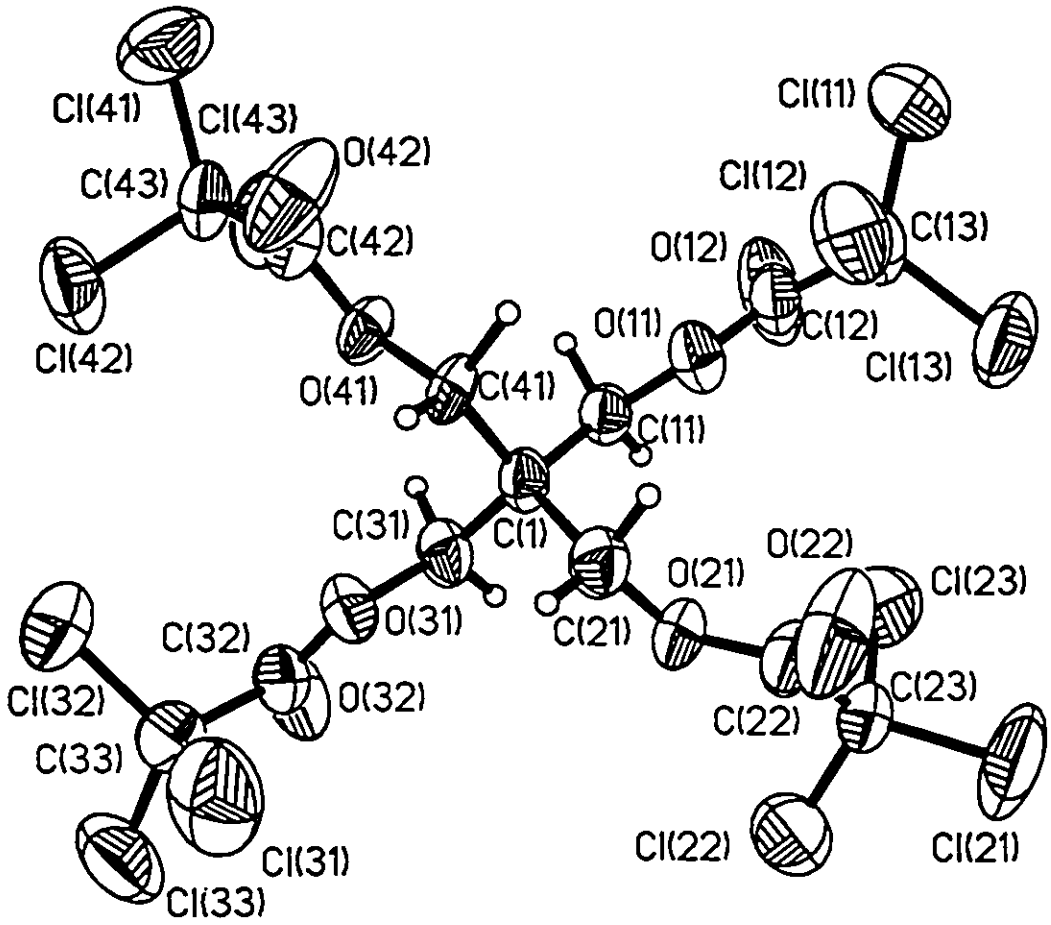

*Figure 6: The X-ray crystal structure of $C(CH_2\text{-}O_2C\text{-}CCl_3)_4$, **16**.*

$C[CH_2\text{-}O_2C\text{-}CCo_3(CO)_9]_4$, **18**, constructed as described above and energy minimized so as to avoid unfavorable steric interactions between carbonyl ligands, appears as Figure 7a; a space-filling representation of **18** is shown in Figure 7b. It is apparent that the desired molecule can indeed adopt a viable conformation but it is less certain that the intermediates involved in the conversion of the CCl_3 groups into tricobalt clusters can be accommodated.

Other potential routes to **18** have been investigated. Thus, although the acylium cation $[(OC)_9Co_3C\text{-}C{=}O]^+$ reacts readily with alcohols, phenols or diols to give mono- or bis-clusters [11], the corresponding reaction with pentaerythritol is thwarted by the very low solubility of the tetra-alcohol in solvents which are themselves unreactive towards the organometallic acylium salt.

2.3 Future Work

Functionalized organic molecules seem like reasonable precursors toward multi-cluster complexes. Other molecules that can be considered are phloroglucinol, and fused-ring systems such as 2,6-dihydroxynaphthalene. Again these two examples should lead to disk-like cluster systems via their trichloroacetate ester intermediates. Phloroglucinol could result in a tris-cluster complex, a system that would be considerably more crowded than **15**. From 2,6-dihydroxynaphthalene, the cluster moieties would be positioned further apart. Also, a chiral cluster system could potentially be synthesized from α-D-glucopyranose. Cluster formation via the acylium cation can also be investigated with alcohols or phenols that are actually soluble in the required solvents.

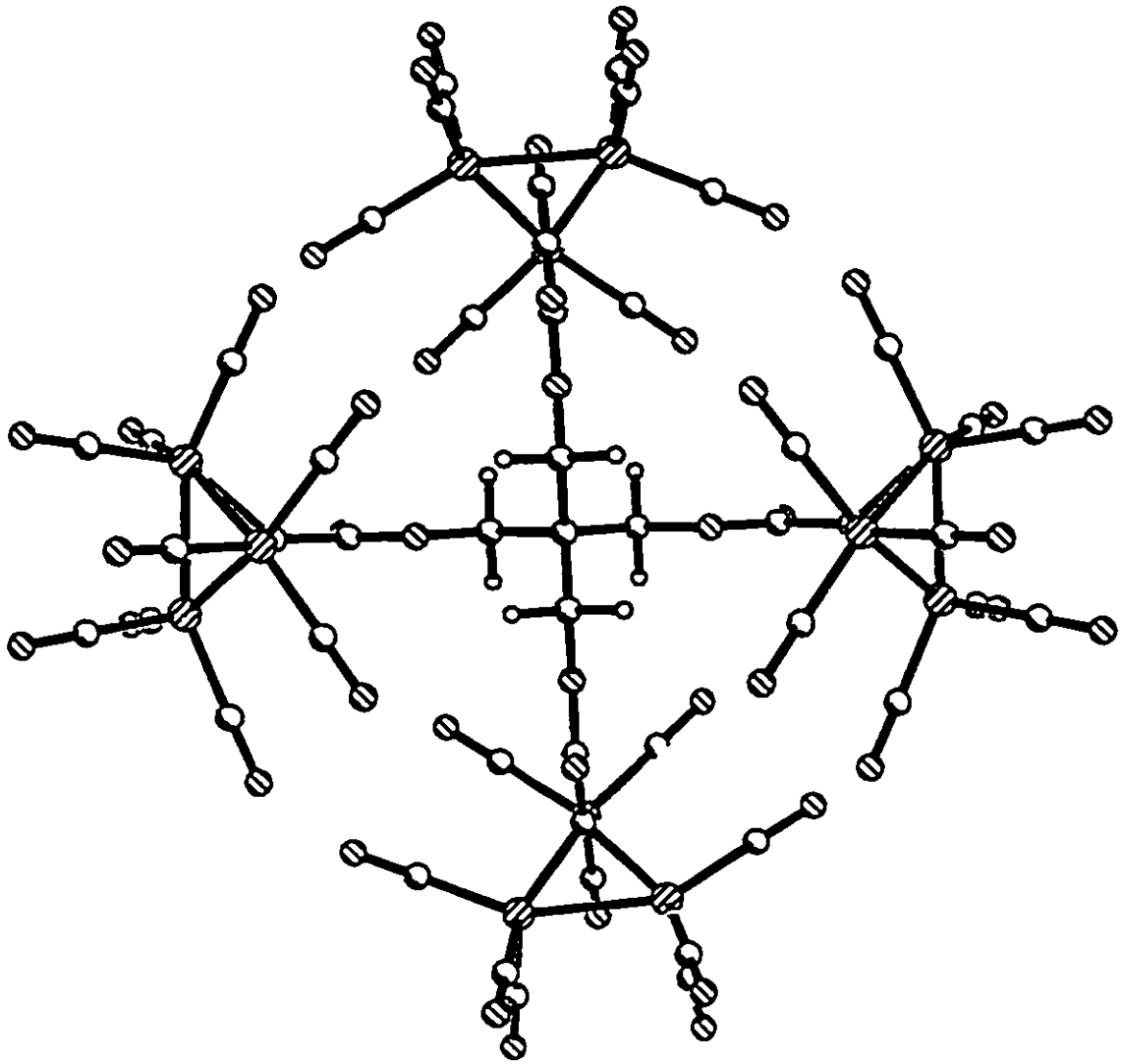

*Figure 7a: Computer-derived model of $C[CH_2\text{-}O_2C\text{-}CCo_3(CO)g]_4$, **18**.*

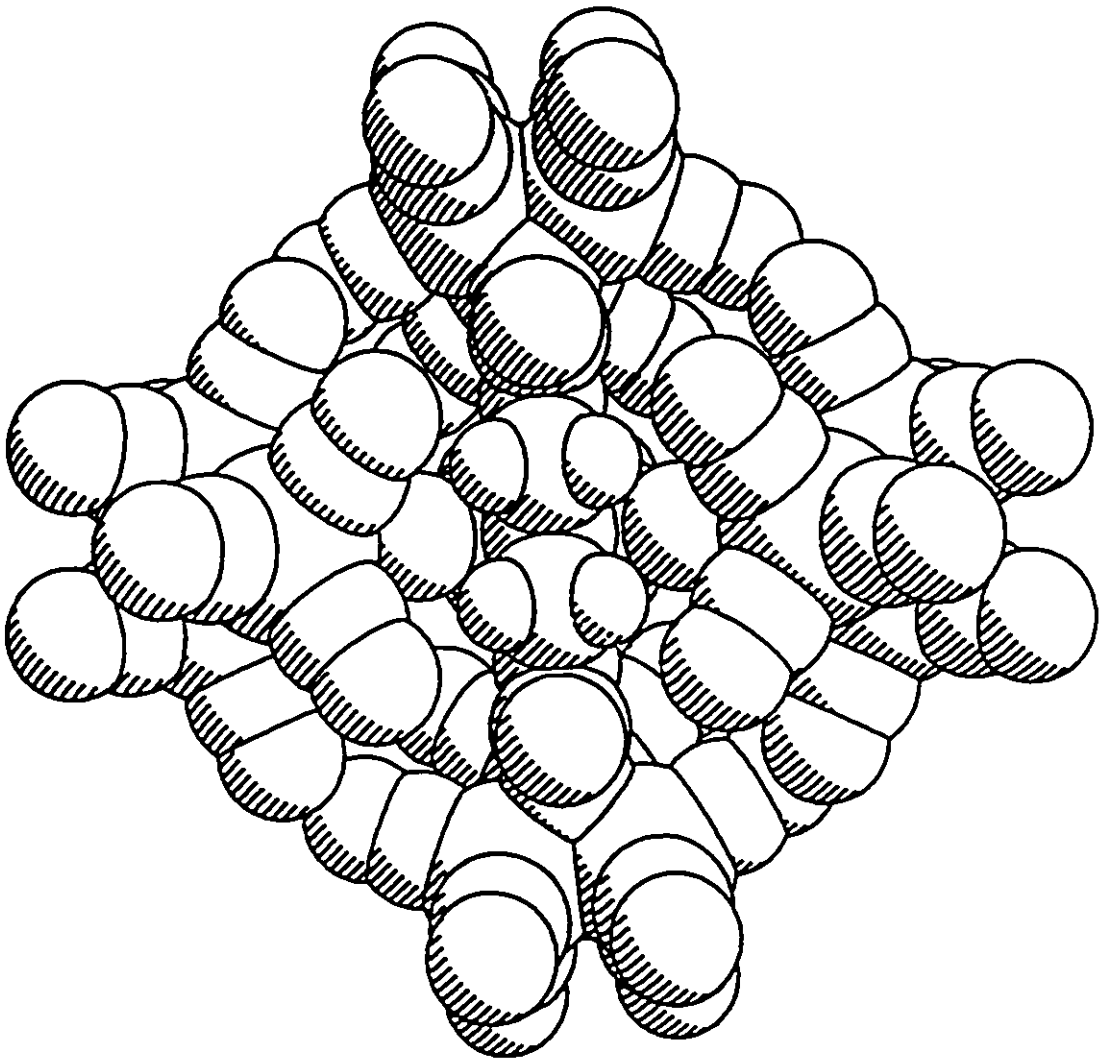

Figure 7b: Computer-derived space filling model of $C[CH_2\text{-}O_2C\text{-}CCo_3(CO)_9]_4$, 18.

CHAPTER THREE

INORGANIC TEMPLATES BEARING MULTIPLE CLUSTER FRAGMENTS

Inorganic precursors may also be considered in the preparation of oligo-cluster complexes. Coordination complexes of selected size and shape can act as templates over which one can coat with a layer of cluster fragments. As in the preparation of the high-nuclearity complexes **7**, **8** (P.19-20), and **11-14** (P.22-23), a bridge between coordination chemistry and organo-tricobalt cluster chemistry can result in the formation of oligo-cluster systems [35,36,38,39]. The exquisite molecules synthesized by Fehlner and Schore depend for their existence on the stability and ready availability of the tri-cobalt cluster carboxylic acid $(OC)_9Co_3C\text{-}CO_2H$. However, the corresponding analogues of acetylacetone, *i.e.* $R^1\text{-}CO\text{-}CH_2\text{-}CO\text{-}R^2$, where one or both R groups are $CCo_3(CO)_9$ moieties rather than methyls, has not yet been prepared. Therefore, while a cluster-substituted acetate ligand was used in the preparation of complexes **7**, **8**, and **11-14**, a cluster-substituted acetylacetonate ligand has not yet been reported.

3.1 Acetylacetone and its Metal Complexes

The ubiquitous acetylacetone, acacH, and its related molecules having the general formula, $R^1\text{-}CO\text{-}CH_2\text{-}CO\text{-}R^2$, are known as β-diketones or β-dicarbonyls [44]. The acacH molecule exists in solution as mixtures of keto, **19**, and enol, **20**, forms.

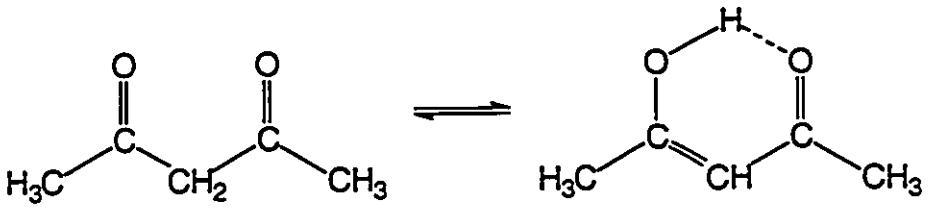

19 20

At 37.3 °C, neat acacH exists 78% as the enol tautomer and this percentage decreases with rising temperature [45]. Replacement of terminal methyl groups with electron-withdrawing or aromatic groups such as CF_3, C_4H_3S, and C_6H_5 shifts the equilibrium in favor of the enol form. Electron-releasing substituents decrease the enol content [46]. The enol tautomer is at least partially stabilized by the intramolecular hydrogen bond.

The two tautomeric forms can be simultaneously observed in the NMR spectrum. The ^1H NMR spectrum of acacH exhibits only two methyl proton signals at 1.97 and 2.14 ppm assignable to the enol and keto methyls respectively, indicating that the two methyls in the enol molecule are equivalent. The enol tautomer must have either the symmetrical C_{2V} structure or exist in the asymmetric C_S forms with a low barrier to intercoversion via the C_{2V} structure (Scheme 16).

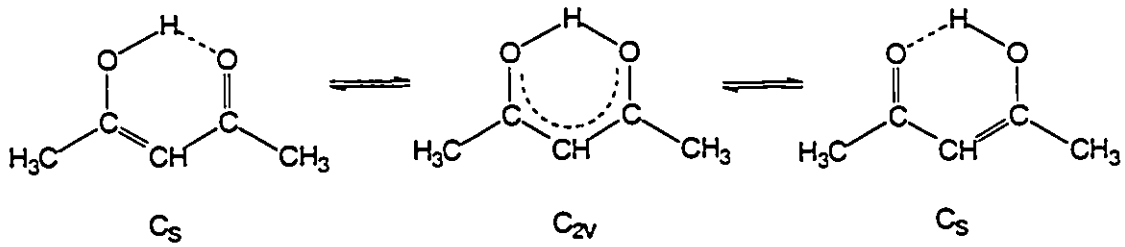

C_S C_{2V} C_S

Scheme 16: The C_{2V} and C_S interconversion of the enol tautomer of acacH.

Camerman *et al.* crystallized a complex of diphenylhydantoin and 9-ethyladenine (an antiepileptic drug) from acacH solution and found that one enol molecule of acacH per asymmetric unit is involved in the crystal lattice [47]. The acacH does not appear to interact with the other components of the lattice. Figure 8 shows a structure in which the bond distances, including the hydrogen bond, are not symmetric but are indicative of localized single and double bonds throughout the molecule.

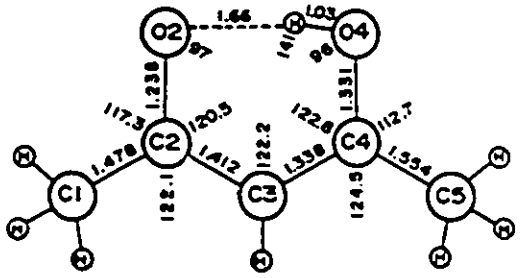

Figure 8: The x-ray crystal structure of acetylacetone [47].

The structures of several derivatives of acetylacetone have been studied. In the solid state, the enol form is generally the sole form observed. The two extreme forms of intramolecular hydrogen bonding, symmetric and asymmetric, have both been observed.

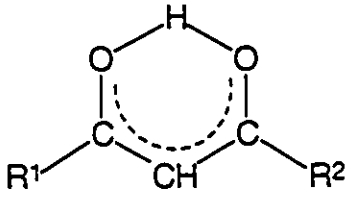

21 a) $R^1 = R^2 = (CH{=}CH)\text{-}Ph$
b) $R^1 = R^2 = Ph$
c) $R^1 = Me$, $R^2 = Ph$

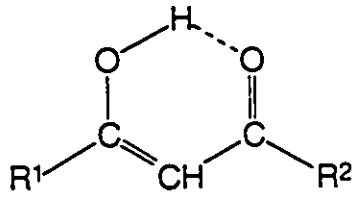

22 a) $R^1 = R^2 = CH_3$

b) $R^1 = R^2 =$ 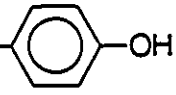

c) $R^1 = CF_3$, $R^2 =$ 

Symmetric hydrogen bonds have been observed in examples having identical substituents, $R^1 = R^2$, **21a, b** [48], or different substituents, $R^1 \neq R^2$, **21c** [49]. Markedly asymmetric hydrogen bonds have been observed both for identical substituents, **22a, b** [47,50], and for different substituents, **22c** [51].

The methine proton in the keto form or the hydroxyl proton in the enol form are acidic and their removal generates the 1,3-diketonate anion. This ligand is a source of a broad class of coordination compounds referred to as diketonates or acetylacetonates.

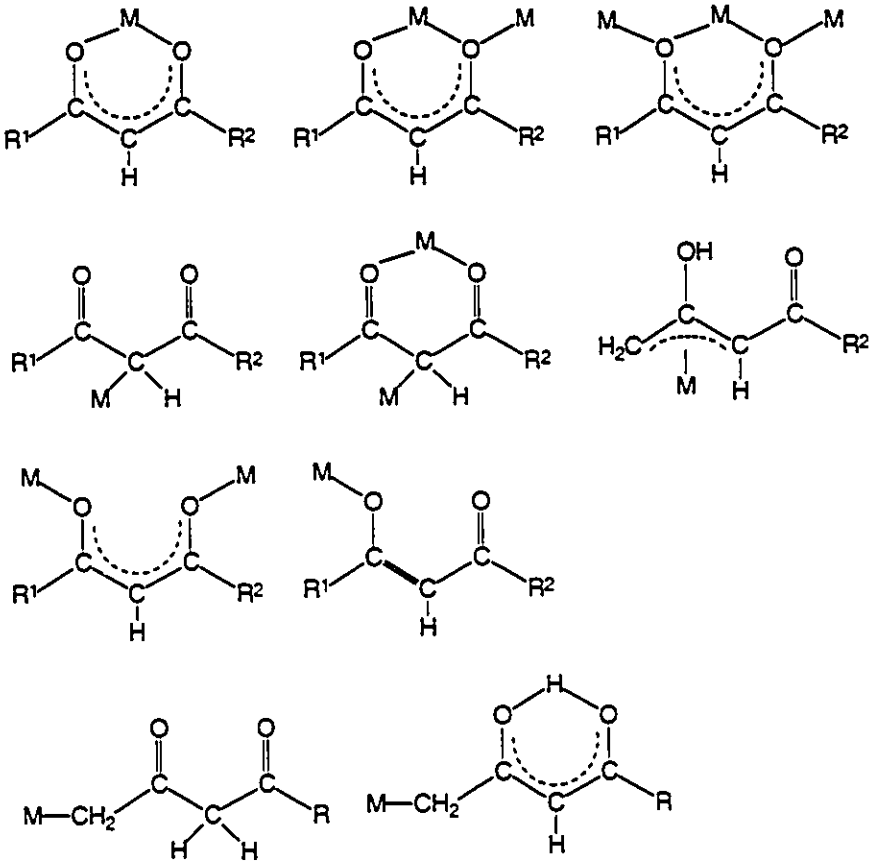

Figure 9: Coordination modes for 1,3-diketonate anions in metal complexes [46].

Diketonate anions are strong chelating agents capable of forming complexes with virtually every transition and main group element [52]. Various coordination modes have been established and are illustrated in Figure 9.

The *O,C'*-chelation and bridging, central carbon bonding, *O*-unidentate linkage, η-allylic coordination, and terminal carbon bonding are the main coordination modes of the monoanion [46]. The *O,O'*-chelation and bridging is the most popular mode of coordination. The $M(diket)_3$ and $M(diket)_2$ are the most common stoichiometries. In $M(diket)_3$ complexes, the six oxygen atoms are octahedrally disposed. These tris(chelate) molecules actually have D_3 symmetry and exist as enantiomers. When these are unsymmetrical diketonate ligands, i.e. $R^1 \neq R^2$, geometrical isomers also exist.

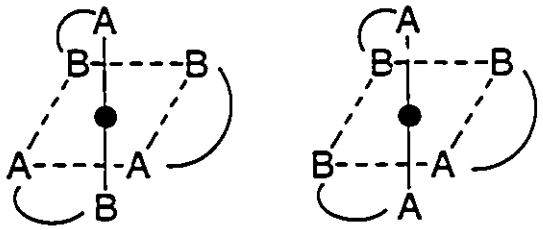

fac mer

There is considerable structural information on these metal complexes [52]. The diketonate ligand is usually planar with nearly equivalent C-C, C-O, and M-O bond distances, consistent with delocalized bonding. Complexes of composition, $M(diket)_2$, have the tendency to adopt oligomeric structures, so that by means of oxygen-bridging diketonate ligands, the central metal atom achieves coordinative saturation. Thus, acetylacetonates of Zn, Ni, and Mn are trimeric (Figure 10) [53,54]. $Co(acac)_2$ is tetrameric (Figure 11) [55].

Monomer-trimer equilibrium for $Ni(acac)_2$ and related compounds have been observed at elevated temperatures [56]. The presence of bulky substituents on the diketonate ligand such as Me_3C groups sterically impedes oligomerization and monomers are formed [57]. These monomers are commonly solvated by H_2O, ROH, or py to give 5- or 6-coordinate complexes, trans-$M(diket)_2L_{1,2}$.

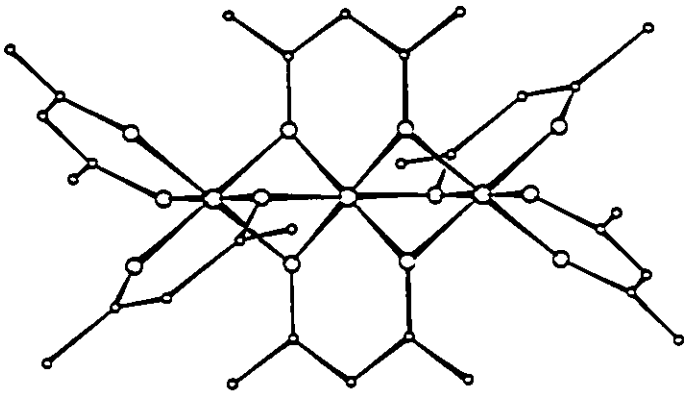

Figure 10: The trimeric structure of $Ni[acac]_2$ [54a].

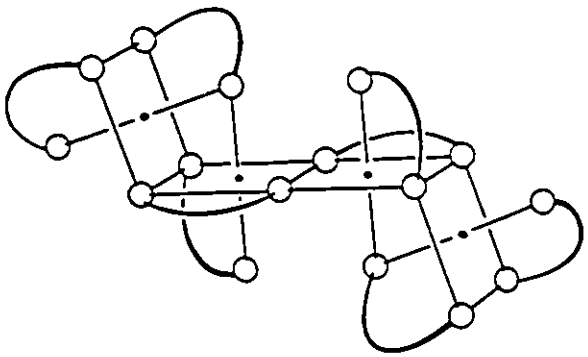

Figure 11: The schematic representation of tetrameric $Co[acac]_2$.

3.2 The Trichloroacetylacetonate Ligand: Its Metal Complexes and Cobalt Cluster Analogues

As discussed in Section **3.1**, much research has been done on acetylacetone and its organic analogues. However, there have been no examples of a cluster-substituted acetylacetone, *i.e.* R^1-CO-CH_2-CO-R^2, where one or both R groups are $CCo_3(CO)_9$ moieties rather than methyls. Since $RCCo_3(CO)_9$ clusters are frequently obtainable by treatment of the corresponding $RCCl_3$ precursors with dicobalt octacarbonyl, the obvious first step was to try to use 1,1,1-trichloropentan-2,4-dione (tcacH), **23**, as the cluster precursor. The ligand tcacH is readily preparable by the reaction of trichloroacetonitrile and pentan-2,4-dione with sodium acetate to give $Cl_3CC(NH_2)$=CHC(O)CH_3; subsequent treatment with concentrated HCl yields tcacH, **23**, as a colorless liquid [58,59] (Scheme 17).

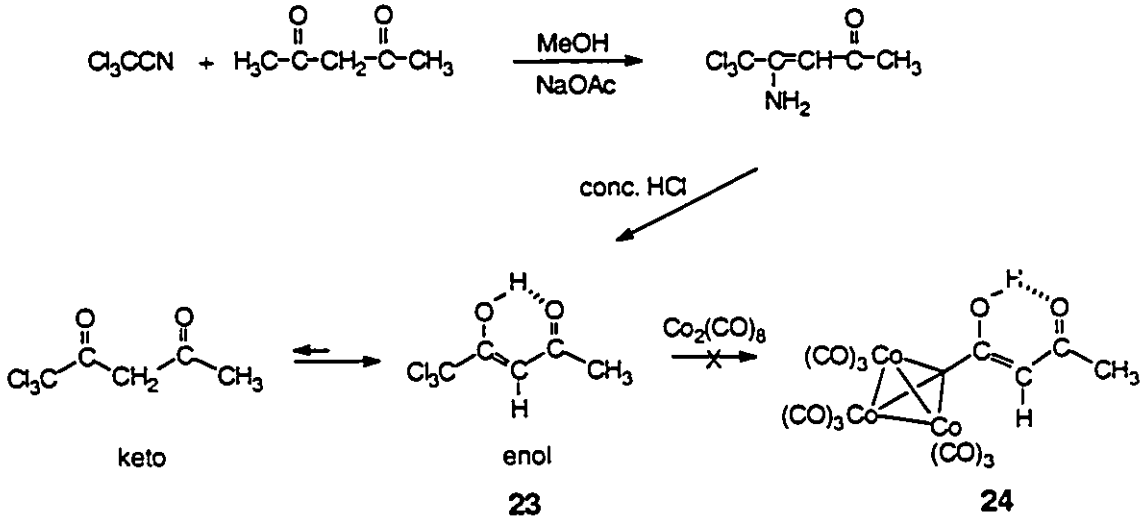

*Scheme 17: The preparation of trichloroacetylacetone, **23**.*

However, the reaction of **23** with $Co_2(CO)_8$ does not yield useful quantities of the desired complex CH_3-CO-CH-C(OH)-$CCo_3(CO)_9$, **24**. This behavior is reminiscent of Seyferth's report that the presence of hydroxyl functionalities in the trichloromethyl precursor often limits the utility of this approach. Specifically, $Co_3(CO)_9C$-CH_2OH can not be obtained directly from $Co_2(CO)_8$ and CCl_3CH_2OH [15].

From the ^1H and ^{13}C NMR spectra of tcacH, it is evident that the ligand exists in solution primarily as an enol tautomer; indeed, other electron-withdrawing groups are well-known to have a marked influence on the keto-enol equilibrium [46]. The ^{13}C NMR spectrum is shown in Figure 12.

1,1,1-Trichloroacetylacetone, **23**, has been reported to yield complexes with a variety of di- and trivalent metals such as Cr(III), Mn(II), Fe(III), Co(II), Cu(II) and Al(III), just as many other β-diketones [60]. By using this approach of the prior coordination of $[CCl_3$-CO-CH-CO-$CH_3]^-$ to a metal center before treatment with $Co_2(CO)_8$, we avoid the presence of a hydroxyl group in the ligand. These complexes can now serve as the inorganic precursors that are to be coated with cobalt cluster fragments.

Typically, $Al(tcac)_3$, **25**, reacts with excess dicobalt octacarbonyl to yield the corresponding cluster-substituted complex **26** (Scheme 18). The cluster **26** is conveniently identified by its $[FAB]^+$ mass spectrum (Figure 13) which exhibits a [P-1CO] peak and sequential loss of 23 carbon monoxide fragments. Moreover, one sees loss of a $Co_3(CO)_9C$-C(O)CHC(O)CH_3 fragment from the molecular ion followed by loss of 10 additional carbonyls.

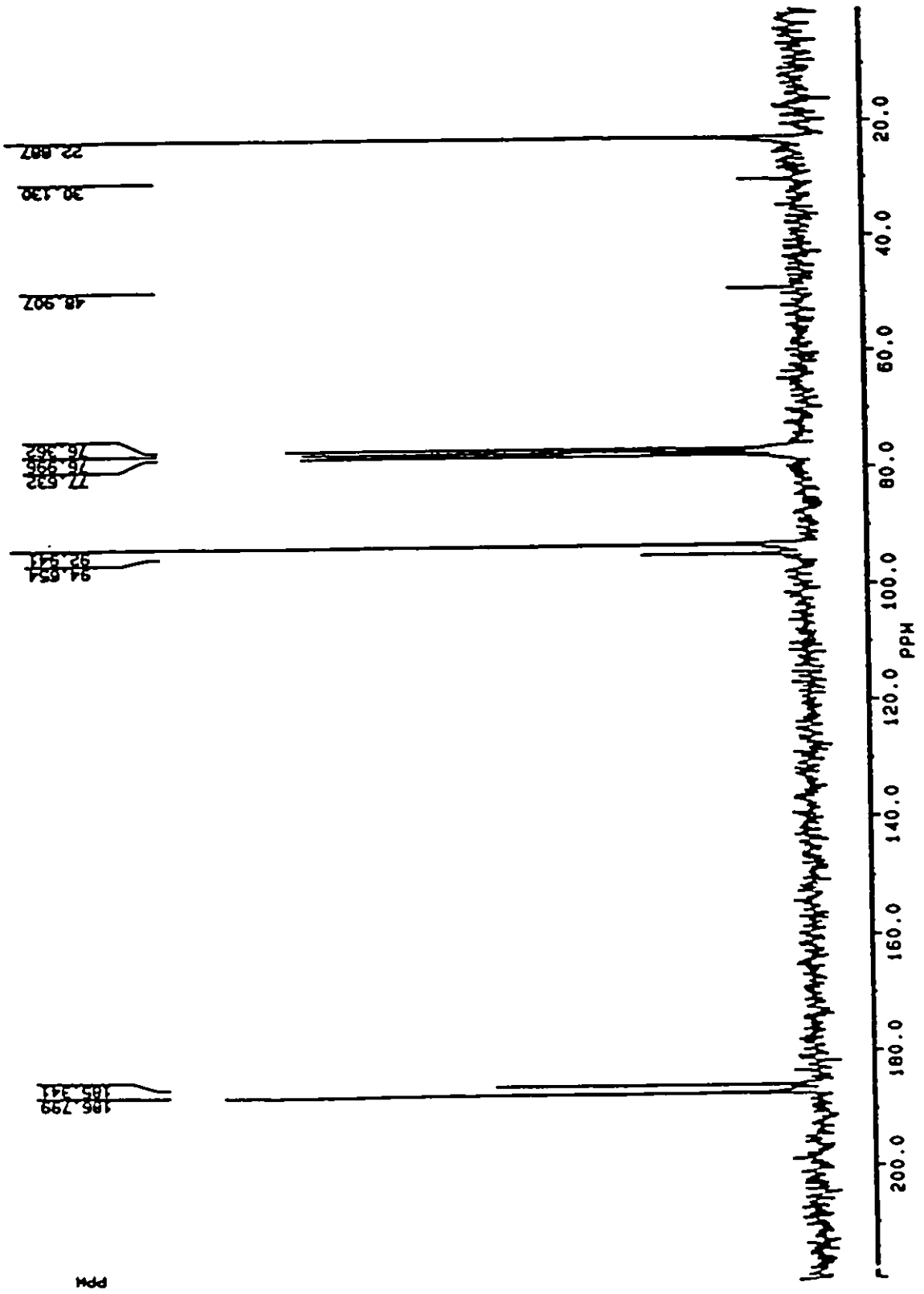

Figure 12: The ^{13}C NMR spectrum of trichloroacetylacetone, 23.

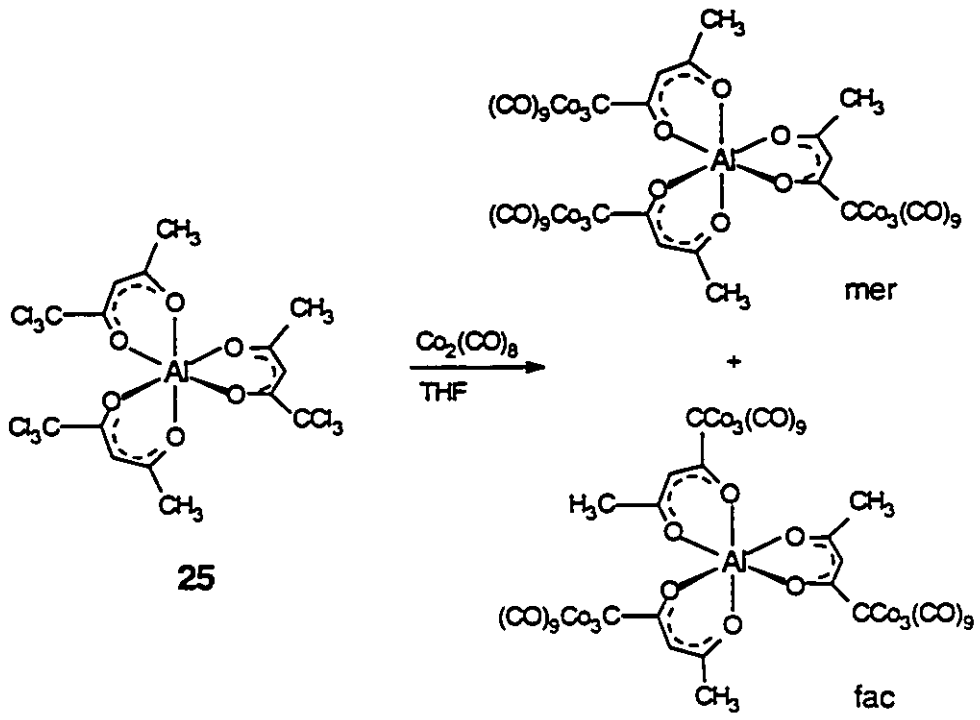

Scheme 18: The preparation of Al[Co_3(CO)$_9$CC(O)CHC(O)CH_3]$_3$, 26.

Interestingly, analogous treatment of Cu(tcac)$_2$, **27**, yields after chromatographic separation of the products, the Co(II) and Co(III) complexes **28** and **29**, respectively (Scheme 19). Evidently, the central cobalt atoms must derive from $Co_2(CO)_8$; this observation is reminiscent of Schore's synthesis of $Co_4O[O_2C\text{-}CCo_3(CO)_9]_6$, **8**, whereby the Co(II) centers arise from decomposition of the original cobalt cluster.

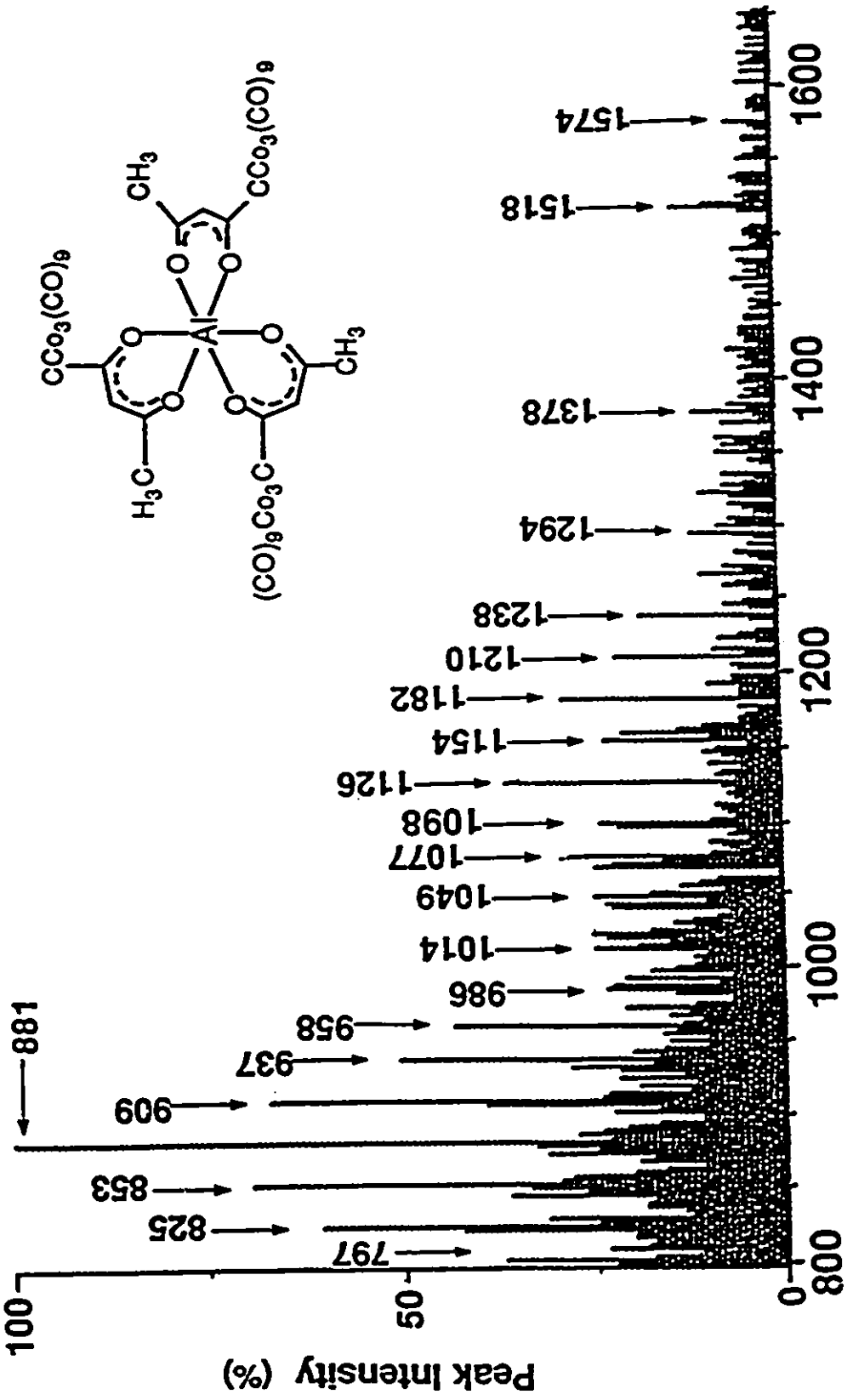

Figure 13: [FAB]+ mass spectrum of $Al[Co_3(CO)_9CC(O)CHC(O)CH_3]_3$, 26.

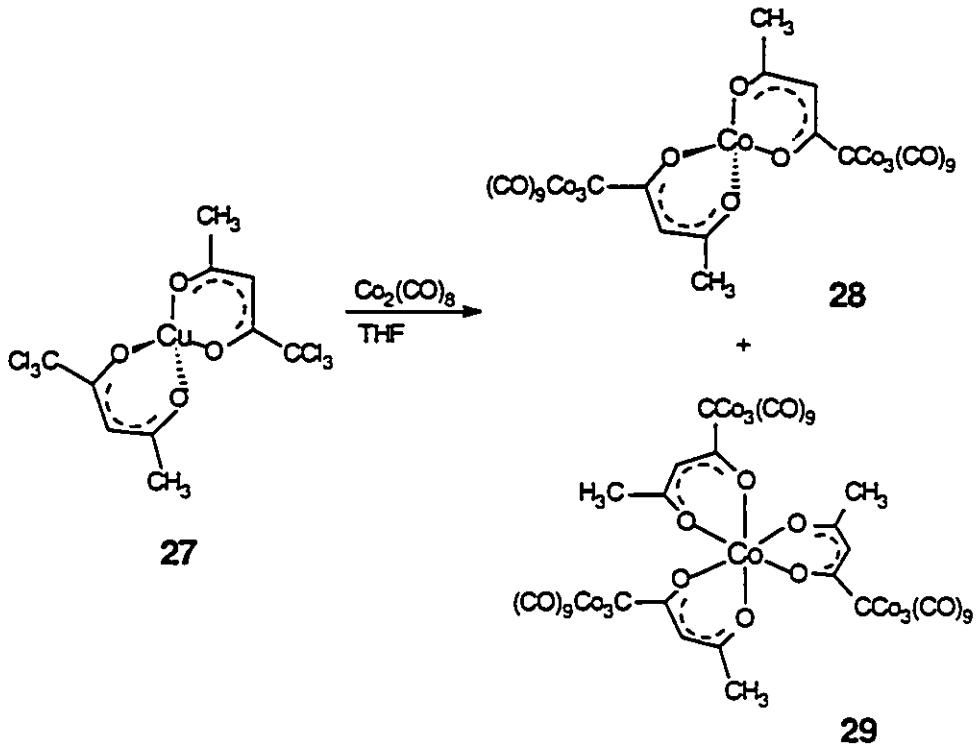

Scheme 19: Preparation of $Co[Co_3(CO)_9CC(O)CHC(O)CH_3]_n$, *where n = 2,3.*

The octahedral systems **26** and **29** derived from trivalent metals yield *mer* and *fac* isomers and, thus far, have not allowed the isolation of single crystals suitable for a diffraction study. However, in an attempt to obtain an x-ray quality crystal of **28**, repeated chromatographic purification yielded black crystals which were subsequently shown to be the parent ligand **24**.

Recrystallization of CH_3-CO-CH-C(OH)-$CCo_3(CO)_9$, **24**, from 50/50 CH_2Cl_2/hexane gave parallelepipeds suitable for an x-ray structure determination. The cluster crystallizes in the orthorhombic space group $Pna2_1$ with four molecules in the unit cell. The crystallographic collection parameters, atomic coordinates and selected bond length and angle data for **24** appear in the Appendix; a view of the molecule appears as Figure 14.

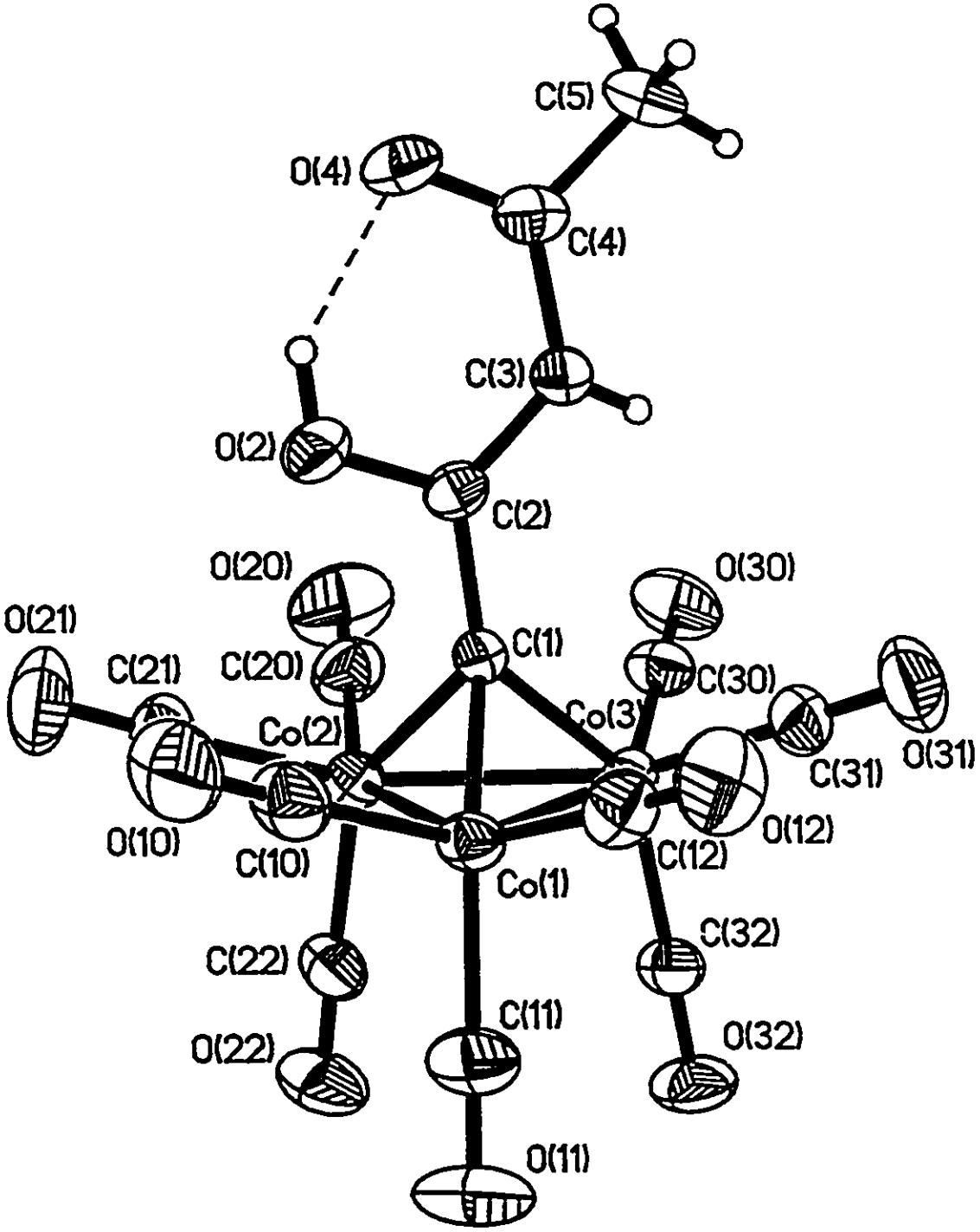

*Figure 14: The x-ray crystal structure of $CH_3C(O)$-CH=C(OH)-$CCo_3(CO)_9$, **24**.*

Each molecule has approximate C_S symmetry with the two oxygens of the acac-type unit oriented so as to lie over the midpoint of a cobalt-cobalt vector. The tetrahedral Co_3C core exhibits typical bond lengths: Co-Co (2.47 Å), Co-CO (1.81 Å) and Co-C_{cap} (1.90 Å). In the solid state, the molecule exists in the enol form $CH_3C(O)$-CH=C(OH)-$CCo_3(CO)_9$, rather than as the keto tautomer. The hydroxyl moiety is at the cluster end of the five-carbon chain and the OH proton is hydrogen-bonded to the ketonic oxygen neighboring the methyl carbon. This tautomeric structure is evident from the C(2)-C(3), C(2)-O(2), C(3)-C(4) and C(4)-O(4) distances of 1.389(8), 1.320(7), 1.408(8) and 1.262(8) Å, respectively. In this structure, the C-O distances are significantly different; moreover, the enolic hydrogen can be seen in the final difference map.

One other organometallic acac-type derivative has been structurally characterized: the x-ray crystal structure of the ferrocenyl complex **30** has recently been reported, and the molecule was shown to adopt the tautomeric form in which the site of enolization is remote from the electron-donating ferrocenyl moiety [61]. Analogously, in the thiophene derivative, **31**, the enol-H is bonded to the oxygen adjacent to the electron-withdrawing CF_3 group [51].

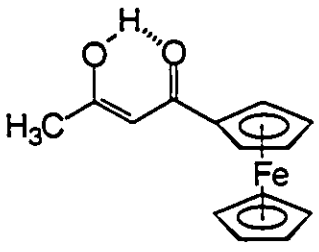

30

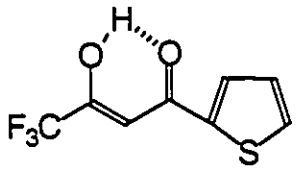

31

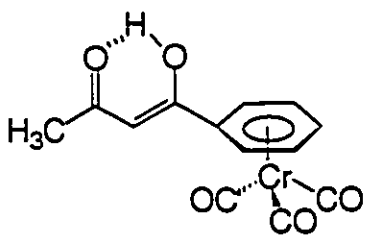

32

In an attempt to rationalize the favored site of enolization found in the cobalt cluster **24**, molecular orbital calculations at the extended Hückel level were carried out. The crystallographically observed tautomer, in which the enol is adjacent to the cluster, is favored by ≈ 3.4 kcal/mol relative to the case when the OH is sited at C(4), as in CH_3-C(OH)=CH-C(O)-$CCo_3(CO)_9$. Figure 15 depicts the changes in the HOMO of **24** as the enol-H migrates from O(2) to O(4) and the C(2)-C(3) and C(3)-C(4) distances are modified accordingly. Initially (Figure 15a), there is an in-plane π^* interaction between C(2) and O(2) which is augmented as the migration proceeds (Figure 15b); that is, the system is somewhat destabilized. However, this rather simplistic approach does not account for the observed tautomer of the ferrocenyl-acac complex **30**, and it may be that a higher level of theory is needed to rationalize the behavior of such systems.

The cobalt cluster **24** can also be compared to (benzoylacetone)$Cr(CO)_3$, **32**. It has been noted previously [62] that replacement of a methyl group in acacH by an (η^6-phenyl)$Cr(CO)_3$ substituent, as in **32**, leads predominantly to an enol tautomer of unknown structure. To resolve this dichotomy, an x-ray quality crystalline sample of **32** was prepared and its structure determined. (Benzoylacetone)$Cr(CO)_3$, **32**, crystallizes in the tetragonal space group $P4_32_12$ with eight molecules in the unit cell. The crystallographic collection parameters, atomic coordinates and selected bond length and angle data for **32** appear in the Appendix; a view of the molecule appears as Figure 16.

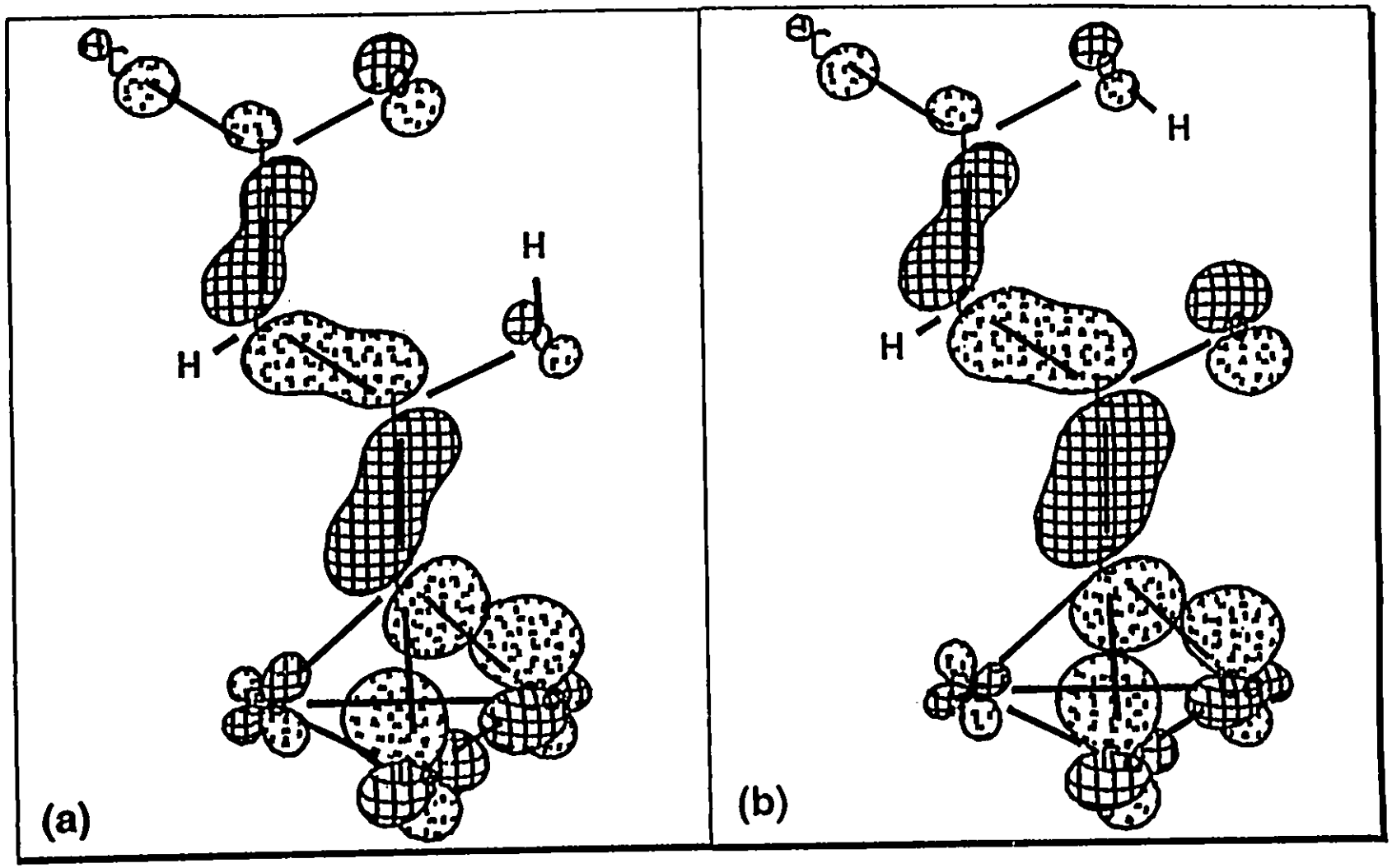

*Figure15: The HOMO of $CH_3C(O)$-CH=C(OH)-$CCo_3(CO)_9$, **24**, as the enol H migrates from (a) O2 to (b) O4.*

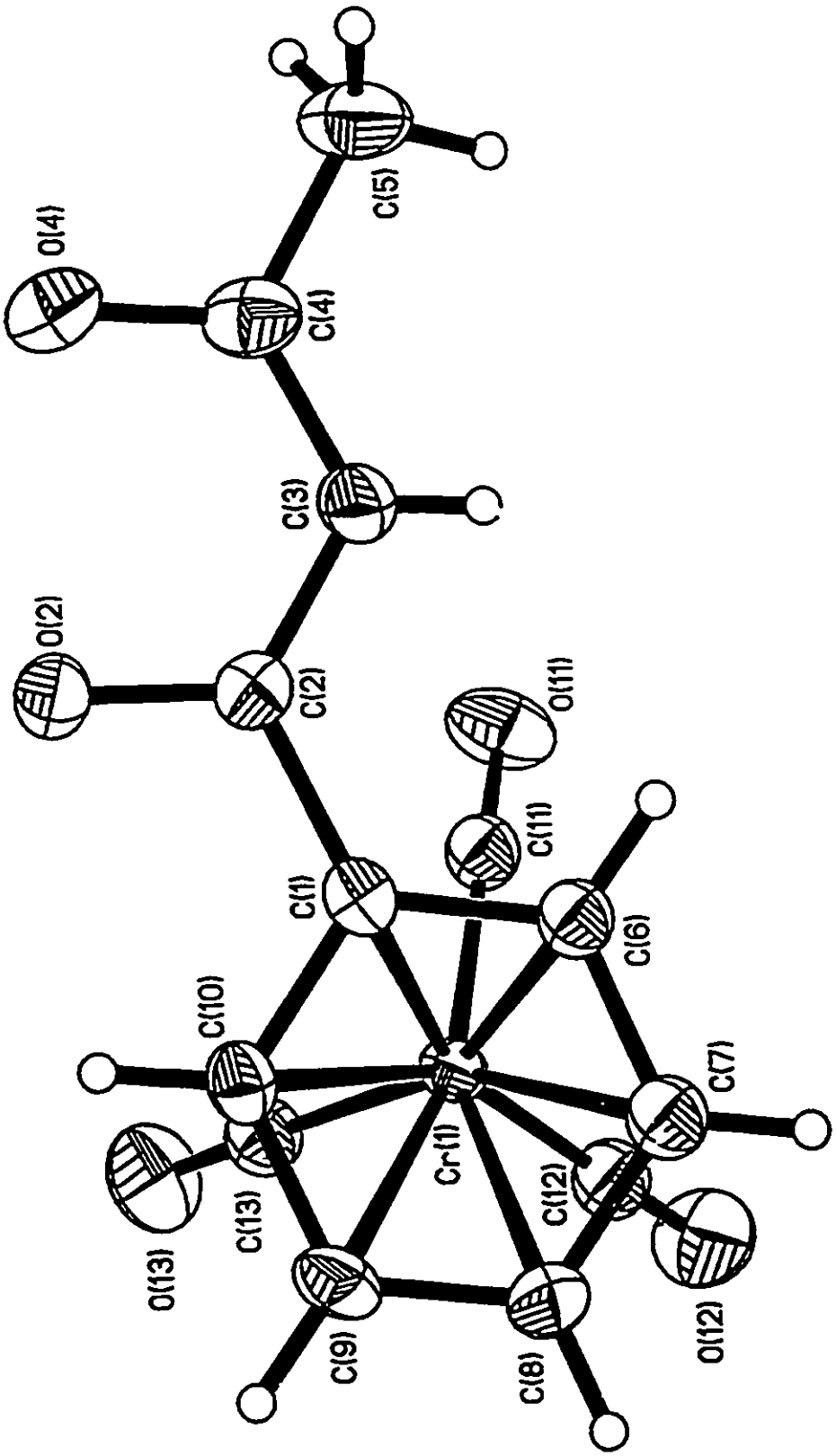

Figure 16: X-ray crystal structure of (benzoylacetone)Cr(CO)$_3$, 32.

The acac and phenyl rings are essentially coplanar and the $Cr(CO)_3$ tripod adopts an almost staggered orientation with respect to the phenyl carbons. Although the acac portion of the molecule is clearly an enol, and the C(3) carbon is sp^2-hybridized, the C(2)-O(2) and C(4)-O(4) distances, 1.288(4) Å and 1.285(5) Å, are not significantly different. Likewise, the C(2)-C(3) and C(3)-C(4) distances, 1.390(5) Å and 1.392(5) Å, are essentially the same, perhaps indicating that the enolic H is symmetrically bonded to both oxygens. In accord with the x-ray data, the ^{13}C CPMAS spectrum of **32** exhibits peaks only for the enol tautomer.

3.2 Future Work

It has been demonstrated that coordination of the 1,1,1-trichloro-acetylacetonate ligand to a variety of metal centers facilitates the construction of a range of oligo-cluster systems. The ligand, $CH_3C(O)$-CH=$C(OH)$-$CCo_3(CO)_9$, **24**, has been isolated, however an effective route for its preparation needs to be developed. One possibility is the protection of the hydroxyl moiety in trichloroacetylacetone, **23**, by a silyl enol ether. The trichloromethyl group might then be free to convert to the tetrahedral cluster upon treatment with $Co_2(CO)_8$. This organometallic ligand could subsequently be bonded to a wide variety of metal cations. Coordination of other organometallic acac-type ligands to metal centers can also be examined. The ferrocenyl derivative, **30**, and the (benzoylacetone)$Cr(CO)_3$ complex, **32**, both of which are easily prepared, may be coordinated to various di- and trivalent metal ions. The use of these organometallic ligands could facilitate the preparation of a whole range of novel inorganometallic clusters.

CHAPTER FOUR

INTRODUCTION TO STERICALLY DEMANDING ORGANIC LIGANDS

4.1 Chemical Exchange

Molecules are in constant motion, for example, interconverting between different conformations by bond rotation, and this allows magnetic site exchange or chemical exchange. This exchange results in NMR spectra that are dependent on the rate of this dynamic process. The rate must be compared to the "NMR time scale" which generally refers to lifetimes of the order of 1s to 10^{-6}s [63]. Two extreme types of NMR behaviour can be readily distinguished. If the exchange litetime is longer than the NMR time scale, the spectrum (at lower temperatures) will be in the slow exchange regime. The slow exchange spectra will be the superposition of the spectrum of each species present (i.e. a mixture). At higher temperatures, the exchange lifetime is shorter than the NMR time scale and the fast exchange regime results. The observed spectrum in this case would appear to be the average of the two species. The temperature at which fast and slow exchange meet is the coalescence temperature, T_C. The condition for slow exchange is that the exchange rate must be slower than the difference in frequency between the two states [64].

For NMR, the frequency difference, $\Delta\nu$, is expressed in Hertz. At coalescence, the rate constant, k, for the interconversion between two equally populated sites, A and B, is defined by

$$k = 1/\tau$$

where τ, the life time of either state A or state B is defined by

$$\tau = \sqrt{2}/\pi\Delta\nu$$

The rate of interconversion between state A and state B is a function of the free energy of activation ($\Delta G^{\neq}$) where

$$k = (RT_C/Nh)\exp(-\Delta G^{\neq}/RT_C)$$

Thus, the free energy of activation, $\Delta G^{\neq}$, at the coalescence temperature, T_C, is

$$\Delta G^{\neq}/RT_C = \ln(\sqrt{2}R/\pi Nh) + \ln(T_C/\Delta\nu)$$
$$= 22.96 + \ln(T_C/\Delta\nu)$$

This equation is only valid for a mutually exchanging, equally populated, non-coupled system.

While an NMR spectrum may lie in the fast or slow exchange regime at any given temperature, fast exchange can only very rarely be achieved on the UV or IR time scales. Frequency differences between peaks are in the range of 10^{14} and 10^{12} Hz respectively for UV and IR spectra, compared to hundreds of Hz separation in the NMR experiment[64]. Since diffusion rates place a limit of 10^9 to 10^{10} s^{-1} on most reaction rates, NMR is the only technique of the three in

which both exchange regimes can be observed.

Information on the structure and dynamics of a molecule can be obtained by collecting a series of spectra over a range of temperatures. Only when the interconversion between sites is slowed can the activation energy be obtained. This technique has been used to elucidate the barriers to substituent rotation as well as organometallic tripodal rotation in many dynamic systems.

4.2 Hindered Rotations in Sterically Crowded Systems

Organometallic complexes containing sterically-demanding ligands have attracted considerable attention for several years [65]. In particular, their

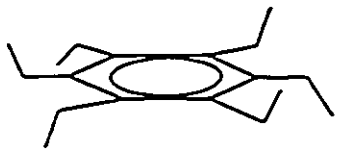

33

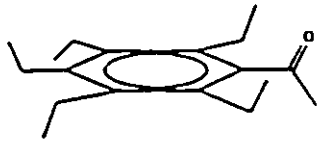

34

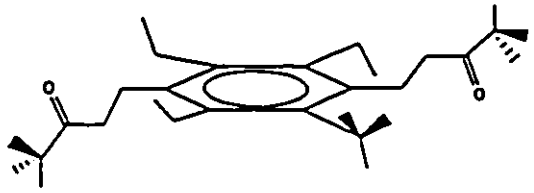

35

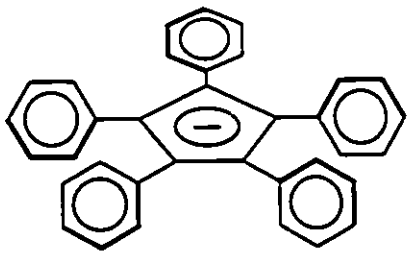

36

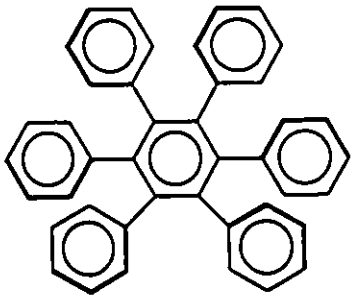

37

fluxional behavior has been studied. Examples of sterically crowded ligands include hexaethylbenzene, **33** [66], pentaethylacetophenone, **34** [67], 1,4-bis(4,4-dimethyl-3-oxopentyl)-2,3,5,6-tetraethylbenzene, **35** [68], pentaphenyl-cyclopentadienyl, **36** [69], and hexaphenylbenzene, **37** [70]. Interest lies in substituent or organometallic tripodal rotation dynamics. By bonding an organometallic fragment to the central ring, one can measure rotational barriers for substituents (e.g. ethyls or phenyls) on the central ring since they can adopt conformations in which they are *proximal* or *distal* with respect to the metal. By using a chiral organometallic fragment, one can measure rotational barriers for the tripod. In many cases, the barrier associated with tripodal rotation was found to be measurably different from that observed for the rotation of the peripheral ethyl or phenyl substituents.

Specifically, in (hexaethylbenzene)$Cr(CO)_3$, **38**, the slowed rotation of the ethyl groups at low temperature is readily detectable by NMR since the *proximal* and *distal* substituents are differentiable in their ^{13}C and ^{1}H regimes [66].

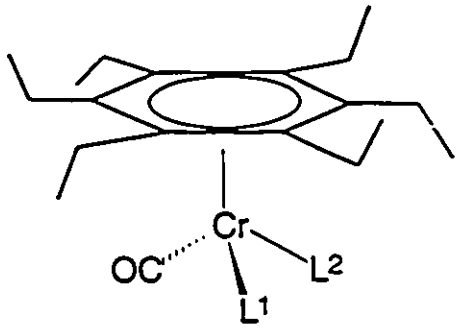

38 $L^1 = L^2 = CO$
39 $L^1 = CS$; $L^2 = NO^+$

The mechanism for the interconversion of *proximal* and *distal* ethyl groups, for which $\Delta G^{\neq}$ = 11.5 kcal/mol, equilibrates not only the two arene ring carbon environments, but also the two methylene and two methyl peaks.

In the solid state, the complex **38** adopts the alternating *proximal* and *distal* arrangement of ethyl groups [71]. Moreover, the organometallic tripod is oriented such that the metal carbonyl ligands lie beneath the *distal* ethyls so as to minimize steric interactions with the *proximal* alkyl groups.

A different approach is required to determine whether the $Cr(CO)_3$ tripod has slowed on the NMR time-scale. The molecule has effective C_{3v} symmetry whether the tripod spins or not; thus it is necessary to break the symmetry as in the chiral molecule $[(C_6Et_6)Cr(CO)(CS)(NO)]^+$, **39**. The observed slowed rotation, for which $\Delta G^{\neq}$ = 9.5 kcal/mol, results in six different ring carbons (and also six CH_3 and six CH_2 environments) at low temperature [66a]. Thus the chiral tripod renders all 18 carbons in the hexaethylbenzene ligand nonequivalent. The large difference in activation energies between the ethyl rotation and tripodal rotation indicates that the two processes in the system are not correlated. Fluxional processes in organometallic systems such as **39** are often hidden and can therefore only be detected when the molecular symmetry is broken.

Chirality can arise in various forms in organometallic systems. Metallocenic chirality can be brought about by the clockwise or counterclockwise arrangement of substituents on a central ring. One example is the pentaisopropylcobalticenium cation, **40**, reported by Astruc *et al.* [72] The diastereotopic methyls of the isopropyl groups are equilibrated via rotations of the five substituents. This process, for which $\Delta G^{\neq}$ = 17 kcal/mol, interconverts

the enantiomers of **40**.

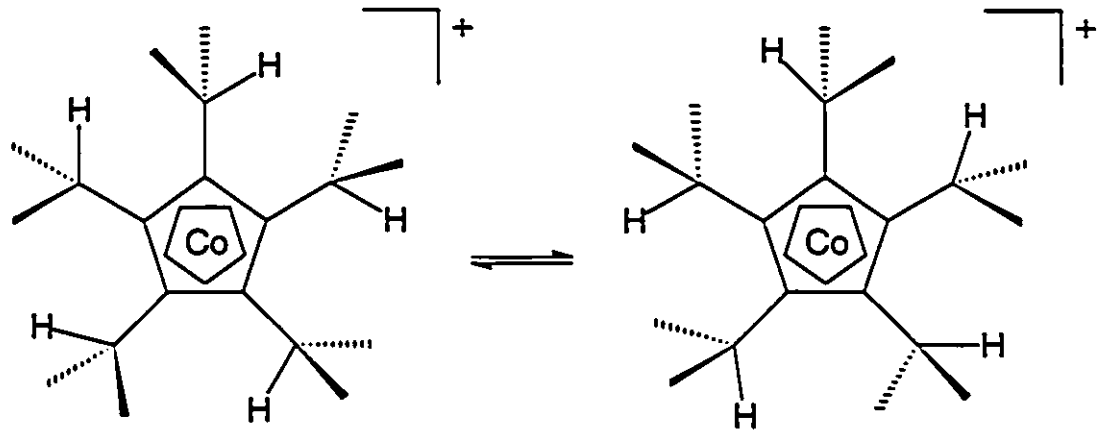

40

Such chirality is also found in polyaryl metal complexes since the phenyl rings can be canted in a clockwise or counterclockwise manner. In fact, the dynamics of rotation of the aryl rings have been studied in both organic and organometallic complexes. Mislow *et al.* have elucidated the mechanics of hindered rotations in many polyaryl systems [73]. These studies included triaryl systems such as Ar_3CH, Ar_3N, Ar_3P, Ar_3B, and Ar_3C^+. The incorporation of bulky substituents in the *ortho* or *meta* positions resulted in slowed aryl rotations. For instance, when the aryl rings of triarylsilanes Ar_3SiX possess *o*-methyl groups, the rotations of the phenyls may be slowed on the NMR time scale [74]. The $\Delta G^{\neq}$ values for enantiomerization, when X = H, or Cl, lie in the range of 11 - 12 kcal/mol. It has been shown that motions of these aryl rings are coupled in such a way that no ring moves independently of the others; such processes are called *correlated rotations*.

The π-bonding of $Cr(CO)_3$ groups to the triaryl systems has also been

studied in an attempt to raise the phenyl rotation barriers into the NMR-detectable range. In contrast to Mislow's studies where he effectively "paints the edges differently", π-bonding of an organometallic fragment "paints the faces differently". The $(Ph_3SiOH)[Cr(CO)_3]_3$ molecule, **41**, unlike the *o*-substituted triarylsilanes, exhibits unrestricted rotation of the phenyl rings. In contrast, slowed phenyl ring rotation is observed for $(Ph_3COH)[Cr(CO)_3]$, **42**. Their x-ray crystal structures show that the phenyls are arranged in a propellor-type fashion [75]. For **41**, as shown in Figure 17, the dihedral angles, θ, O-Si-C_{ipso}-C_o, are 39.8° for all three complexed rings. The dihedral angles, θ, in **42** are 32, 36, and 65° for the complexed and the two noncomplexed rings respectively.

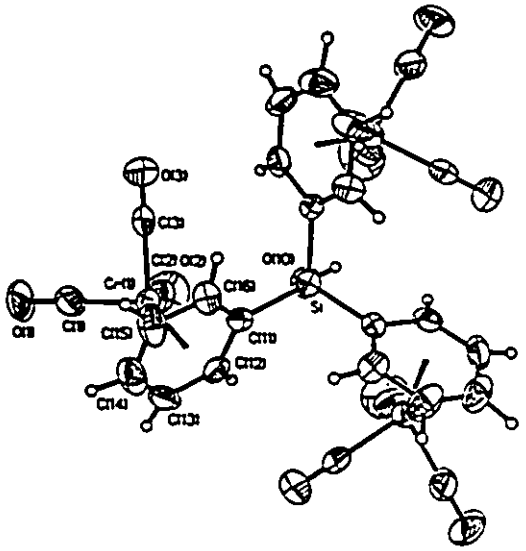

*Figure 17: X-ray crystal structure of $(Ph_3SiOH)[Cr(CO)_3]_3$, **41**.*

Multiple fluxional processes can arise when a pentaphenylcyclo-pentadienyl ligand is bonded to a chiral tripod. The x-ray crystal structure of the $(C_5Ph_5)Fe(CO)(PMe_3)(HC{=}O)$ complex, **43**, reported by Li *et al.*, shows that the phenyls adopt a paddle-wheel orientation and are tilted an average of 50.1°

relative to the plane of the five-membered ring [69] (Figure 18).

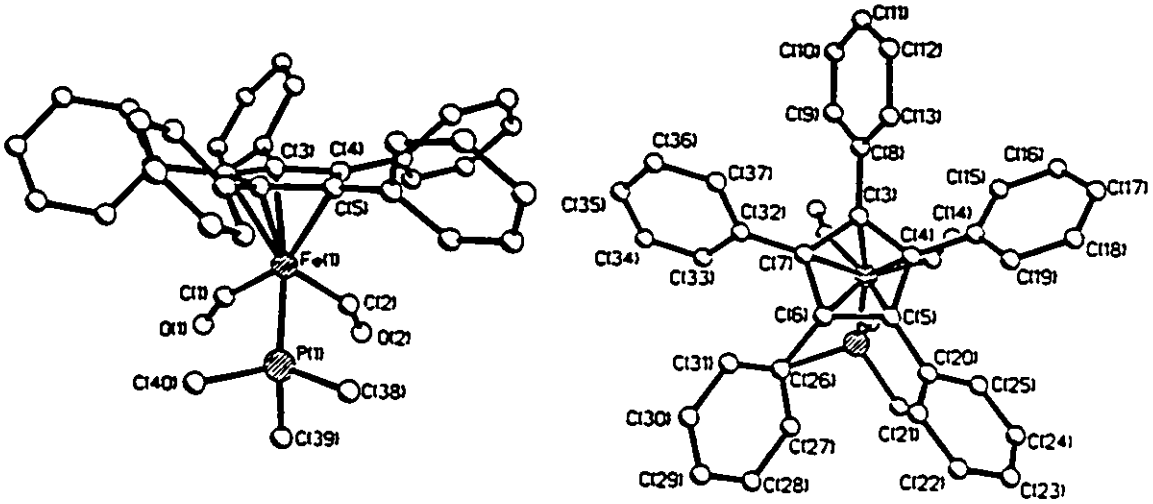

*Figure 18: X-ray crystal structure of $(C_5Ph_5)Fe(CO)(PMe_3)(HC{=}O)$, **43**, (a) sideview (b) topview.*

These peripheral phenyls adopt a compromise between the sterically favored orthogonal orientation, $\theta = 90°$, and the completely coplanar arrangement, $\theta = 0°$, which would maximize π-overlap but lead to severe steric strain. This phenomenon confers a chiral array on the pentaphenylcyclopentadienyl ligand.

The variable-temperature NMR spectra of a similar complex, $(C_5Ph_5)Fe(CO)(PMe_2Ph)C(O)Et$, **44**, reveal two fluxional processes. The chiral tripod together with the clockwise or counterclockwise canting of the peripheral phenyl rings of the C_5Ph_5 ligand yields a diastereomeric mixture (65/35 ratio at 300 K). It is apparent from Figure 19 that slowed rotation of the chiral tripod can occur on the NMR time scale, causing the room temperature ^{13}C singlet of the cyclopentadienyl ring to be split into five peaks (two of which overlap) at 173 K. The barrier to rotation is 8.7 kcal/mol.

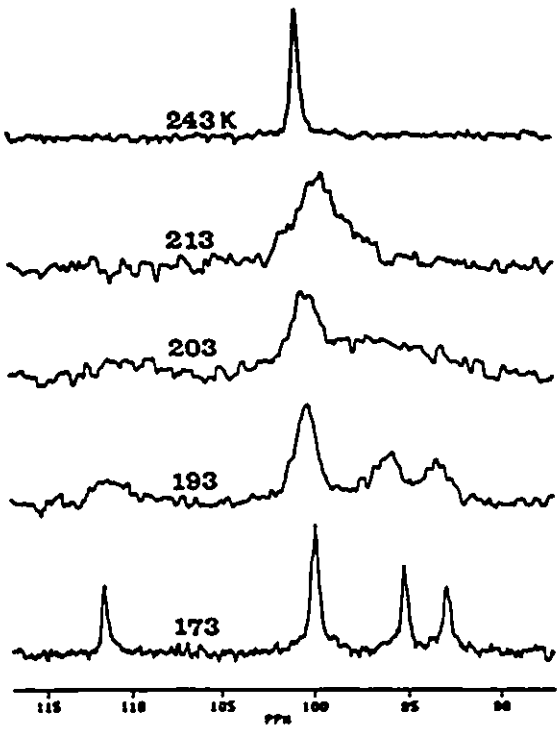

Figure 19: Variable temperature 125.7 MHz ^{13}C NMR spectra of $(C_5Ph_5)Fe(CO)(PMe_2Ph)C(O)Et$, 44.

Placement of the organometallic tripod on one face of the C_5 ring also allows detection of slowed phenyl rotation since each aryl ring would have a *proximal* or *distal* edge with respect to the metal. Since the ^1H and ^{13}C NMR resonances of the peripheral phenyl rings in **44** are very severely overlapped at low temperatures, the CH_3 groups in the Me_2PPh ligand can be used as probes. The acquired activation barrier of 11.7 kcal/mol is significantly different from the 8.7 kcal/mol for the tripodal rotation, thus the two processes in the system are not correlated.

Other sterically crowded ligands of the type C_nAr_n have also been investigated [76,77]. The more sterically demanding hexaphenylbenzene, **37**, molecule has been crystallographically characterized and it has been shown that the peripheral phenyl rings are canted 67° relative to the central six membered

ring [78]. In solution, one could envisage all six peripheral rings turning in a concerted manner so as to interchange the ring edges with respect to one face of the central arene. To evaluate the barriers to peripheral ring rotation, Gust *et al.* labelled one or more phenyls with *ortho* or *meta* substituents [76]. His studies concluded that interconversions, in fact, occur via mechanisms involving uncorrelated rotations of the aryl rings and that the incorporation of an *ortho* methyl or methoxy group brings about an activation energy of 33 kcal/mol while a *meta* substituted system has a barrier of 17 kcal/mol.

In order to study π-bonded addenda on polyphenylarenes, the $Cr(CO)_3$ complex of the hexaphenylbenzene, **45**, was prepared [70]. The metal is π-bonded to one of the peripheral rings. At -80 °C, the complexed phenyl exhibits slowed rotation on the NMR time-scale and is effectively orthogonal to the central six membered ring. The fluxional process involves rotation of the chromium-bonded phenyl ring. The barrier to rotation is 12.2 kcal/mol, a value much lower than those reported for non-complexed hexa-aryl benzenes bearing *ortho* or *meta* substituents.

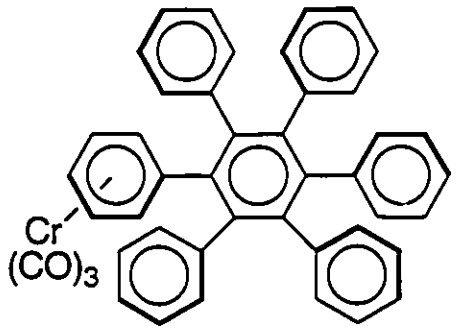

45

4.3 Statement of the Problem

The investigation of sterically demanding ligands of the C_nAr_n type can be taken one step further. The heptaphenylcycloheptatrienylium or heptaphenyltropylium cation, $C_7Ph_7^+$, **46**, although previously reported, has not been found in organometallic complexes [79,80]. One can view these polyaryl complexes in terms of the angle, ω, subtended by adjacent phenyls at the center of the internal ring: in $C_5Ph_5^-$, ω= 72°, in C_6Ph_6, ω = 60°, and in $C_7Ph_7^+$, ω = 51.4°. While it is true that increasing the ring size lengthens the radial distance of the external phenyls from the center of the molecule, this is more than compensated for by the diminishing value of ω. The increased steric strain in a C_7Ph_7 system may "freeze-out" the entire molecule, leading to interesting dynamic studies. For example, the spinning of the organometallic moiety about the C_7 axis and the rotation of the peripheral phenyls might be correlated, as in the molecular bevel gears discussed by Iwamura and Mislow [81,82]. Therefore, a study of potential routes to organometallic complexes of the type $(C_7Ph_7)ML_n$ was undertaken.

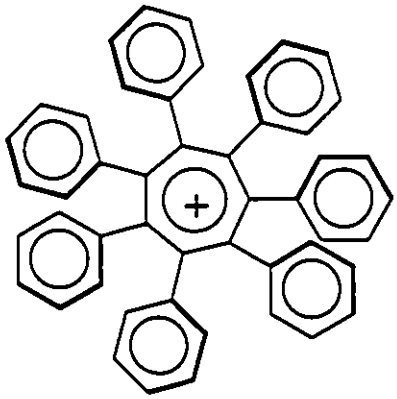

46

CHAPTER FIVE

THE HEPTAPHENYLCYCLOHEPTATRIENE, C_7Ph_7H, LIGAND

5.1 Introduction

Heptaphenylcycloheptatriene, C_7Ph_7H, **47**, was originally synthesized by Battiste in 1961 [83], and the $C_7Ph_7^+$, **46**, and $C_7Ph_7^-$, **48**, ions and also the $C_7Ph_7^\bullet$, **49**, radical have since been reported [79,80]. However, there are no structural or molecular dynamics studies on these systems; moreover, despite the elegant work of a number of groups on $(C_7H_7)ML_n$ derivatives [84], there are no reports of organometallic complexes containing the C_7Ph_7 unit. This chapter will describe the dynamic behavior and structure of heptaphenylcycloheptatriene.

5.2 Dynamic Behaviour and Structure of Heptaphenylcycloheptatriene

Heptaphenylcycloheptatriene, **47**, is conveniently synthesized by the Diels-Alder addition of tetraphenylcyclopentadienone (commonly known as tetracyclone) and 1,2,3-triphenylcyclopropene to give the tricyclic ketone, **50**. The reaction is normally carried out at elevated temperatures and loss of CO yields C_7Ph_7H directly [83]; however, if the Diels-Alder addition is performed at room temperature, the intermediate ketone, **50**, can be isolated.

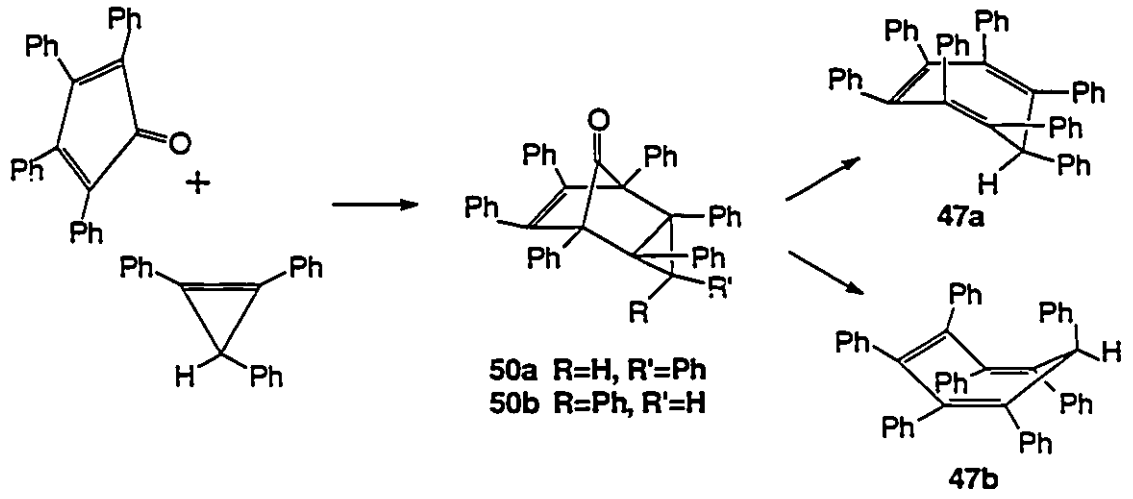

The 500 MHz ^{1}H and 125 MHz ^{13}C NMR spectra of C_7Ph_7H can be completely assigned by means of ^{1}H-^{1}H COSY and ^{1}H-^{13}C shift-correlated experiments, together with selected nOe measurements. The labelling scheme of C_7Ph_7H, **47**, is shown in Figure 20. The ^{1}H-^{1}H COSY and ^{1}H-^{13}C shift-correlated spectra for **47** are shown in Figures 21 and 22, respectively, while the NMR data are collected in Table 3.

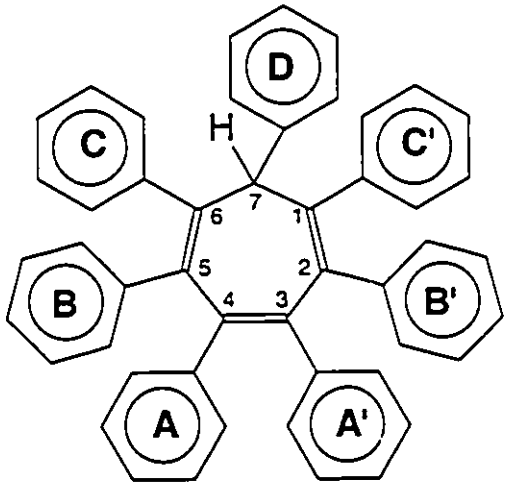

Figure 20: Labelling scheme for C_7Ph_7H, 47.

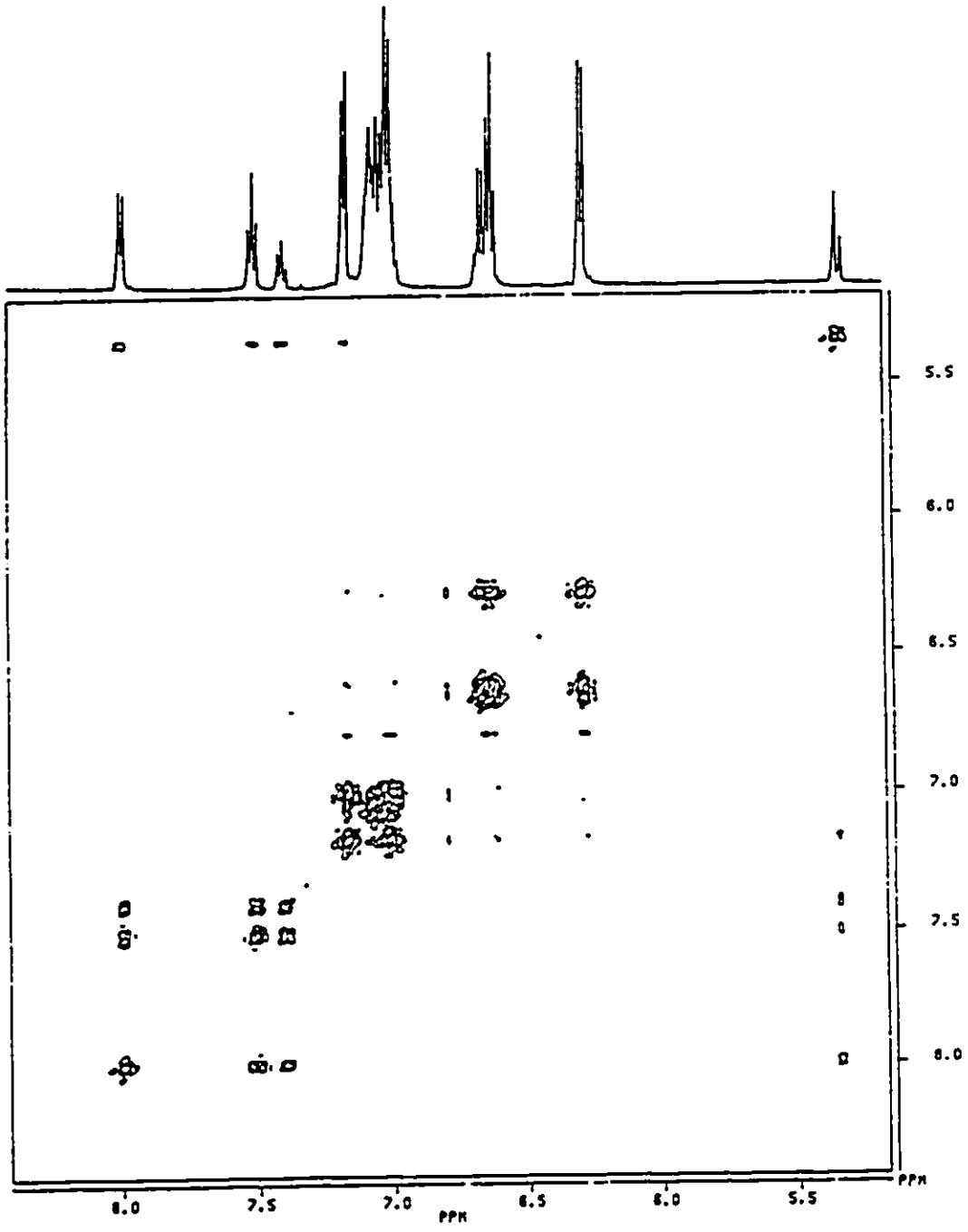

Figure 21: ^{1}H-^{1}H COSY spectrum of C_7Ph_7H, 47.

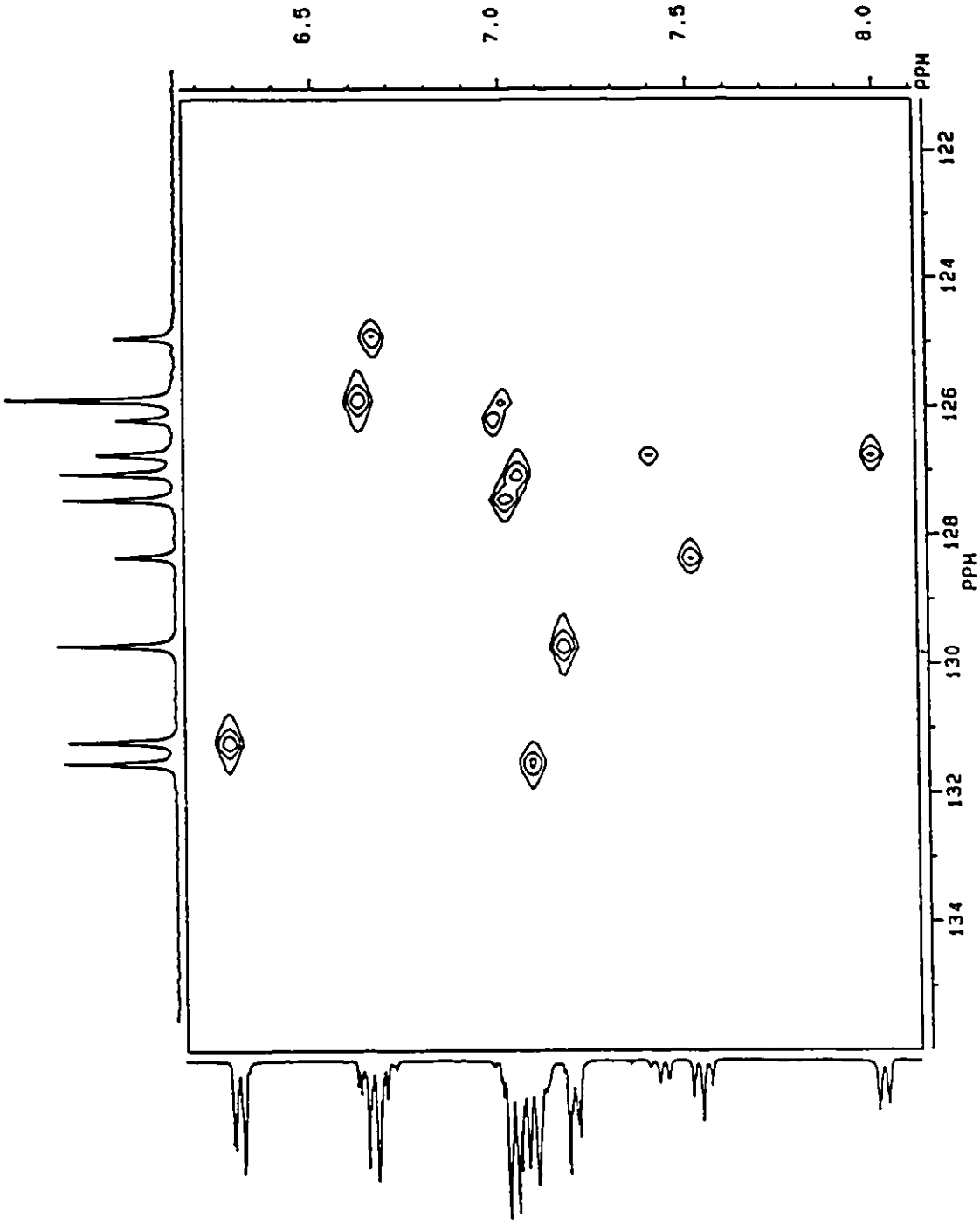

Figure 22: ^{1}H-^{13}C shift-correlated spectrum of C_7Ph_7H, 47.

Table 3: ^{1}H and ^{13}C NMR data for C_7Ph_7H, 47, and $C_7Ph_5Me_2H$, 51.

	PHENYL A/A'		PHENYL B/B'		PHENYL C/C'		PHENYL D		OTHER	
C_7Ph_7H, 47[a]	^{1}H, δ	^{13}C, δ	^{1}H, δ	^{13}C, δ	^{1}H, δ	^{13}C, δ	^{1}H, δ	^{13}C, δ	^{1}H, δ	^{13}C, δ
ortho	6.29 (4H) d of d, 8.2, 1.5 Hz	130.71	7.09 (4H, m)[b]	131.04	7.18 (4H) d of d, 8.1, 1.4 Hz	129.22	8.00 (2H) d of t, 8.3, 1.2 Hz	126.26		
meta	6.63 (4H, m)	125.39	7.08 (4H, m)[c]	126.55	7.03 (4H, m)	126.95	7.51 (2H) d of d, 8.3, 7.5 Hz	127.84		
para	6.67 (2H, m)	124.44	7.03 (2H, m)	125.39	7.03 (2H, m)	125.71	7.40 (1H) t of q, 7.5, 1.2 Hz	126.26		
ipso carbon		140.00		140.24		143.10		142.53		
ring carbon		142.75		136.35		138.72		57.17		
sp^3 H									5.35 (1H, s)	57.17
$C_7Ph_5Me_2H$, 51[d]										
ortho	6.51 (2H, b)	130.27	B 7.07 (2H, m) B' 7.23 (2H, m)	B 130.71 B' 131.62	7.17 (2H, m)	130.44	7.61 (2H) d of t, 8.3, 1.2 Hz	126.43		
meta	6.94 (2H, m)	127.35	B 7.17 (2H, m) B' 7.23 (2H, m)	B 127.74[e] B' 128.21[e]	7.16 (2H, m)	128.21[e]	7.34 (2H) d of d 7.5, 8.3 Hz	128.03		
para	6.91 (1H, m)	125.94	B 7.61 (1H, m) B' 7.08 (1H, m)	B 126.64[f] B' 126.19[f]	7.14 (1H, m)	126.77[f]	7.20 (1H, m)	126.43		
sp^3 H									4.84 (1H, s)	56.90
1-Me									1.87 (3H, s)	25.03
4-Me									1.20 (3H, s)	20.43

d=doublet, q=quartet, s= singlet, t=triplet, m=multiplet, b=broad

a. Spectra obtained in CD_2Cl_2 on 500 MHz NMR spectrometer; b. At -90°C, splits into two peaks at 7.5 and 6.7 ppm; c. At -90°C, splits into two peaks at 7.3 and 6.9 ppm; d. Spectra obtained in CD_2Cl_2 on 125.721 MHz NMR spectrometer; e. Peak assignments of meta carbons may be interchanged; f. Peak assignments of para carbons may be interchanged.

The phenyl protons of **47** are spread over a 2 ppm range. The protons of the unique phenyl (ring **D** in Figure 20) are markedly deshielded relative to those of the **A** rings; moreover, the nOe data reveal a clear interaction between the *ortho*-protons of the **D** and **A** rings, suggesting the structure **47b**, whereby the **D** ring is pseudo-axial and the single hydrogen substituent is sited equatorially. At room temperature, the **B** and **C** phenyl protons are heavily overlapped. However, upon cooling the sample, the doublet attributable to the *ortho*-protons of the **B** rings broadens and splits to give a pair of doublets separated by no less than 0.73 ppm; likewise, as shown in Figure 23, the *meta*-protons of the **B** rings also decoalesce to give a pair of triplets 0.44 ppm apart. At -90 °C, the *ortho*-protons of the **A** rings, and of the **C** rings, have also broadened and disappeared into the base-line. Comparable splittings are seen in the variable-temperature ^{13}C spectra of C_7Ph_7H (see Figure 24), and the barrier to rotation of the **B** rings may be evaluated as 11.0 ± 0.5 kcal mol^{-1}. This relatively high barrier tells us that these phenyls are in a very crowded environment; moreover, the large chemical shift differences observed for the protons of the **B** ring when its rotation is slow on the NMR time-scale suggest that the *ortho* protons in particular experience very different ring current effects from their neighboring phenyls.

To clarify these points, C_7Ph_7H, **47**, was structurally characterized by x-ray crystallography (see Appendix) and views of the molecule are shown in Figure 25. In the solid state, **47** possesses close to C_S symmetry such that the pseudo mirror plane contains the sp^3 carbon and bisects the double bond bearing the phenyl **A** rings. It is also evident that the unique phenyl group (the **D** ring in our notation), in accord with the NMR evidence, is axial, and also

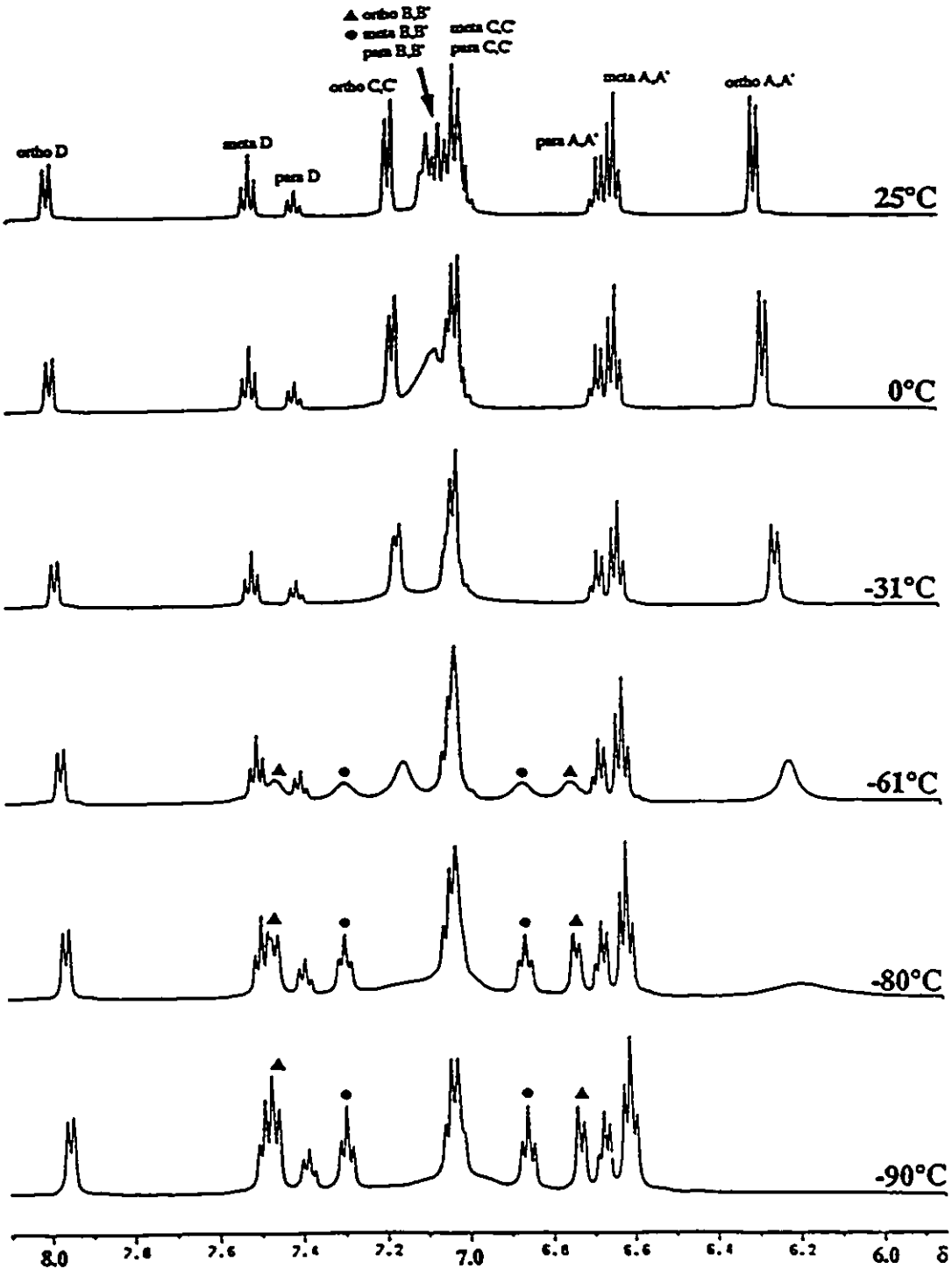

Figure 23: Variable-temperature 500 MHz ^1H NMR spectra of C_7Ph_7H, 47

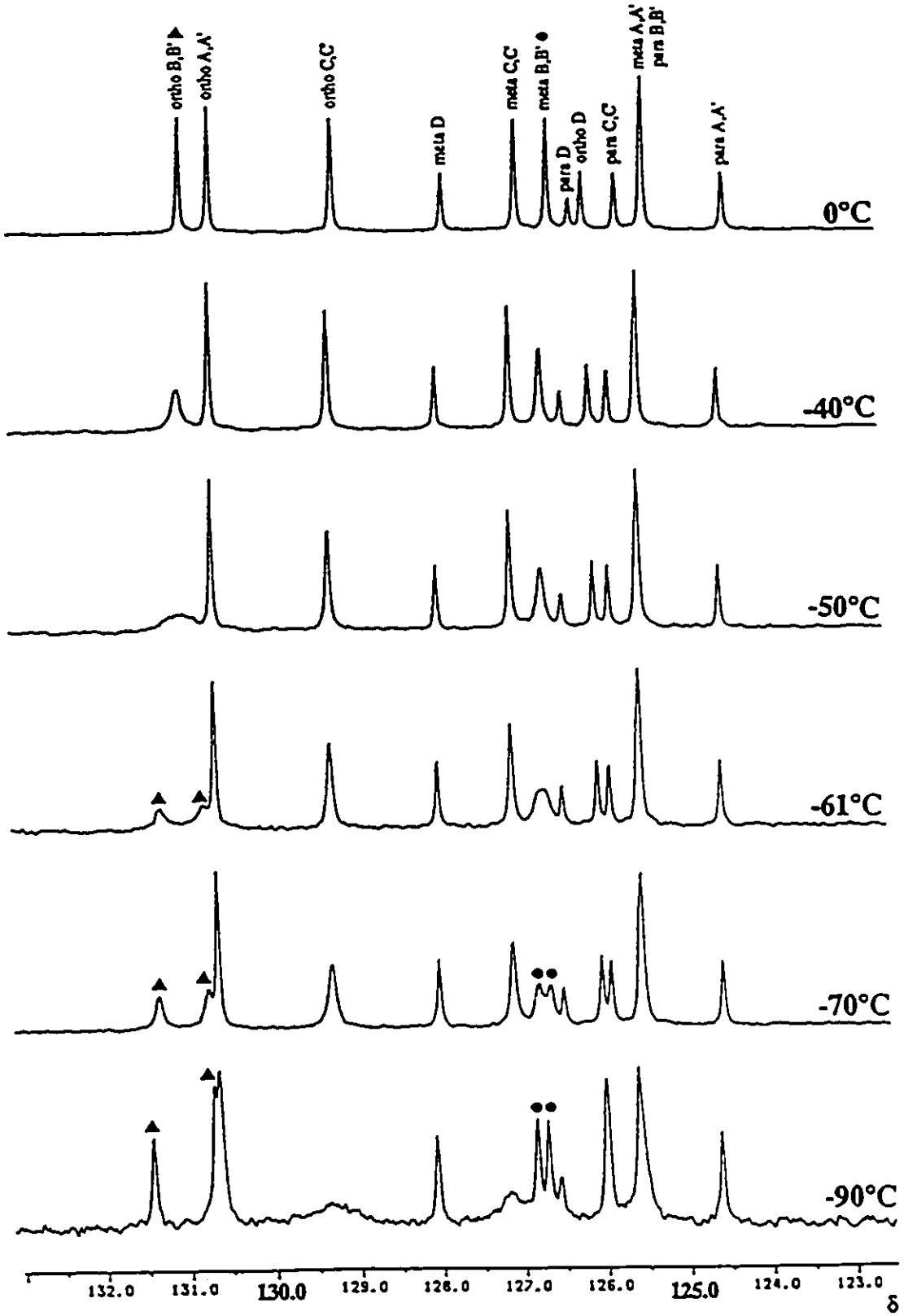

Figure 24:Variable-temperature 125 MHz ^{13}C NMR spectra of C_7Ph_7H, 47

straddles the pseudo mirror plane. As expected, the C_7 ring adopts a boat conformation such that the dihedral angles between the planes containing C(6)-C(7)-C(1) [plane 1], C(1)-C(2)-C(5)-C(6) [plane 2], and C(2)-C(3)-C(4)-C(5) [plane 3] are 125° for [plane 1]/[plane 2], and 145° for [plane 2]/[plane 3]. These may be compared with the corresponding interplanar angles in C_7H_8 which are 144° for [plane 1]/[plane 2] and 140° for [plane 2]/[plane 3] [85]. Thus, the conformation of the seven-membered boat in C_7Ph_7H is markedly different to that found in cycloheptatriene itself, especially with respect to the bending of the sp^3 carbon out of the C(1)-C(2)-C(5)-C(6) plane. In C_7H_8, this deviation from planarity is 36°, but in C_7Ph_7H it has become 55°, presumably to minimize steric interactions between the phenyl substituents.

Our major interest lies with the orientations of the peripheral phenyl rings relative to the central C_7 ring. The phenyl **A** rings are almost perpendicular to their portion of the central ring; typically, the dihedral angles C(2)-C(3)-C(31)-C(32) and C(2)-C(3)-C(31)-C(36) are 92° and 87°, respectively. The **B** rings take up an orientation of 63° ± 4°, while the **C** phenyls are twisted through 50° relative to the plane defined by C(7)-C(1)-C(2) of the central ring. The net result is to place the **B** phenyls in a very restricted locale, and this is illustrated in the space-filling model which appears as Figure 26. Furthermore, we can see from Figure 26 that the *ortho*-hydrogens of the **B** rings are in very different magnetic environments. One proton, H(22), is sandwiched between the adjacent **A** and **C** phenyls and so is unusually highly shielded; its *ortho* partner in the same **B** ring, H(26), is situated on the molecular periphery, far from any aromatic fragments whose ring currents could affect its chemical shift. Since it is clear that the x-ray structure of **47** provides a rationale for the large chemical shift separation

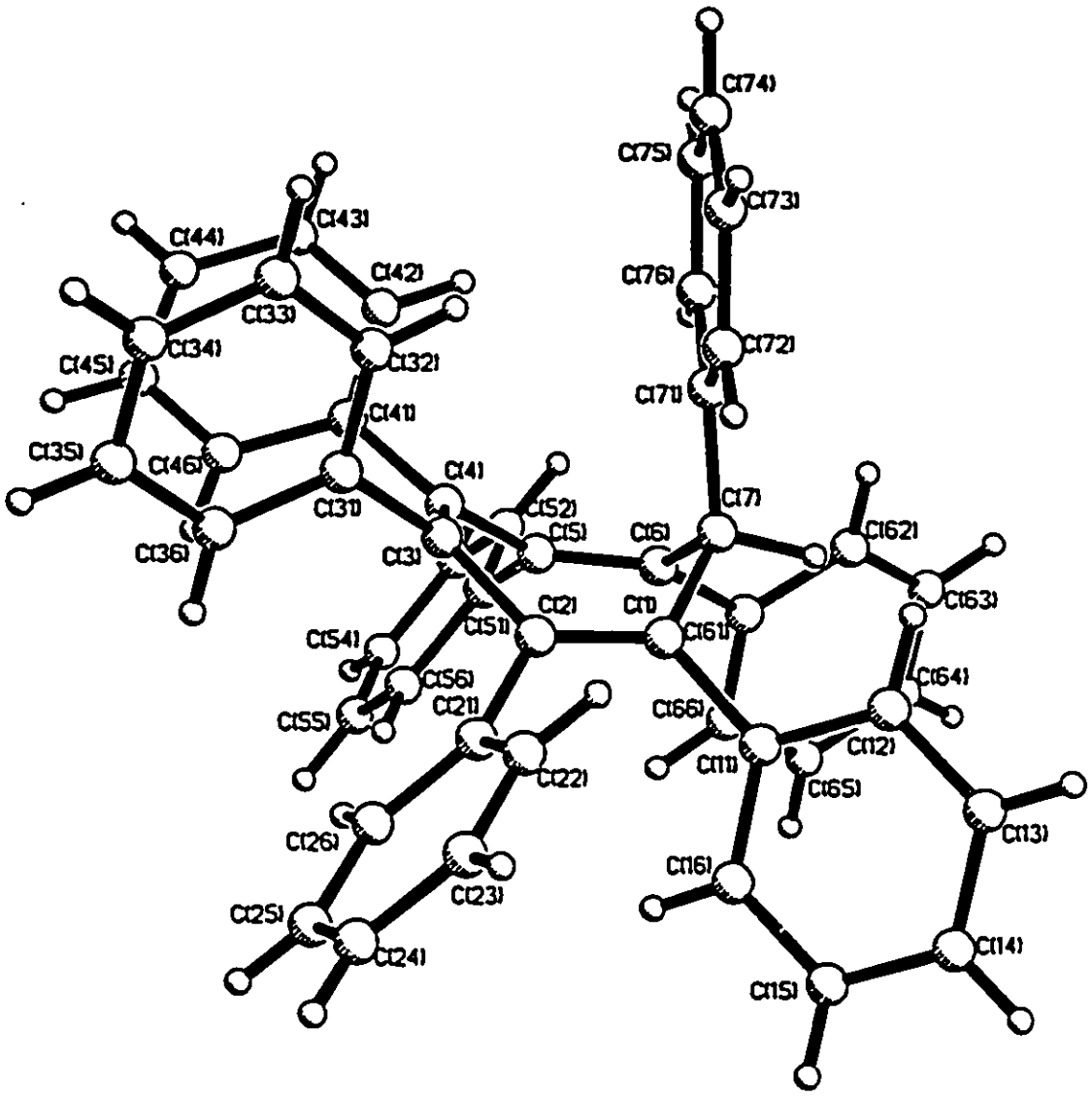

Figure 25: Molecular structure of C_7Ph_7H, 47, showing the atom numbering scheme. (a) side view.

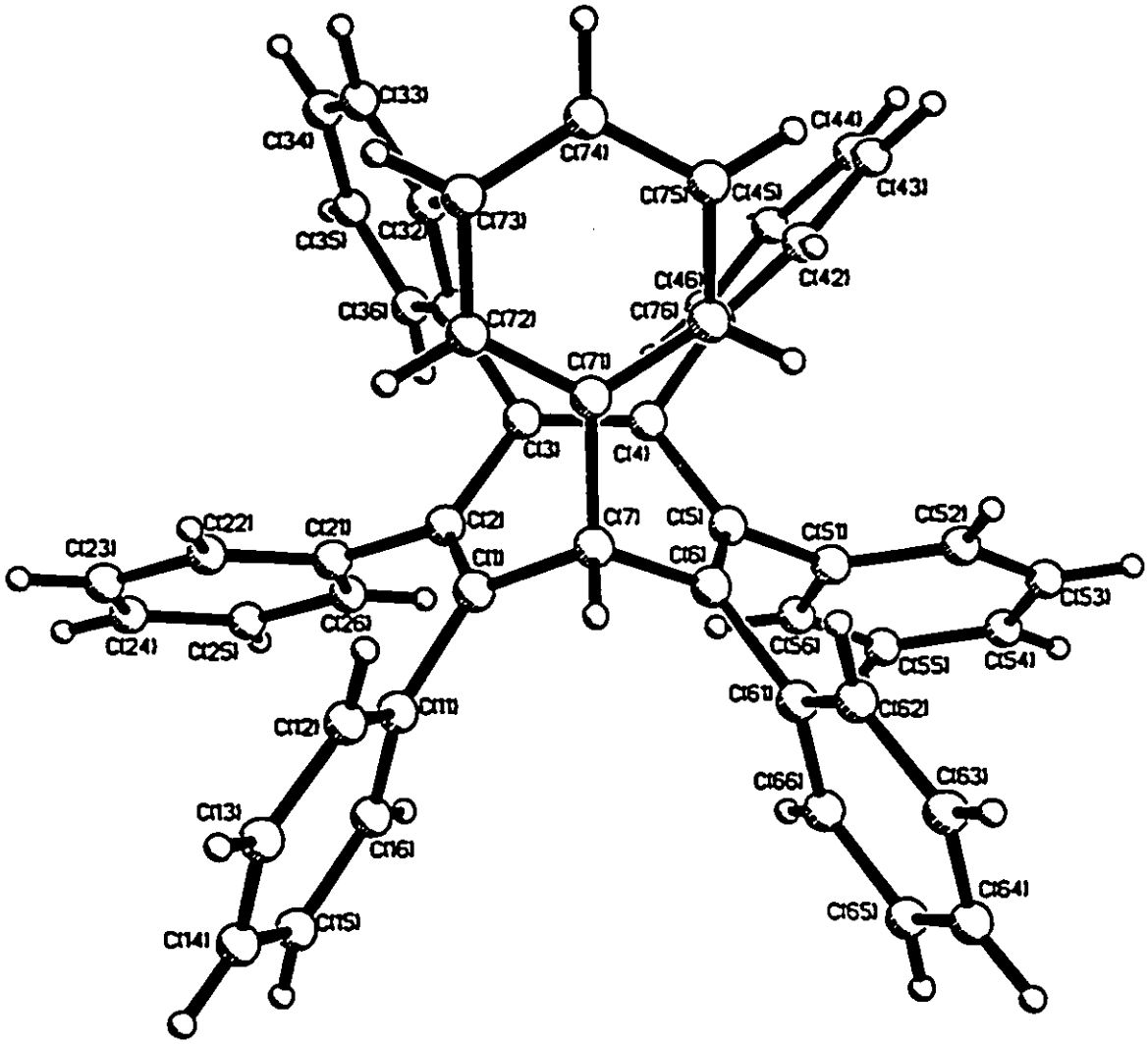

Figure 25: (b) view depicting the pseudo mirror plane

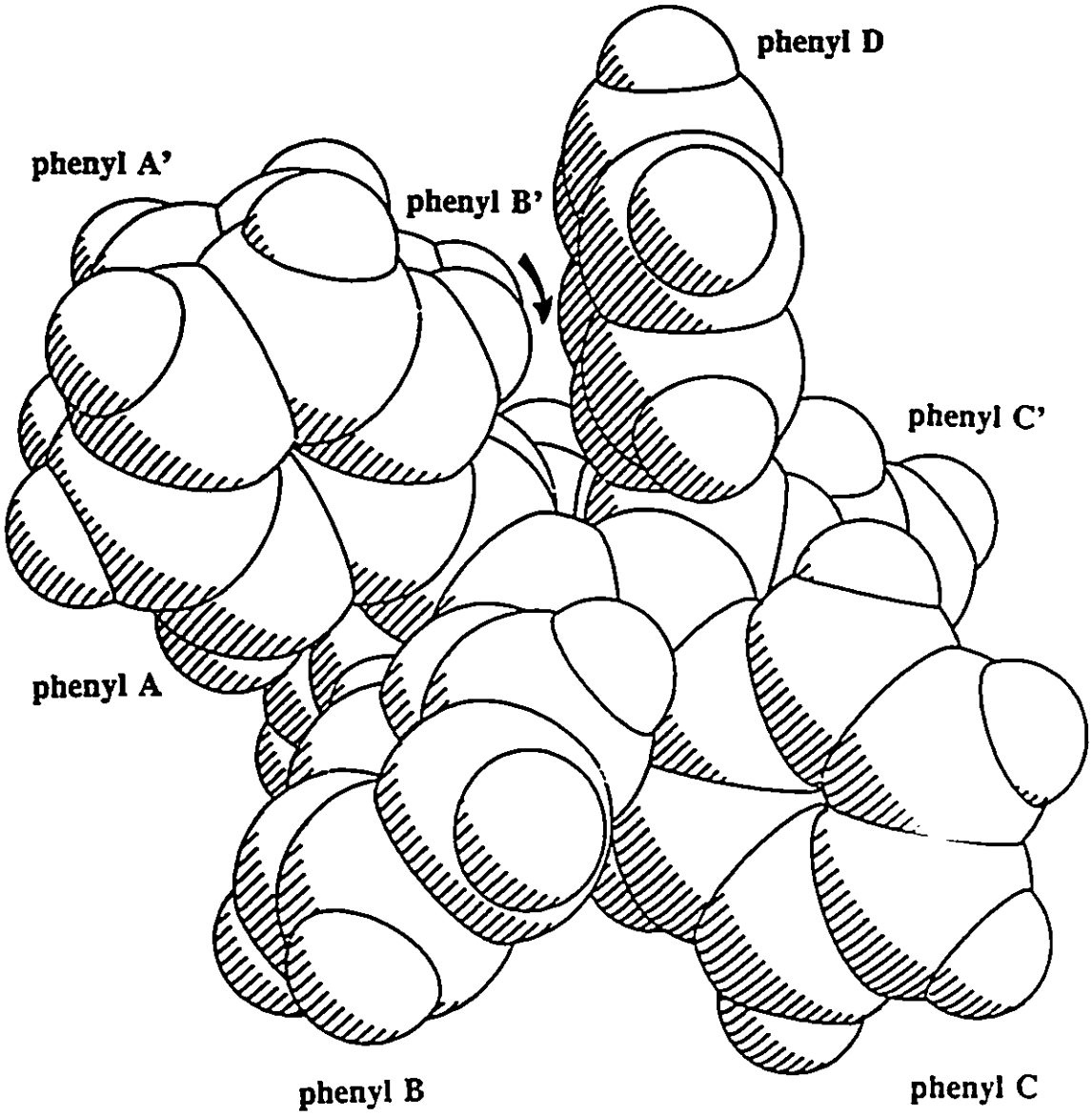

Figure 26: Space-filling model of C_7Ph_7H, 47.

between protons on opposite edges of the **B** phenyl rings, one can conclude that the solid state data provide an excellent model for the most favored conformation in solution.

The marked shielding of the *ortho* protons of the **A** rings may be accounted for by their proximity to the unique phenyl (ring **D**). Indeed, in the room temperature ^{1}H spectrum, these protons exhibit a doublet at δ 6.2 which is, of course, the time-averaged chemical shift for the two environments, H(32)/H(42) and H(36)/H(46). At -70 °C, this resonance has broadened considerably, and by -90 °C it has completely disappeared into the baseline. Since solubility limitations do not allow the observation of a limiting spectrum for slowed **A** ring rotation, it is not possible to extract a barrier for this process. Nevertheless, knowing the coalescence temperature (≈ -70 °C), one could estimate this barrier if the approximate chemical shift difference between H(32) and H(36) could be evaluated. Making the (admittedly naive) assumption that the major contributor to this chemical shift separation is the sum of the ring current effects of the neighboring phenyls, then a simple calculation leads to an estimate of $\Delta\nu$. To test the validity of such an approach, the ring current induced chemical shift difference between the *ortho* protons H(22) and H(26) was evaluated; the x-ray structure of **47** places H(22) 3.51 Å from the centroid of the phenyl **C** ring bonded to C(1) such that the vector connecting these two points makes an angle of 124° with the ring plane. The Johnson-Bovey ring current tables [86] (based on the original model of Waugh and Fessenden [87]) predict that the **C** ring induces an incremental shielding of 0.69 ppm for a proton sited in such a position. In a similar manner, one can evaluate the shielding of H(22) caused by the anisotropic character of the phenyl **A** ring at C(3); the Johnson-

Bovey approach yields a shielding of 0.34 ppm. By using this method, the incremental shifts predicted for H(26), and for the *meta* protons H(23) and H(25), were evaluated. Overall, this calculatory approach suggests chemical shift differences of 0.73 ± 0.1 ppm for the *ortho* H's of the **B** rings, and 0.31 ± 0.1 ppm for the *meta* H's; the experimental shift differences are 0.73 ppm and 0.44 ppm, respectively. The ring current induced chemical shift differences for selected hydrogens are listed in Appendix A15.

The corresponding calculations for the *ortho* proton chemical shifts in the **A** and **C** phenyl rings yield a $\Delta\delta$ value of 0.65 ppm in each case. We note that the **A** ring protons which face the unique **D** ring are particularly strongly shielded. These estimates of $\Delta\nu$, in conjunction with a coalescence temperature of ≈ 203 K, yield a $\Delta G^{\neq}$ value of approximately 9.1 kcal mol^{-1} for the barrier to **A** ring rotation. Likewise, the barrier to **C** ring rotation was also estimated to be ≈ 9 kcal mol^{-1}. After making due allowances for the errors associated with such an approach, the energy requirements for rotation of the **A** and **C** phenyls appear to be considerably less than the 11 kcal mol^{-1} barrier found experimentally for the **B** phenyls. Although the chemical shift differences between *ortho* protons in the **A** and **C** rings have been estimated from ring current calculations rather than measured directly, the experimental coalescence temperatures are available. It is easy to show that, for the **A** and **C** rings to have rotational barriers of ≈ 11 kcal mol^{-1}, the $\Delta\delta$ values for their *ortho* protons would have to be ≈ 3 Hz rather than the estimated separation of approximately 325 Hz. Therefore, we can conclude that the phenyl rotations are not correlated in C_7Ph_7H.

CHAPTER SIX

DERIVATIVES OF THE HEPTAPHENYLCYCLOHEPTATRIENE LIGAND

Variations of the heptaphenylcycloheptatriene ligand, **47**, may be achieved by changing the diene in the Diels-Alder reaction. Ligands such as dimethylpentaphenylcycloheptatriene, **51**, and di-*p*-tolylpentaphenylcycloheptatriene, **52**, not only possess a different degree of steric crowding, but also reveal a cycloheptatriene ring inversion process that is not immediately obvious from the spectroscopic evidence of **47**.

The x-ray crystal structure of the heptaphenylcycloheptatriene molecule, **47** (Figure 25), shows that it does not lie planar, just as cycloheptatriene, C_7H_8. The related $C_7H_7^+$ cation, or tropylium and the $C_7H_7^-$ anion, or tropylide, have both been extensively studied in organometallic systems as π ligands. The analogous $C_7Ph_7^+$ cation, **46**, and $C_7Ph_7^-$ anion, **48**, which have been previously reported [79,80], have not yet been structurally examined nor found in reactions with organometallic fragments.

6.1 Preparation of Dimethylpentaphenylcycloheptatriene, $C_7Ph_5Me_2H$.

The analogous synthesis of $C_7Ph_5Me_2H$, **51**, can be readily envisaged from the Diels-Alder reaction of 1,2,3-triphenylcyclopropene with 2,5-dimethyl-3,4-diphenylcyclopentadienone, **53**. This latter molecule, unlike C_4Ph_4CO which is monomeric, occurs as its Diels-Alder dimer and so must be

cracked before use [88]. When **53** and C_3Ph_3H are either melted together or heated in refluxing xylenes for 4 days, CO is evolved and $C_7Ph_5Me_2H$ is produced. However, the complexity of the NMR spectra, in particular the non-equivalence of the methyl groups in both the ^1H and ^{13}C regimes (Figure 27, 28, and Table 3), reveals that $C_7Ph_5Me_2H$, **51,** cannot be the anticipated symmetrical isomer **51a.** Indeed, the singlet character of both methyl signals in the ^1H spectrum eliminates **51c** and leaves **51b** and **51d** as the only two viable candidates.

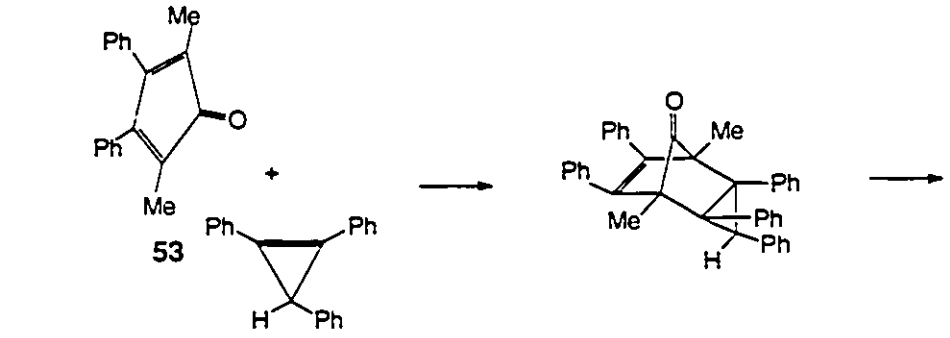

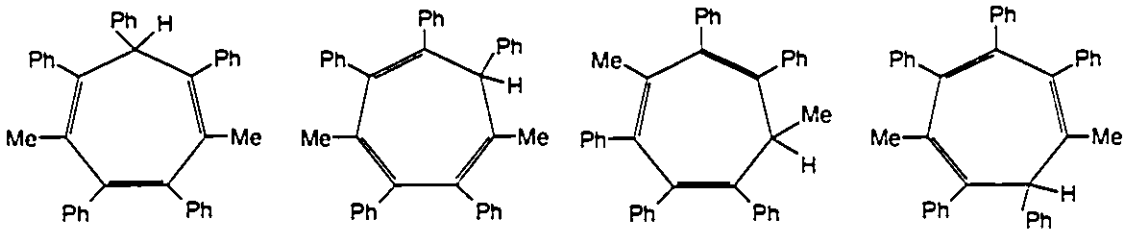

51a **51b** **51c** **51d**

The choice between these two isomers can be made by using a combination of 2D and nOe experiments (Figure 29 and 30). These spectra allowed the ready identification of the phenyl **D** ring (whose *ortho* protons were coupled to the methine hydrogen) and of the methyl and phenyl in the **C**

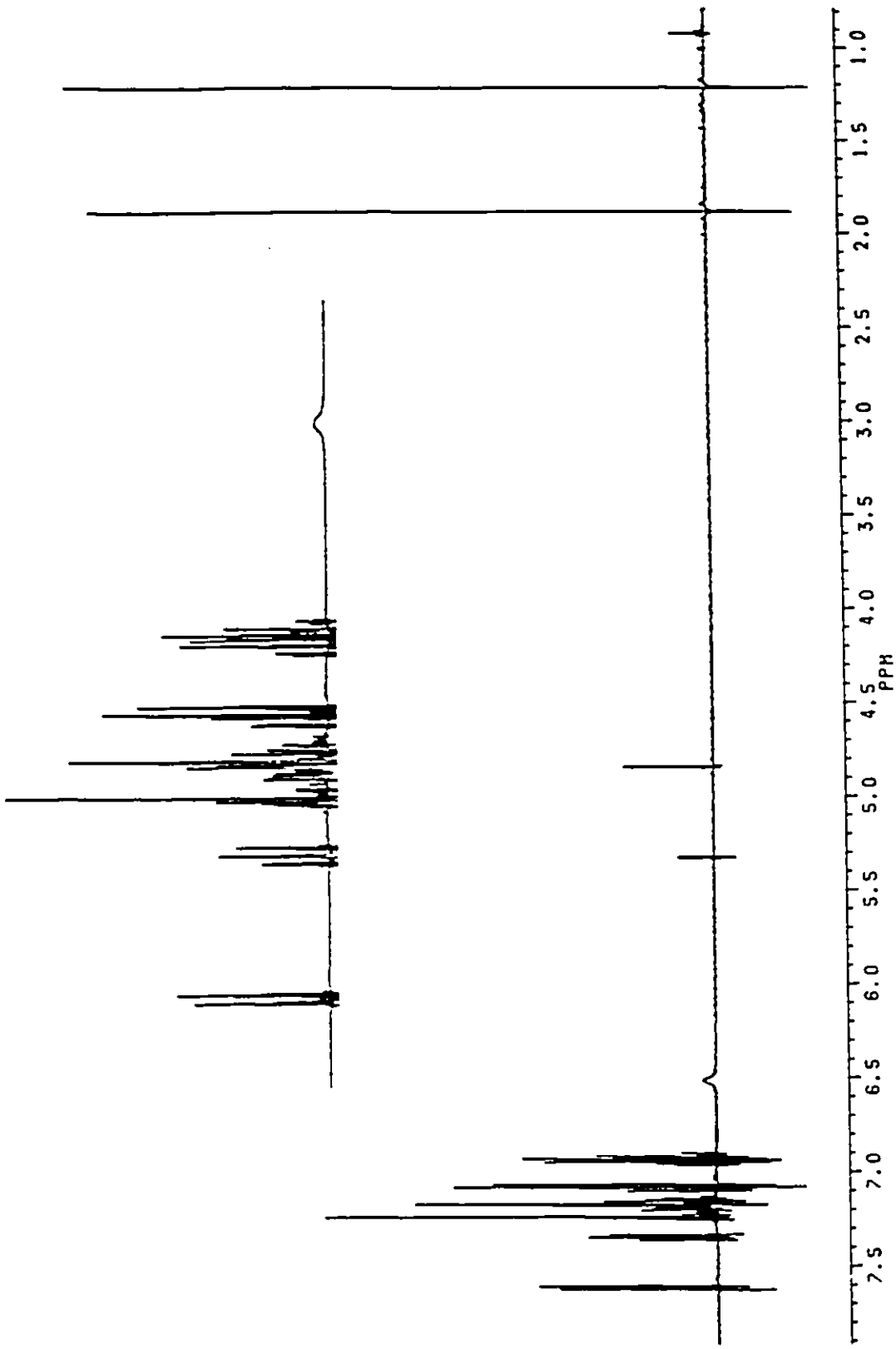

Figure 27: 500 MHz ^1H NMR spectrum of $C_7Ph_5Me_2H$, 51.

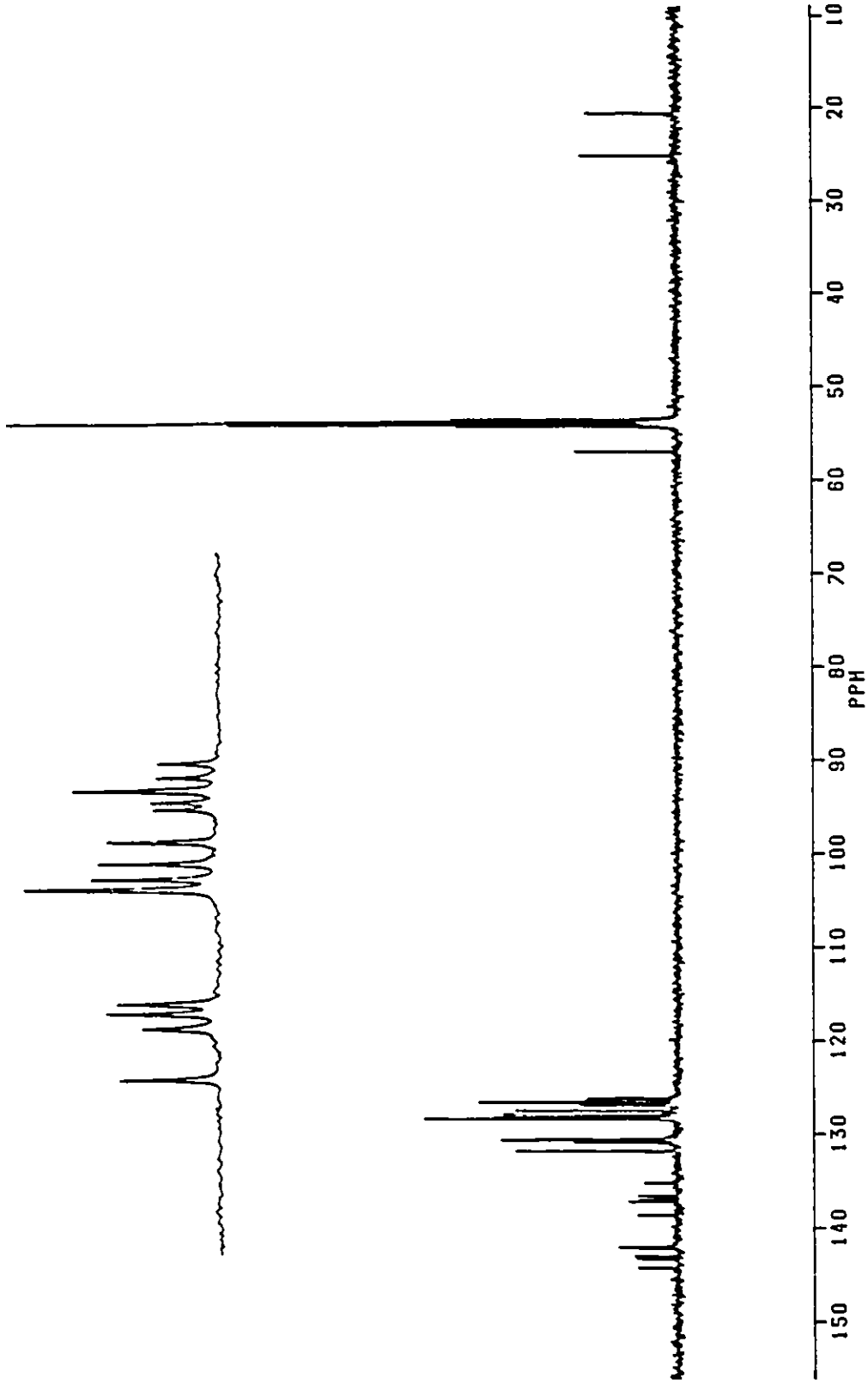

*Figure 28: 125 MHz ^{13}C NMR spectrum of $C_7Ph_5Me_2H$, **51**.*

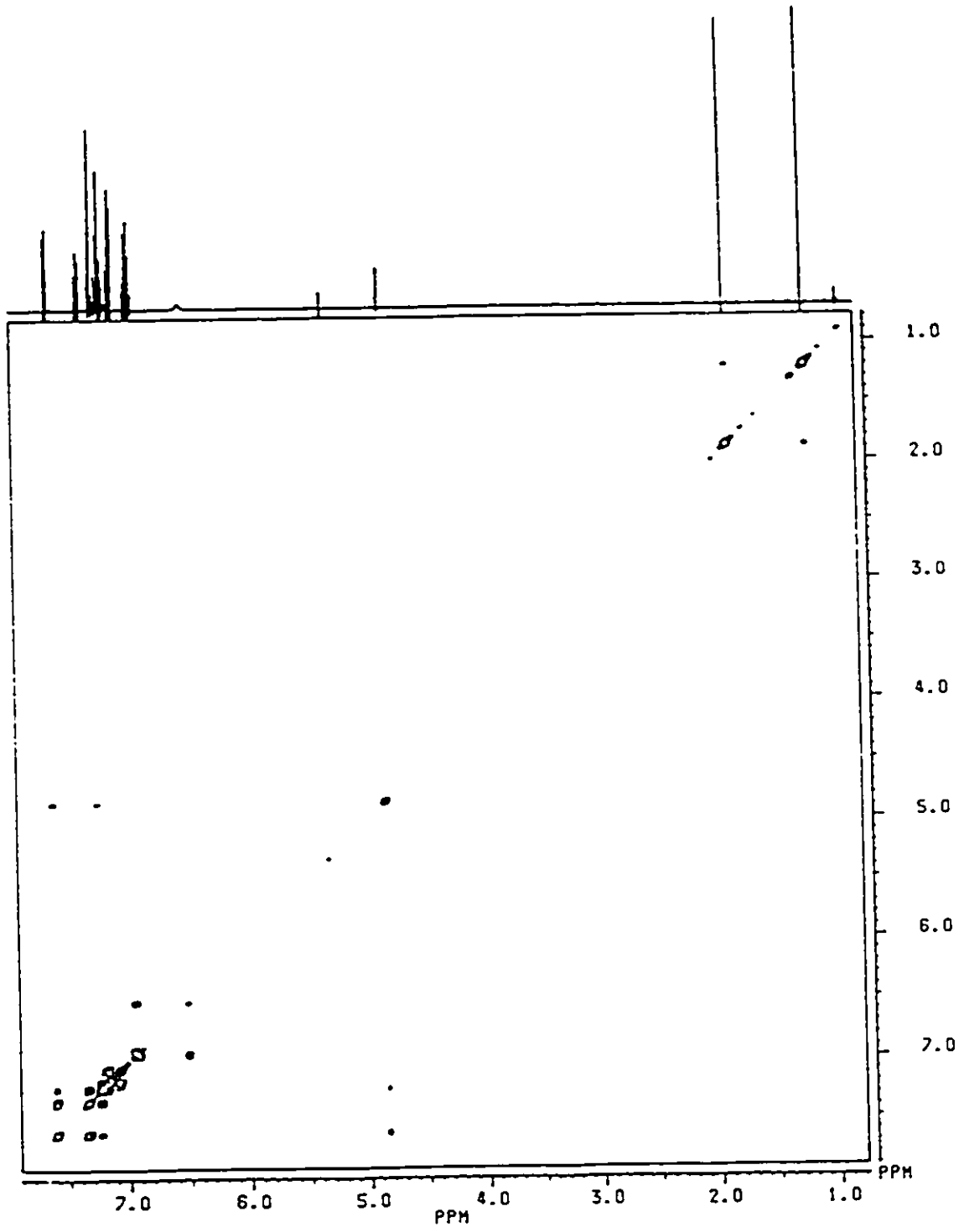

Figure 29: ^{1}H - ^{1}H COSY spectrum of $C_7Ph_5Me_2H$, 51.

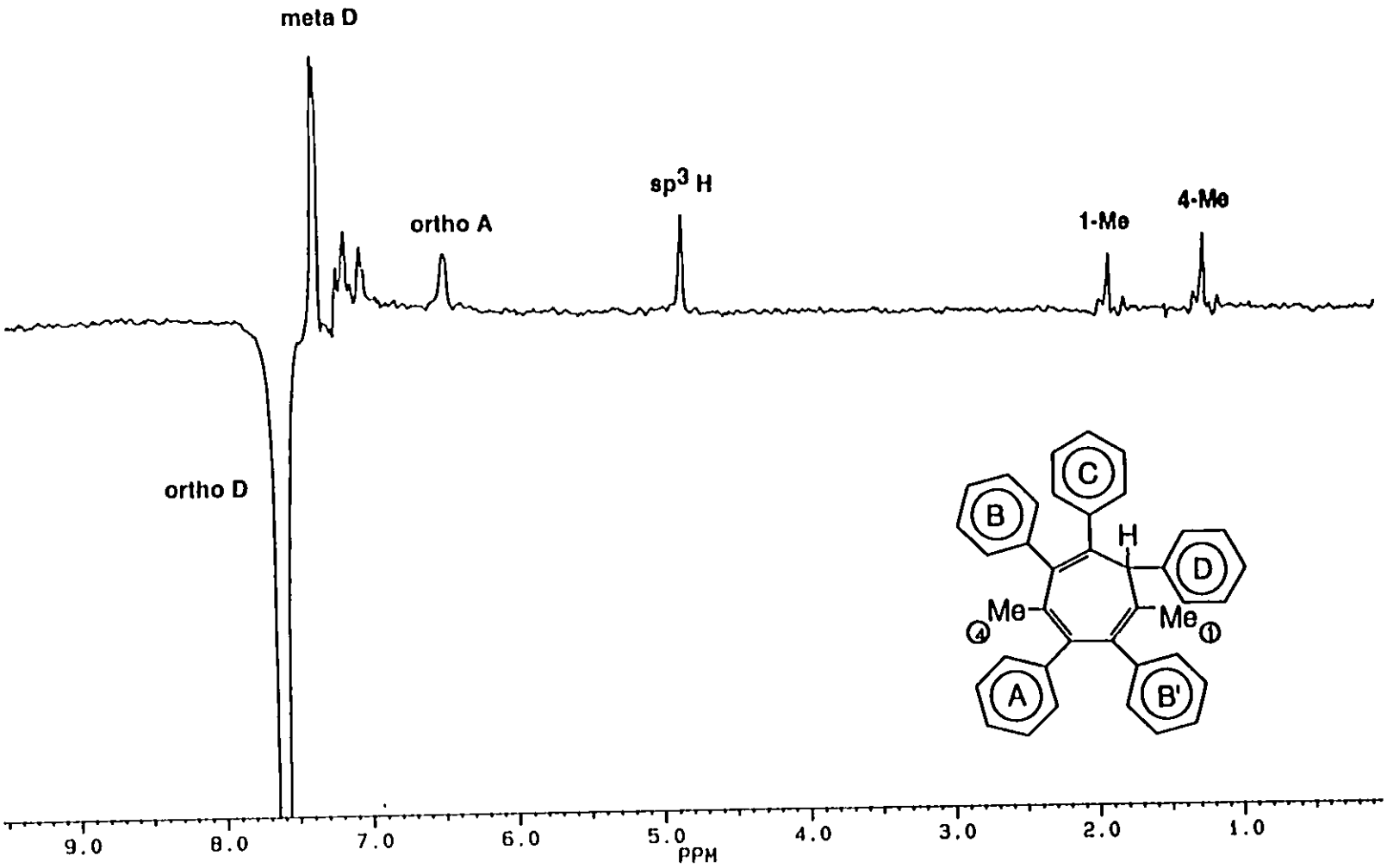

*Figure 30: NOE difference experiment; saturation at 7.60 ppm (ortho protons of phenyl **D** in **51**).*

environment (both of which showed nOe's to this same methine proton). Irradiation of the *ortho*-H's of the **D** ring enhanced the other methyl as well as the single phenyl in the **A** environment. These data were confirmed by irradiation of each methyl in turn; all the data were consistent with structure **51b** in which the methine hydrogen again occupied the pseudo-equatorial site at C(7). Although this structure possesses two phenyl **B** rings, they each have a phenyl and a methyl neighbor, thus avoiding the severe steric crowding which is observed in C_7Ph_7H.

Such molecules must arise via hydrogen migrations, but the symmetry-allowed [1,5] suprafacial sigmatropic shift can only occur when the migrating hydrogen is positioned axially so as to facilitate the rearrangement shown in Scheme 20.

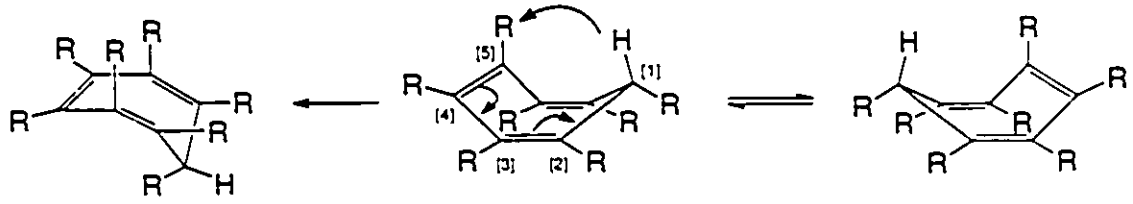

Scheme 20: A [1,5] suprafacial sigmatropic hydrogen shift versus conformational ring flipping.

Since the methine hydrogen at C(7) is positioned pseudo-equatorially, any attempt to equilibrate the methyl environments via hydrogen migrations must first surmount the barrier to cycloheptatriene ring flipping. The ^1H spectrum of **51** was recorded at various temperatures up to 137 °C (410 K) but no broadening or coalescence of the methyl signals was evident. This result yields

a minimum barrier of 19.4 kcal mol^{-1} for C_7 ring inversion. Consequently, a series of selective inversion experiments were carried out since this technique is capable of detecting slow exchange without the need to take the sample to inconveniently high temperatures [89]. However, even at 410 K, no magnetization transfer between methyl sites could be detected, and so a revised estimate of the minimum barrier for ring inversion of 25 kcal mol^{-1} must be made. This minimum estimate for $\Delta G^{\neq}$ exceeds the quoted value of 23.8 kcal mol^{-1} for (1,2)(3,4)(5,6)-tribenzocycloheptatriene [90].

6.2 Structure of the Tricyclic Ketone, C_7Ph_7HCO.

A crucial factor in rearrangements is the ring conformation; it may well be the case that [1,5] hydrogen shifts also occur during the formation of C_7Ph_7H but, since such a process would be degenerate, the same final product would result [91]. The crystallographically characterized C_7Ph_7H, **47b**, in which the methine hydrogen at C7 is equatorial, could not undergo [1,5] hydrogen shifts without flipping to the other boat conformer, as in Scheme 20. The activation energies for such conformational flips vary from 6.3 kcal mol^{-1} for C_7H_8 to more than 20 kcal mol^{-1} for cycloheptatrienes bearing bulky groups [92]. Clearly, the conformation of the initially formed C_7Ph_7H is dependent on the structure of the precursor tricyclic ketone, **50a** or **50b**. The geometry of **50** could not be assigned unequivocally since, even at 500 MHz, overlap of the phenyl peaks is too severe. Consequently, the problem was again resolved by x-ray crystallography and the resulting structure, **50a**, appears as Figure 31. It is evident that all three phenyls derived from the cyclopropene ring are mutually cis

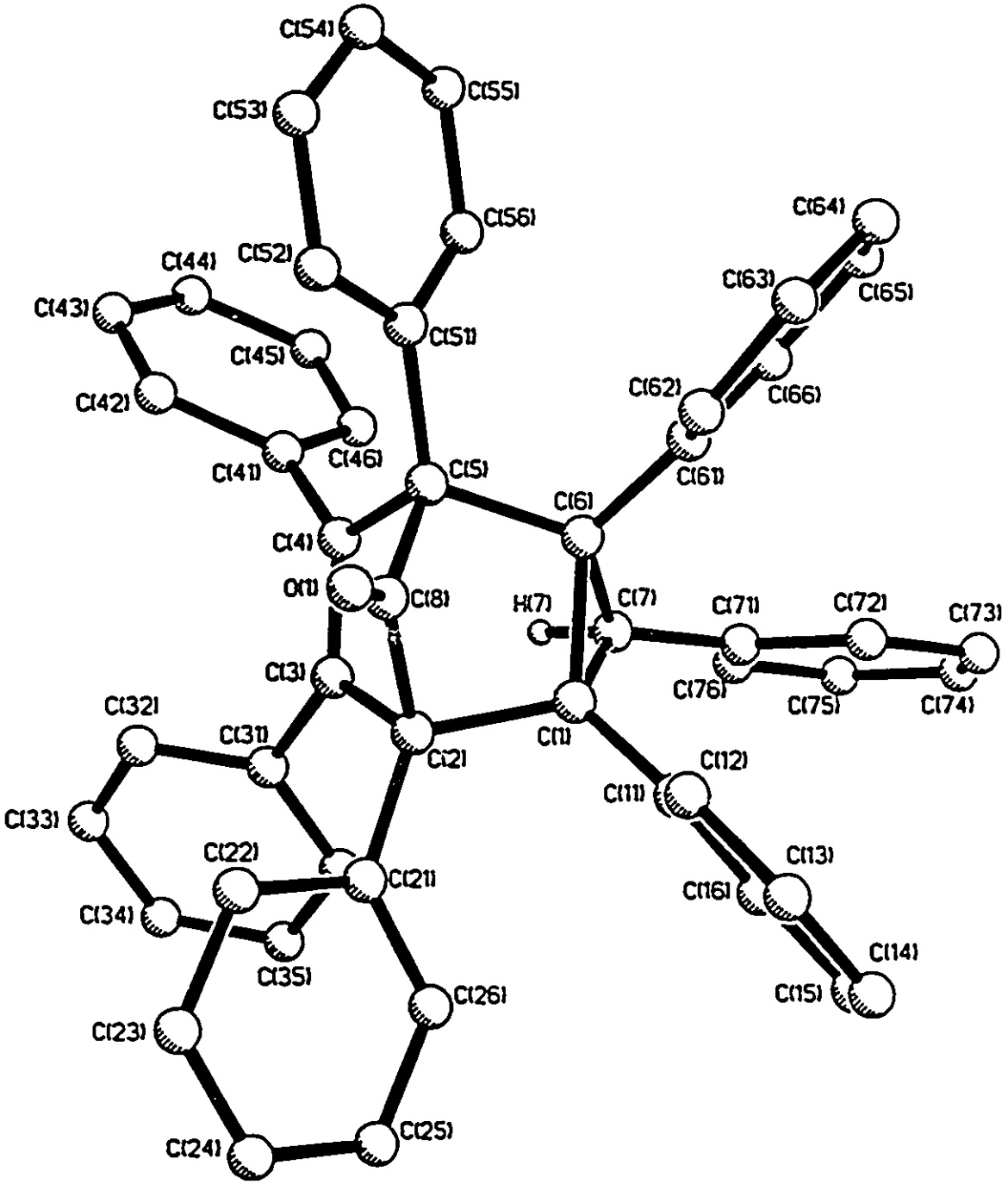

Figure 31: Molecular structure of C_7Ph_7HCO, 50, showing the atom numbering scheme.

in the Diels-Alder adduct, leaving the methine hydrogen axially positioned (structure determination tables in the Appendix).

The tricyclic ketone **50a** possesses several interesting structural features. The C(1)-C(6) distance is rather long at 1.569(6) Å, reflecting its somewhat strained environment as a member of three different sized rings (a cyclopropane, a cyclopentanone, and a cyclohexene). It is this bond that is broken when CO is lost and C_7Ph_7H is formed. However, it is also interesting that the C(1)-C(2) and C(5)-C(6) bonds are also long, 1.607(6) Å and 1.600(6) Å, respectively; these are the bonds that are made during the Diels-Alder reaction to form **50a**, and their weakness may account for the ready reversibility of this process. Indeed, as shall be seen presently, this factor presumably comes into play during the reaction of **50a** with $Mo(CO)_6$. Only one other closely related tricyclic ketone structure has been reported, the Diels-Alder adduct of tetracyclone with cyclopentadiene, where both the *endo* and *exo* isomers are known. In the *endo* adduct, the bonds formed in the Diels-Alder addition (corresponding to C(1) - C(2) and C(5) - C(6) in **51**) average 1.569 Å reflecting the less crowded nature of the product [93].

Battiste has noted that *endo*-tricyclo[3.2.1.$0^{2,4}$]octen-8-ones undergo facile decarbonylation to yield cycloheptatrienes directly, while their *exo*-isomers apparently decompose via norcaradiene intermediates [94]. Thus, it is apparent that cheletropic loss of CO from **50a** will yield **47a**, in which [1,5] hydrogen shifts are viable. However, the structure determined for C_7Ph_7H is **47b** in which a boat-to-boat conformational flip has occurred. An examination of molecular models confirms that the initially formed conformer, **47a**, engenders severe steric problems between the pseudo-equatorial phenyl (ring **D**) and its neighbors in the **C** positions.

6.3 Preparation of Di-*p*-tolylpentaphenylcycloheptatriene, $C_7Ph_5Tol_2H$.

To demonstrate the intermediacy of conformer **47a**, where the methine hydrogen is axial, 2,5-diphenyl-3,4-di-*p*-tolylcyclopentadienone was used to prepare $C_7Ph_5Tol_2H$, **52**, and its Diels-Alder adduct, **54**, analogous to **47** and **50**. Thermolysis of **54** resulted in elimination of CO and formation of the isomers **52a** through **52d**.

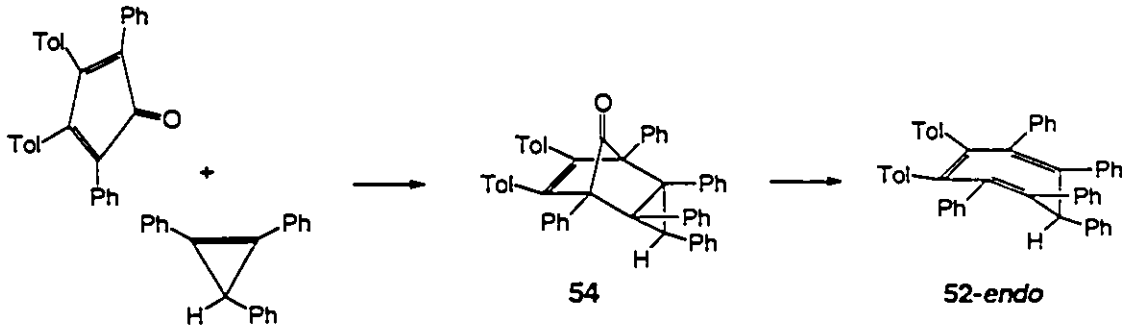

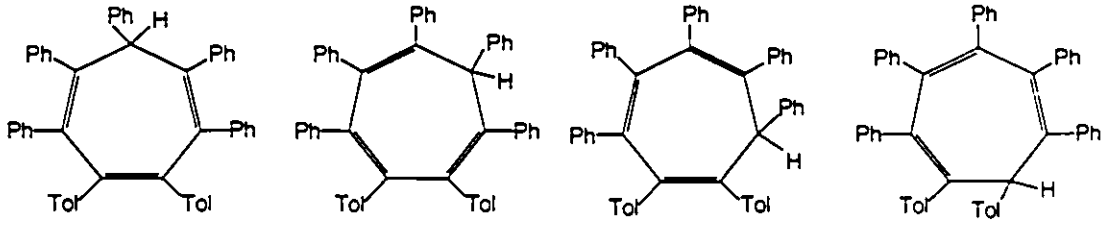

52a **52b** **52c** **52d**

The peripheral tolyl rings in the isomers of **52** give rise to seven equally intense ^1H methyl resonances; moreover, the aromatic protons in the D-ring environment clearly reveal the presence of both phenyl and tolyl groups in a 5:2 ratio. Evidently, conformation **52-*endo*** has a finite life-time which allows the [1,5] hydrogen shifts to occur and yields ultimately the mixture 52a through 52d.

Unlike the $C_7Ph_5Me_2H$ analogue, **51**, where only one favored isomer was isolated, these isomers must have roughly equal steric crowding. The formation of the isomers of **52** demonstrates that in the parent heptaphenylcyclo-heptatriene, conformation **47a** is sufficiently long-lived to allow rapid [1,5] suprafacial sigmatropic hydrogen shifts before ring flipping to **47b** prevents any further rearrangement.

6.4 The Heptaphenyltropylium ion, $[C_7Ph_7]^+$

The study of heptaphenylcycloheptatriene and its analogues have provided important information on hydrogen migrations and conformational ring flipping in seven-membered rings. However, in order to compare this molecule to polyaryl systems such as $C_5Ph_5^-$ and C_6Ph_6, the $C_7Ph_7^+$ ion must be examined. The central ring of the $C_7Ph_7^+$ ion is a 6π system and is expected to lie planar. This cation could potentially be treated with an organometallic anion to form a complex in which the organometallic fragment is bonded to the central seven-membered ring. These complexes could then be compared to the organometallic derivatives of other polyphenylated systems as well as those of the tropylium ion, $C_7H_7^+$ [69,70,84]. The $C_7Ph_7^+Br^-$ salt, **46a**, is prepared by treating C_7Ph_7H, **47**, with bromine in carbon tetrachloride [79].

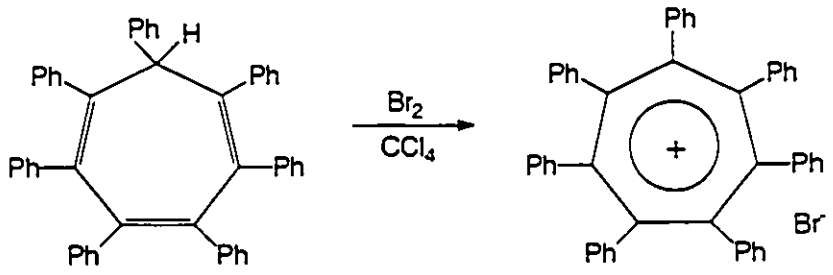

47 **46a**

This bright red solid, **46a**, possesses a simple NMR spectrum in trifluoroacetic acid suggesting a symmetrical molecule with a planar central ring. The ^{1}H spectrum shows one broad peak in the phenyl proton region, while the ^{13}C NMR spectrum shows one peak each for the *para*, *meta*, *ortho*, and *ipso* carbons. The $C_7Ph_7^+$ salt is only slightly soluble in acetonitrile and chloroform and insoluble in benzene, ether, THF, and acetone, making subsequent reactions with organometallic moieties difficult.

It was then considered that a different counter anion might change the solubility of the salt. The $C_7Ph_7^+BF_4^-$ salt, **46b**, is prepared by first treating the $C_7Ph_7^+Br^-$ salt, **46a**, with water or methanol in CH_3CN to form C_7Ph_7OH, **55**, or C_7Ph_7OMe, **56**, respectively [79]. These two molecules will likely have similar structures and dynamics as the parent C_7Ph_7H, **47**.

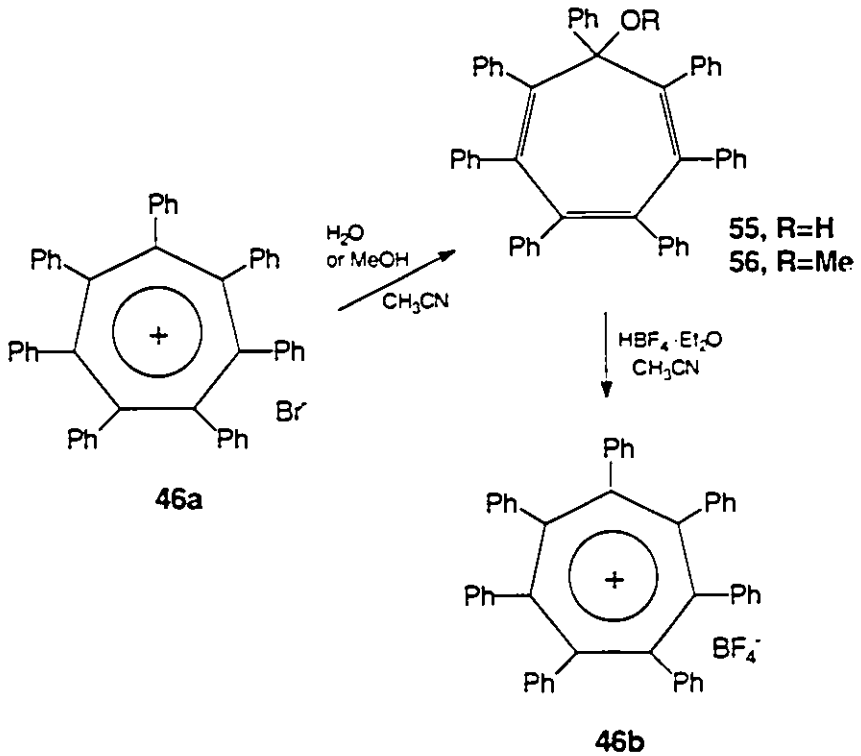

46a

46b

Molecule **55** or **56** is then treated with $HBF_4 \cdot Et_2O$ to form the salt, $C_7Ph_7^+BF_4^-$, **46b**, which is soluble in most organic solvents. This salt also exhibits a simple NMR spectrum, suggesting a planar seven-membered ring. X-ray data has been collected on **46b**, however its structure remains unsolvable. There appear to be three independent molecules in the unit cell. The structure crystallizes in the monoclinic space group $P2_1$ where a = 15.402 (5), b = 21.783 (7), c = 17.125 (6), and β = 94.21 (2). For **46a**, problems have been encountered in obtaining a single crystal suitable for x-ray diffraction studies.

In order to gain an understanding of the crowding in the $C_7Ph_7^+$ ion, a molecular modelling study was carried out. The study showed that the seven peripheral phenyl rings prefer to adopt an orientation that is orthogonal, θ = 90°, to the central seven-membered ring (Figure 32). This arrangement minimizes interaction between the bulky groups but prevents orbital overlap between the central and peripheral π-systems. Such a conformation is in contrast to that of the solid state structure of hexaphenylbenzene where the exterior rings are canted ≈ 67° with respect to the central six-membered ring.

By "painting the edges differently", information on solution dynamics could, in principle, be determined. Just as Gust and Mislow labelled the peripheral phenyl rings of polyaryl systems with methyl or methoxy groups [73,76], the edges of these phenyl groups could be marked so that a barrier to phenyl rotation can be measured. Two of the phenyl rings can be labelled as in di-*m*-methoxy-phenylpentaphenylcycloheptatriene, **57**, which was prepared by treating 1,2,3-triphenylcyclopropene with 2,5-diphenyl-3,4-di(*m*-methoxyphenyl) cyclopentadienone, **58**.

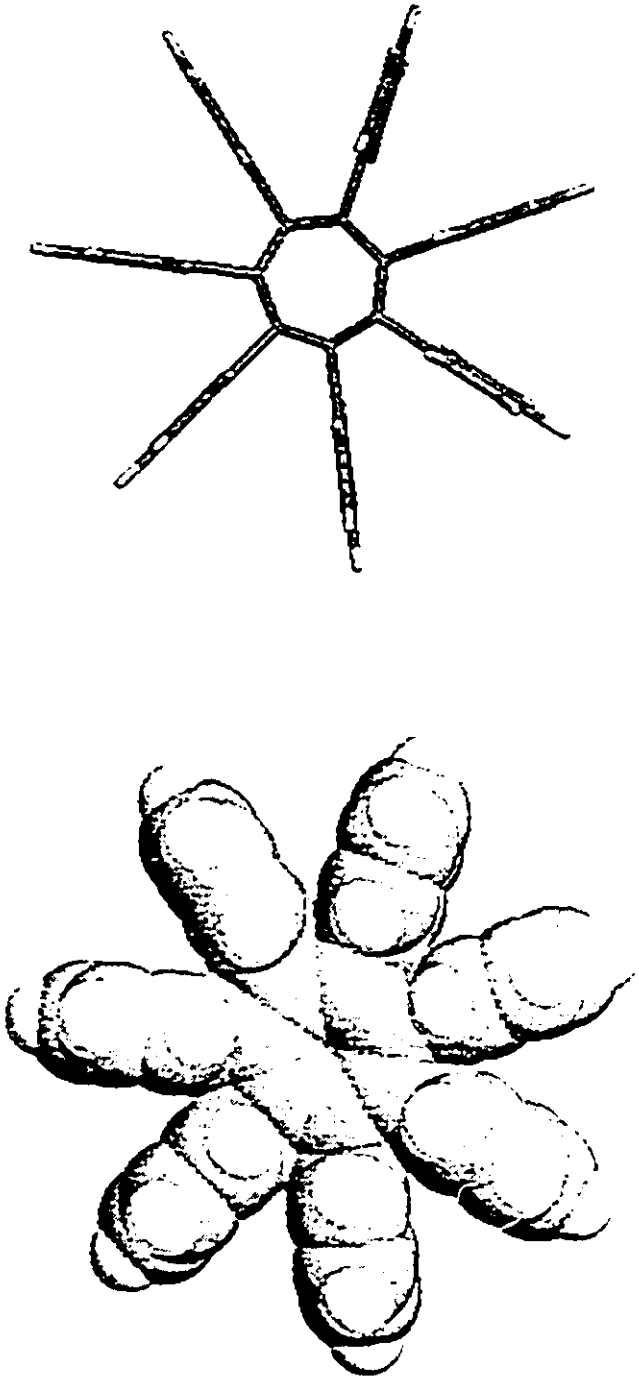

*Figure 32: Models of $C_7Ph_7^+$, **46**; (a) ball and stick (b) space-fill.*

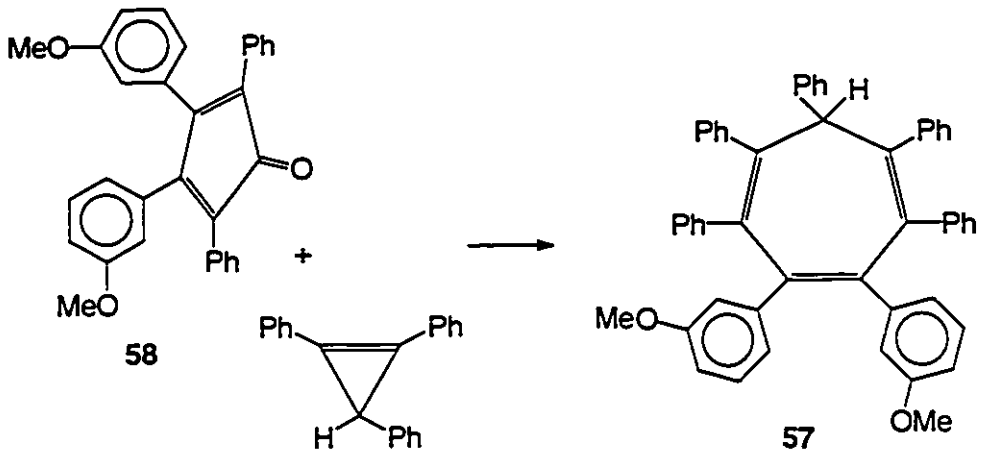

The product, **57**, is a mixture of which only one isomer is illustrated above. The formation of this mixture again demonstrates that [1,5] sigmatropic hydrogen shifts occur before a conformational ring flip places the unique phenyl axial. The $C_7(m\text{-PhOMe})_2Ph_5H$, **57**, was then treated with bromine in carbon tetrachloride in anticipation of the $C_7(m\text{-PhOMe})_2Ph_5^+Br^-$ salt, **59**. However, the cation was not formed as the *ortho* and *para* directing character of the methoxy groups resulted in a non-ionic perbrominated molecule, **60**. The mass spectrum of **60** exhibits a parent ion peak corresponding to a molecule with seven bromo substituents.

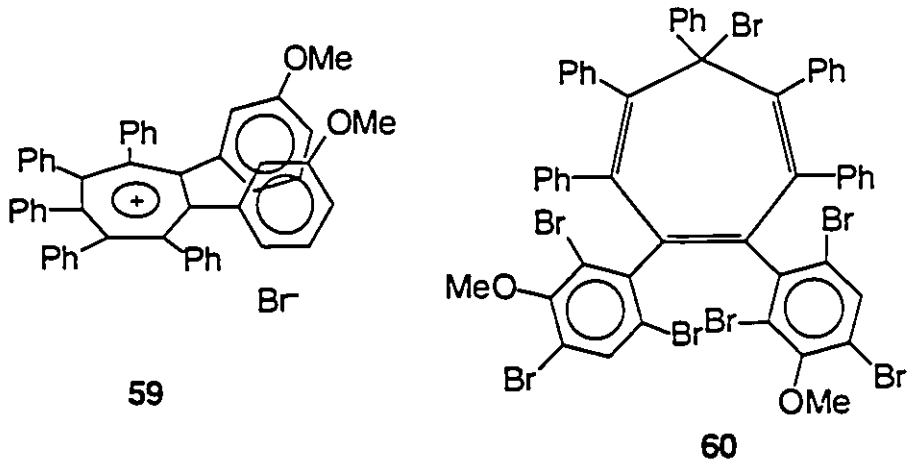

In order to perfom dynamic studies, other substituents such as fluoro or methyl groups would be ideal. An organometallic fragment bonded to the central ring could also give insight on the solution dynamics of the $C_7Ph_7^+$ ion since the phenyls would have a *proximal* and *distal* edge with respect to the metal.

6.5 The Heptaphenylcycloheptatrienide anion, $[C_7Ph_7]^-$

The heptaphenylcycloheptatrienide anion, **48**, is also a very interesting polyaryl system. The anti-aromatic 8π character of the central ring should result in its non-planar arrangement. To prepare **48**, the $C_7Ph_7^+Br^-$ salt, **46a**, is treated with potassium metal in dry diethyl ether [80]. The formation of the anion is indicated by an intense blue colour.

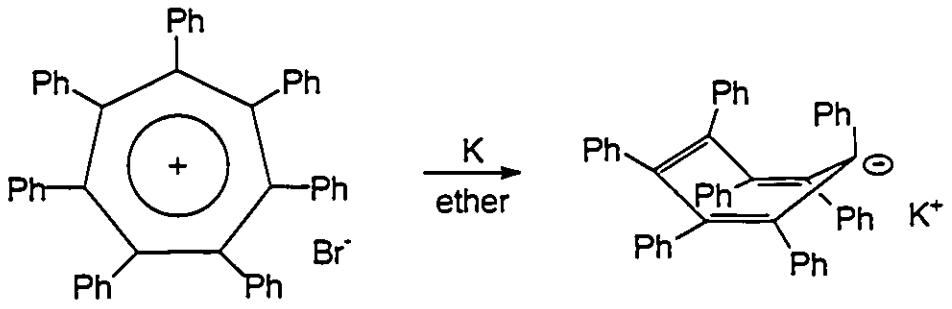

46a **48**

At this point, a number of organometallic cationic complexes can be introduced resulting in organometallic fragments either sigma bonded to the sp^3 carbon or π-bonded to the central seven-membered ring.

6.6 Conclusion

The Diels-Alder reaction of tetracyclone (or of $C_4Ph_2Me_2CO$, **53**) with triphenylcyclopropene yields the adduct with an *endo* hydrogen at C(7); thermolysis to bring about elimination of CO produces the appropriately substituted cycloheptatriene in which [1,5] hydrogen shifts can occur. However, this initially formed isomer with a pseudo-equatorial phenyl substituent at the sp^3 position is sterically hindered and undergoes a conformational flip which allows the phenyl group to occupy the favored pseudo-axial site.

This methine hydrogen can also be removed as a hydride resulting in the heptaphenyltropylium ion which appears to possess a planar central ring. As well, the methine hydrogen can be removed as H^+, resulting in the $C_7Ph_7^-$ anion.

CHAPTER SEVEN

ORGANOMETALLIC DERIVATIVES OF HEPTAPHENYLCYCLOHEPTATRIENE AND RELATED LIGANDS

Now that a better understanding of the dynamics and structure of heptaphenylcycloheptatriene and related ligands has been achieved, the study of their organometallic derivatives is warranted. To begin, a brief look will be taken at the numerous organometallic derivatives of C_7H_8 and $C_7H_7^+$.

7.1 η^6-Cycloheptatriene and η^7-Tropylium Complexes

Cycloheptatriene complexes of chromium, molybdenum, and tungsten are generally prepared by heating the ligand with the hexacarbonyl in a high boiling solvent. The C_7H_8 ligand is a 6π donor in these triolefin complexes. In the x-ray crystal structure of η^6-$(C_7H_8)Mo(CO)_3$, **61**, there is an *exo*-bending of the non-coordinated CH_2 group about 0.67Å from the plane of the other six carbon atoms. The study also reveals alternating C-C bond lengths [95a] (Figure 33a).

The $C_7H_7^+$ ligand is usually regarded as an aromatic 6π donor. The abstraction of hydride from the η^6-triene ligand is one route to these tropylium complexes. Hydride elimination from η^6-$(C_7H_8)Mo(CO)_3$ with $[Ph_3C]^+[BF_4]^-$ results in the air-stable $[\eta^7$-$(C_7H_7)Mo(CO)_3]^+[BF_4]^-$, **62**. The structure of the

tropylium complexes are quite different from the cycloheptatriene derivatives. In $[\eta^7(C_7H_7)Mo(CO)_3]^+$, the C_7H_7 ring lies planar with equal C-C bond distances [95b] (Figure 33b).

(a)

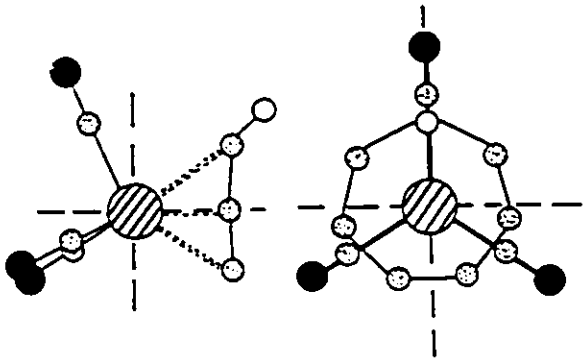

(b)

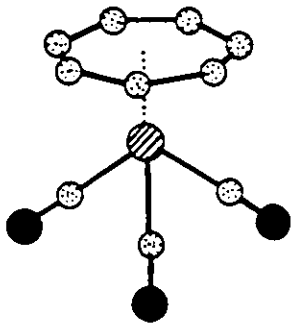

Figure 33: X-ray crystal structure of (a) η^6-$(C_7H_8)Mo(CO)_3$, 61, and (b) $[\eta^7$-$(C_7H_7)Mo(CO)_3]^+[BF_4]^-$, 62.

The C_7H_7 ligand can also act as an η^3 or η^4 donor. The η^4-$(C_7H_8)Fe(CO)_3$ complex can be prepared by refluxing $Fe(CO)_5$ and cycloheptatriene in methylcyclohexane [96]. This complex can be deprotonated with n-BuLi to give $[(\eta^3$-$C_7H_7)Fe(CO)_3]^-[Li]^+$, 63. Partially coordinated seven-membered rings such as 63 can form additional bonds to a second transition

metal. This quite often results in the formation of metal-metal bonds as well as fluxional behavior of the bridging ligand as demonstrated by the dinuclear complex, **64**, reported by Takats *et al.*[97]

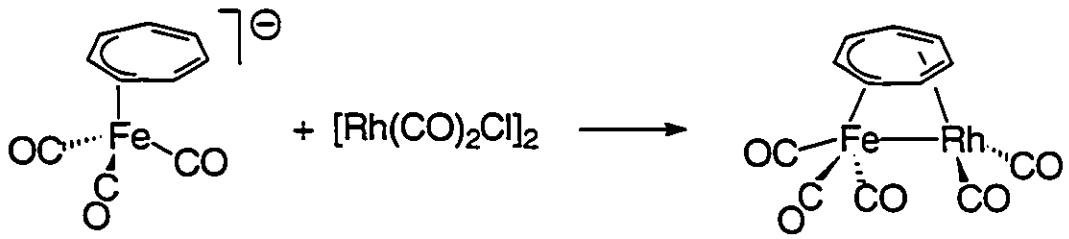

63 **64**

7.2 Reactions of C_7Ph_7H and Related Ligands with Metal Carbonyls

It is known that 7-phenylcycloheptatriene reacts with $Cr(CO)_6$ or $(pyridine)_3Cr(CO)_3$ to give the *exo*- and *endo*-phenyl isomers, **65** and **66**, respectively, in which the metal is η^6-coordinated to the 7-membered ring [98].

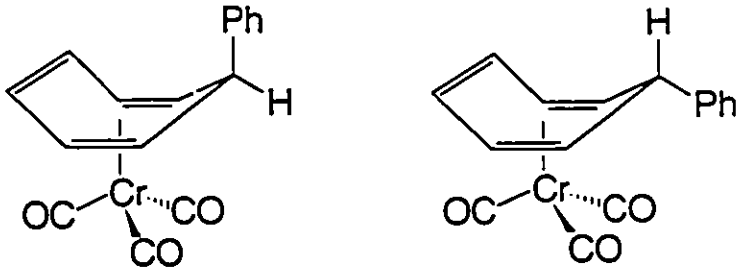

65 **66**

Treatment of C_7Ph_7H, **47**, with $Cr(CO)_6$ yields a yellow complex, **67**, in which the $Cr(CO)_3$ moiety is attached to an external phenyl ring. The marked

shielding of the ^{1}H and ^{13}C resonances in the chromium-complexed ring, together with the symmetrical character of the remaining phenyl ^{13}C signals, indicates that the metal is coordinated to the unique **D** ring. The preference for the peripheral phenyl ring is analogous to the previously mentioned polyaryl complex, (hexaphenylbenzene)$Cr(CO)_3$, **45** [70].

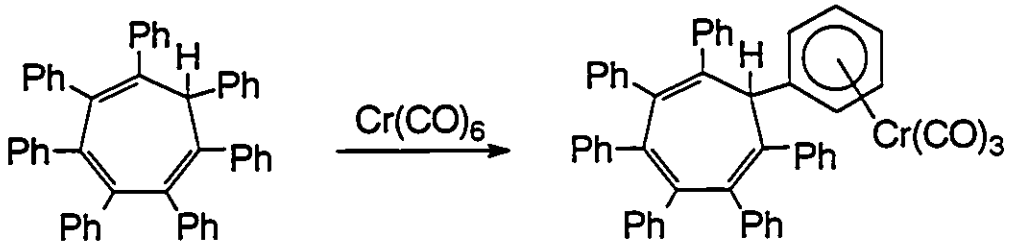

47 **67**

Likewise, when $C_7Ph_5Me_2H$, **51**, was treated with $Cr(CO)_6$, the $(C_7Ph_5Me_2H)Cr(CO)_3$ complex, **68**, resulted.

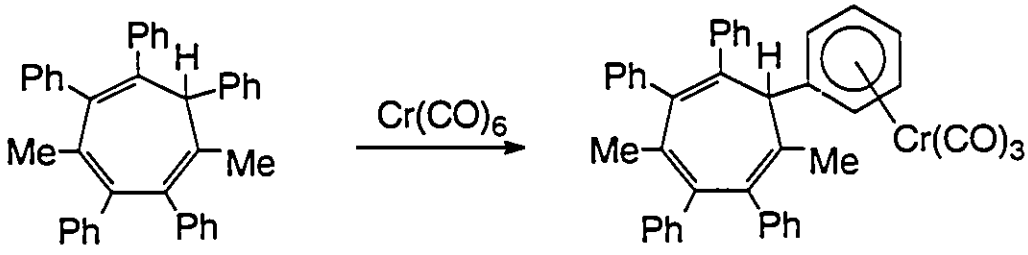

51 **68**

The observation of five distinct protons in the complexed phenyl ring suggests that, like **51**, the molecule lacks a mirror plane. Thus, in both complexes, whether the metal merely attacked the most sterically accessible

ring, or rather the product resulted from hydrogen migration after complexation, remains an open question at present. Recall that hydrogen migrations proceed 10^3 times more rapidly in $(\eta^6\text{-}C_7H_8)Mo(CO)_3$ than they do in free cycloheptatriene; deuterium labeling studies suggest that, in the complex, it is the *endo* hydrogen which migrates, presumably through a metal hydride intermediate [99].

The reactions of $Mo(CO)_6$ or $(CH_3CN)_3W(CO)_3$ with C_7Ph_7H, **47**, gave relatively unstable products, but a more interesting result was obtained when the tricyclic ketone, C_7Ph_7HCO, **50**, was heated under reflux with $Mo(CO)_6$. The intent was to try to coordinate a molybdenum carbonyl fragment onto the open face of **50** in the expectation that subsequent metal-assisted cyclopropane ring-opening and loss of CO would yield a complex in which the molybdenum was bonded to the central ring, as in **69**.

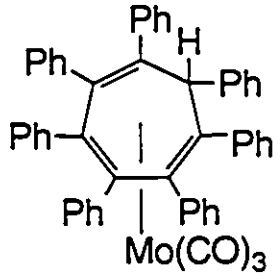

69

However, upon heating the reactants, a blue coloration appeared indicating the formation of tetracyclone, presumably as the result of a retro-Diels-Alder reaction. The product, **70**, that was finally isolated was shown by mass spectrometry to possess a molecular weight corresponding to

$C_7Ph_7H_3Mo(CO)_3$, and its identity was not immediately evident from the NMR data. The structure of **70**, determined by x-ray crystallography, is shown in Figure 34, and reveals that it contains an η^5-1-hydroxy-2,3,4,5-tetraphenyl-cyclopentadienyl ligand, and also an η^3-1,2,3-triphenylallyl moiety coordinated to a dicarbonylmolybdenum center (structure determination tables in the Appendix). Although the Ph_4C_5OH moiety is not a common ligand, ruthenium and molybdenum complexes are known [100,101]. The molybdenum-C_5(centroid) distance of 2.052 Å in **70** compares well with the value of 2.034 Å found in $[Mo_2(CO)_3(\mu\text{-}\sigma\text{:}\eta^5\text{-}C_4Ph_4CO)(\eta^5\text{-}(C_5Ph_4OH)]$ [101].

The four peripheral rings of the η^5-Ph_4C_5OH ligand adopt a propeller-type geometry in which the phenyls are twisted relative to the central 5-membered ring by θ values of 41°, 52°, 66° and 44°. This contrasts with their orientations in $[Mo_2(CO)_3(\mu\text{-}\sigma\text{:}\eta^5\text{-}C_4Ph_4CO)(\eta^5\text{-}(C_5Ph_4OH)]$ where they were described as taking up a cup-shaped arrangement [101].

Subsequently, it was shown that the molybdenum complex **70** (and also its dimethyl analogue, **71**) can be prepared by heating $Mo(CO)_6$, C_3Ph_3H and tetracyclone (or $C_4Ph_2Me_2CO$, **53**) in refluxing toluene; it is not necessary to use the tricyclic ketone **50** as the precursor.

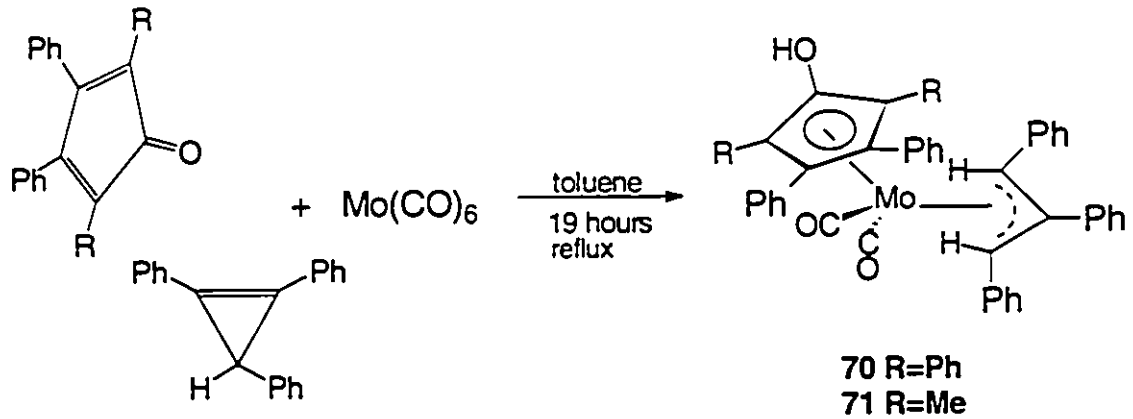

70 R=Ph
71 R=Me

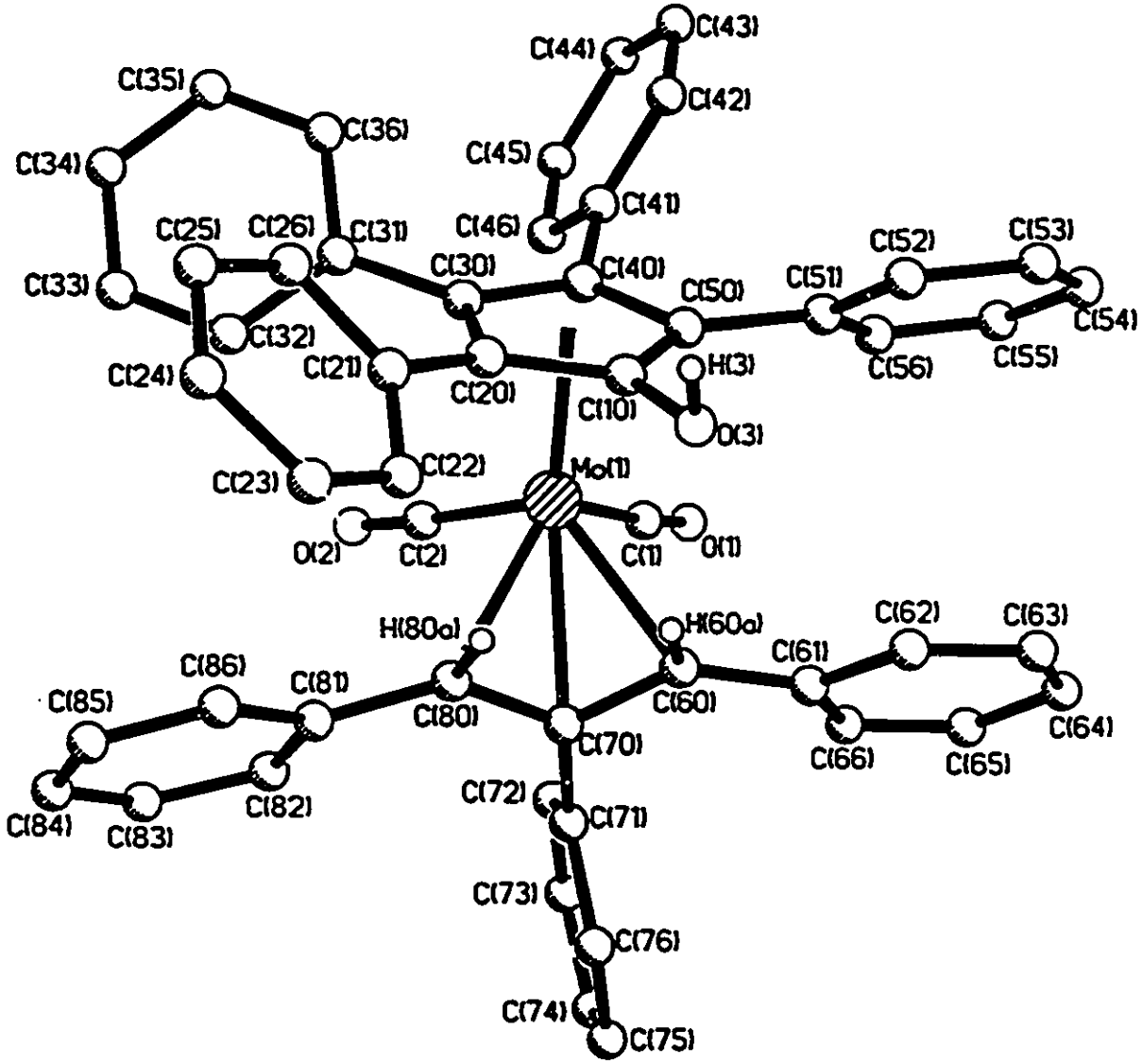

Figure 34: Molecular structure of $(\eta^5\text{-}C_5Ph_4OH)(\eta^3\text{-}C_3Ph_3H_2)Mo(CO)_2$, ***70***.

The reaction of $Mo(CO)_6$ with tetracyclone has been investigated previously [101]. In the presence of acetonitrile, the (dienone)$Mo(CO)_3(NCCH_3)$ complex, **72**, is formed but, in the absence of a coordinating solvent, one can obtain either the oxygen-bridged dimer, **73**, or the bis(dienone)$Mo(CO)_2$, **74**, depending on the ratio of reactants.

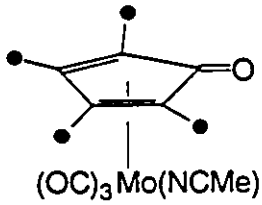

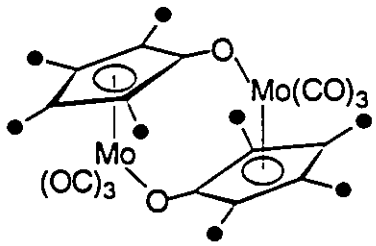

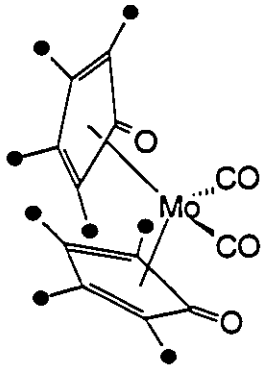

● = phenyl

72 **73** **74**

A number of reactions of C_3Ph_3H or of the $C_3Ph_3^+$ cation with organometallics have been reported [102]. Schrock [103] and Hughes [104] have investigated the experimental barrier to rotation of the η^3-C_3R_3 ligand, where R is a bulky substituent such as *tert*-butyl or phenyl, in a series of tungsten, molybdenum and ruthenium complexes. It was shown that in $CpMX_2(C_3R_3)$ systems the frontier orbitals of the $CpMX_2$ fragment play a crucial role in determining the rotational barrier [102h,104].

Of particular relevance to this work are a series of products, **75** through **79**, resulting from the treatment of $[Ph_3C_3]^+$ $[PF_6]^-$ or C_3Ph_3H with several coordinatively unsaturated organometallics. In the first four cases shown in Scheme 21, the opening of the cyclopropenyl ring has proceeded to a different

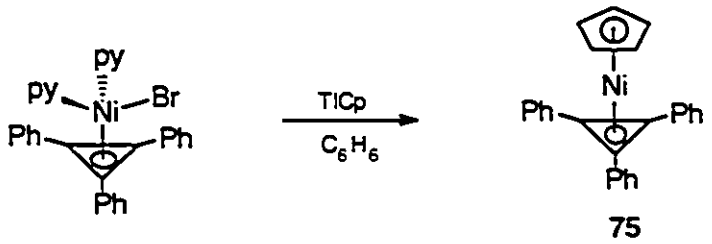

75

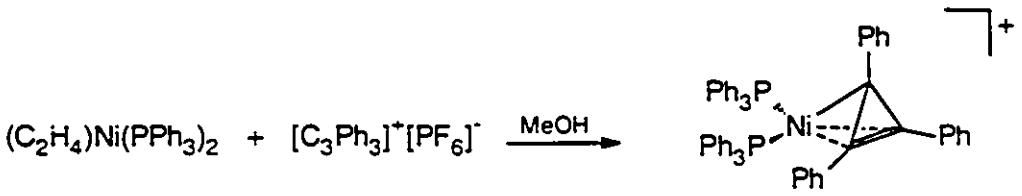

76

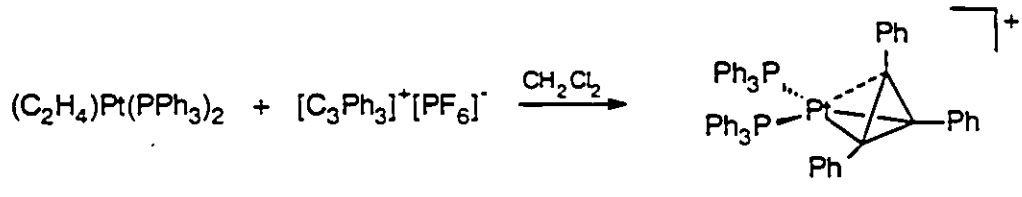

77

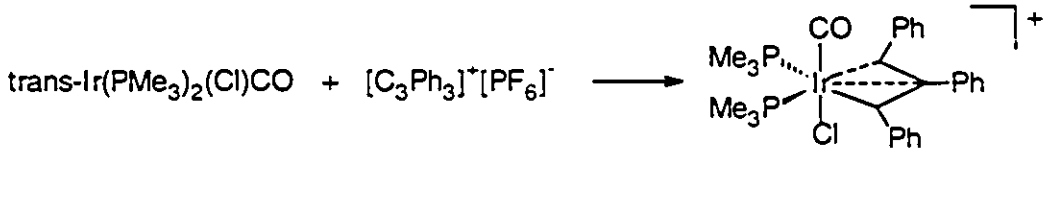

78

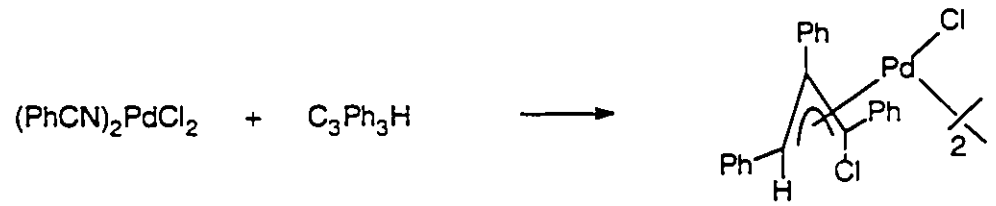

79

Scheme 21: Reactions of $[Ph_3C_3]^+[PF_6]^-$ and C_3Ph_3H with a series of organometallic complexes.

extent, culminating in the iridocycle, **78** [102c]. In **70**, the cyclopropene ring-opening is now complete, and the addition of hydrogen has generated the η^3-1,2,3-triphenylallyl ligand. The C_3Ph_3H molecule is reported to react with $(PhCN)_2PdCl_2$ to give $[(\eta^3$-1-chloro-1,2,3-triphenylallyl)$PdCl]_2$, **79** [102g]; however, x-ray crystallographic data on this molecule has not been reported.

One might envisage a route to **70** that involves an intermediate of the type (tetracyclone)$Mo(CO)_3(C_3Ph_3H)$, **80**, which subsequently undergoes cyclopropene ring-opening, perhaps via a metallacyclobutene, **81** [102i]. Another possible avenue might entail hydrogen transfer to give $(\eta^5$-$Ph_4C_5OH)Mo(CO)_2$ $(\eta^3$-$C_3Ph_3)$, **82**. However, such mechanistic proposals must remain speculative until deuterium-labelling studies can establish the source of the additional two hydrogens.

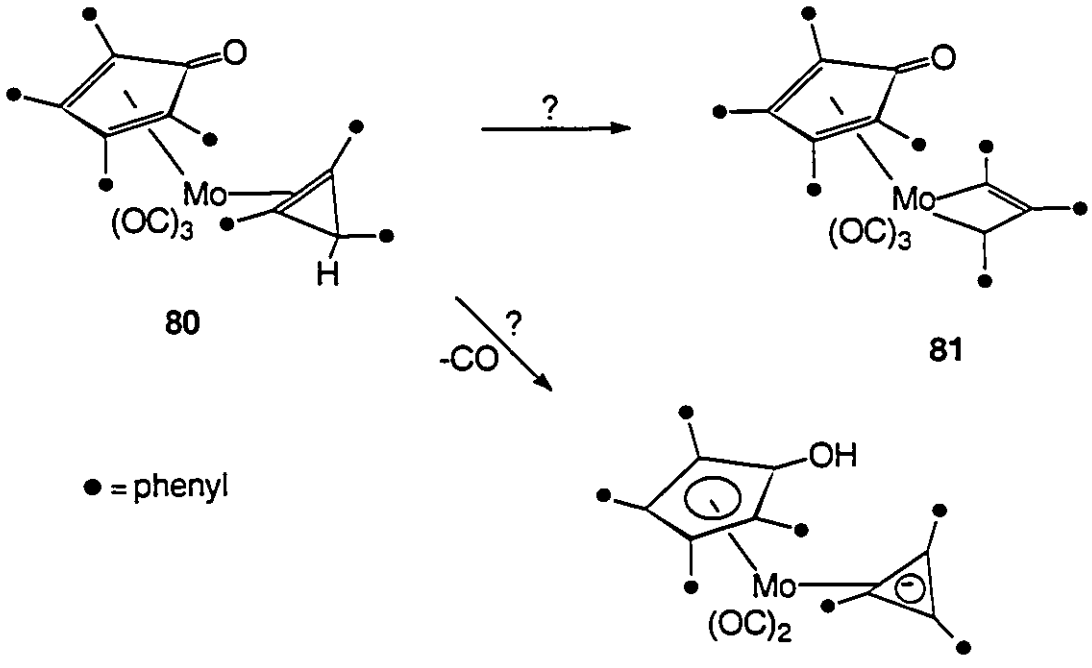

82

7.3 Complexes of $C_7Ph_7^+$ and $C_7Ph_7^-$

The reactions of C_7Ph_7H, **47**, or $C_7Ph_5Me_2H$, **51**, with $Cr(CO)_6$ revealed the preference of the organometallic moiety to bind to the peripheral ring rather than to the central ring. As mentioned previously, the seven-membered ring of triolefin complexes is oriented such that six sp^2 carbon atoms are coplanar and the methylene carbon is bent out of this plane. Perhaps such a conformation is not favorable for the considerably more crowded C_7Ph_7H ligand. The preparation of heptaphenyltropylium complexes, $[C_7Ph_7ML_n]^+$, in which the organometallic moiety could be coordinated to the planar tropylium ring, was also investigated. However, reactions of $C_7Ph_7^+$, **46**, with organometallic anions such as $[CpFe(CO)_2]^-Na^+$ and $[CpMo(CO)_3]^-Na^+$ did not lead to isolable products. This suggests that the bulkiness of the seven peripheral phenyl groups impedes the binding of metal fragments.

Subsequently, reactions with the $C_7Ph_7^-$ anion, **48**, were investigated. Once the orange-red colour of $C_7Ph_7^+Br^-$, **46a**, turned to the intense blue of the anion, it was treated with Me_3SnCl, resulting in the formation of the light yellow product, $C_7Ph_7SnMe_3$, **83**.

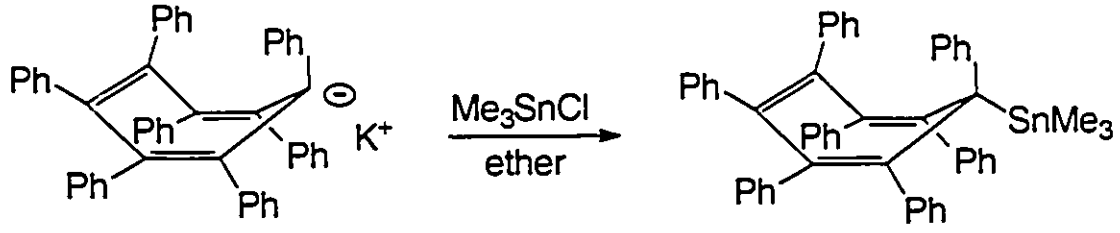

48 **83**

The dark blue colour of $C_7Ph_7^-K^+$ immediately disappeared as it reacted with the ethereal solution of Me_3SnCl. The light yellow product clearly exhibits a parent ion peak of 788 in its mass spectrum. The Me_3Sn moiety is expected to be σ bonded to the sp^3 carbon, as in its $C_7H_7SnMe_3$ analogue [105]. The NMR data do not permit an unequivocal assignment of the trimethyltin group as being axial or equatorial, and x-ray crystallographic data are required.

Treatment of $SiMe_2HCl$ with $C_7Ph_7^-K^+$ also results in the immediate decolorization of the blue anion and formation of a yellow cloudy solution. After removal of the insoluble salts by filtration, a light yellow product, **84**, was isolated whose ^1H NMR spectrum exhibits a septet at δ 4.72 corresponding to the Si-H linkage, and a doublet at δ 0.22 attributed to the methyls. In the IR spectrum, an Si-H stretch is clearly seen at 2126 cm^{-1}. Again, this $SiMe_2H$ moiety is expected to be σ-bonded to the sp^3 carbon. The structure of this derivative is expected to be similar to the boat conformation of the parent C_7Ph_7H as suggested by the rather similar ^1H and ^{13}C NMR spectra.

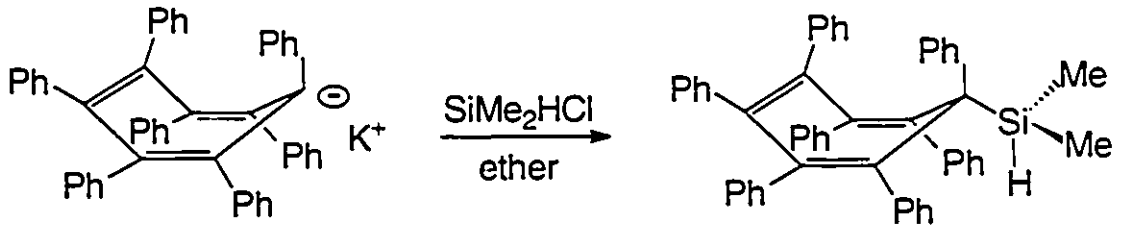

48 **84**

7.4 Conclusion

To conclude, the reaction of $Cr(CO)_6$ with C_7Ph_7H leads to incorporation of a $Cr(CO)_3$ group on a peripheral phenyl ring; attempts to coordinate $Mo(CO)_3$ or $W(CO)_3$ to the 7-membered ring have so far been unsuccessful. The corresponding $(\eta^6\text{-}C_7H_8)M(CO)_3$ complexes, where M = Cr, Mo, W, adopt geometries whereby the six coordinated sp^2 carbons are almost coplanar, and only the methylene group is bent substantially out of this plane [95a]. Such a conformation may be energetically disfavored for the C_7Ph_7H ligand, and it has not yet been possible to characterize any molecules in which a metal is coordinated to the central ring of the heptaphenylcycloheptatriene ligand. However, the tricyclic ketone **50** which is the precursor to **47**, reacts with $Mo(CO)_6$ to give the complex $(\eta^5\text{-}C_5Ph_4OH)Mo(CO)_2(\eta^3\text{-}C_3Ph_3H_2)$.

Although there appears to be a steric problem in binding of organometallic moieties to the central cycloheptatriene or tropylium ring, σ-bonding of small groups can be accomplished at the sp^3 carbon via the reactive $C_7Ph_7^-$ anion, **48**.

CHAPTER EIGHT

FUTURE WORK ON HEPTAPHENYLCYCLOHEPTATRIENE AND RELATED LIGANDS

8.1 Further Studies on Organometallic Derivatives of C_7Ph_7H

From the crystal structures and NMR data of the polyphenylated ligands, it is apparent that the phenyl groups lead to considerable crowding in the molecule. This steric hindrance may account for the difficulty in binding organometallic fragments to the central ring. Since there has been some success with reactions of the $C_7Ph_7^-$ anion, it may provide a route to complexes in which initially σ-bonded organometallic fragments could be induced photochemically or thermally to rearrange to a π-bonded product.

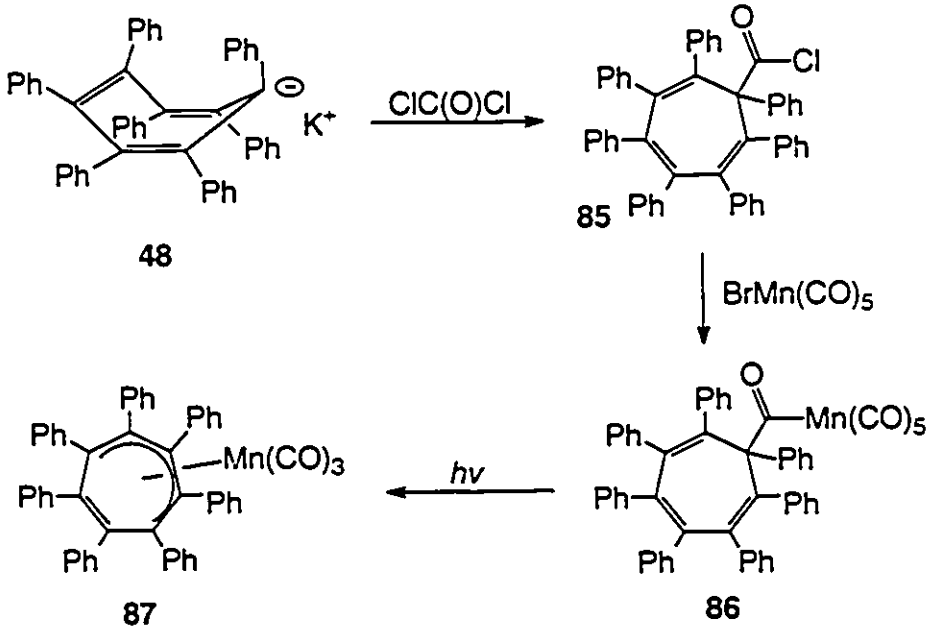

Just as the $C_7H_7C(O)Mn(CO)_5$ complex rearranges to $(\eta^5\text{-}C_7H_7)Mn(CO)_3$ upon irradiation [106], $C_7Ph_7C(O)Mn(CO)_5$, **86**, which could be prepared from $C_7Ph_7C(O)Cl$, **85**, and $BrMn(CO)_5$, may rearrange to $(\eta^5\text{-}C_7Ph_7Mn(CO)_3$, **87**.

The reaction of $C_7Ph_7^-$ with such compounds as Me_3SnCl or $SiMe_2HCl$ requires further investigation. In terms of structure, will there be a competition between the phenyl and one of these substituents for the axial position at the sp^3 carbon? Structural studies will have to be done as well as additional reactions with other compounds such as Me_3SiCl, Ph_3SiCl, or Ph_3SnCl. Further reactions, for example at the reactive Si-H bond, can also be investigated. This hydrogen could be replaced by an isolobal organometallic moiety such as $Co(CO)_4$ to give **88**.

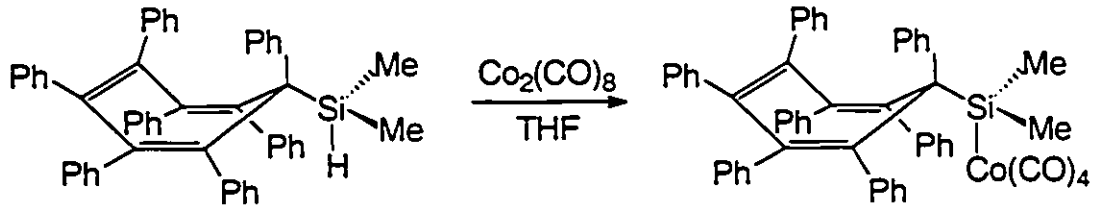

84 **88**

8.2 Preparation of C_7Cl_8 and Related Ligands

Since these polyaryl systems are quite crowded, perhaps replacing one or more of the phenyl groups with chloro substituents could reduce the steric problem. We have undertaken some preliminary studies on seven-membered rings containing chloro groups. Tetrachlorocyclopentadienone, C_4Cl_4CO, would

be an ideal diene in a Diels-Alder reaction with 1,2,3-triphenylcyclopropene to make tetrachlorotriphenylcycloheptatriene, $C_7Cl_4Ph_3H$. There is an old report that fluorosulfonic acid converts C_5Cl_6, **89**, into the required ketone which undergoes Diels-Alder self-dimerization to give **90** [107].

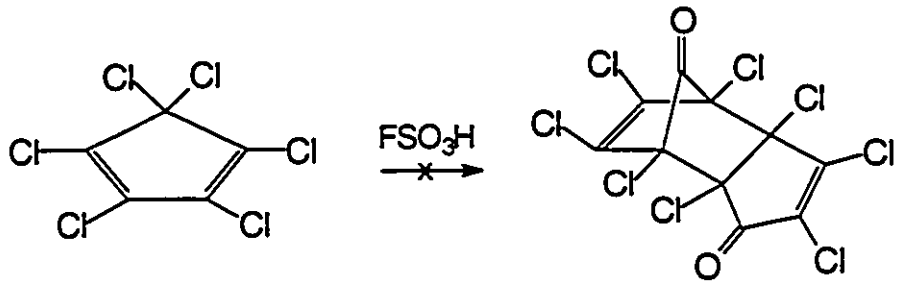

89 **90**

Subsequent work suggested that this was not true and that a cubane-type system is formed [108]. We repeated this preparation and what resulted was the product, **91**, whose x-ray crystal structure is shown in Figure 35. **91** crystallizes in the orthorhombic space group $Pna2_1$ with a = 25.449 (4) Å, b = 8.465 (2) Å, c = 8.880 (3) Å, and V = 1913.0 (7) $Å^3$ for Z = 4. The cubane-like structure of **91** contains two cyclopentane rings connected by four single bonds. The connection of the two five-membered rings actually produces a cage structure of two four-membered cyclobutane rings and four cyclopentane rings. The two apex carbon atoms are in a trans relationship with each other, with one OSO_2F group attached to apex carbon, C1. There is a crystal structure of the analogous chlorosulfate ester system which was derived from film data; the molecular parameters were not as good as can be obtained with modern automated diffractometer techniques [109].

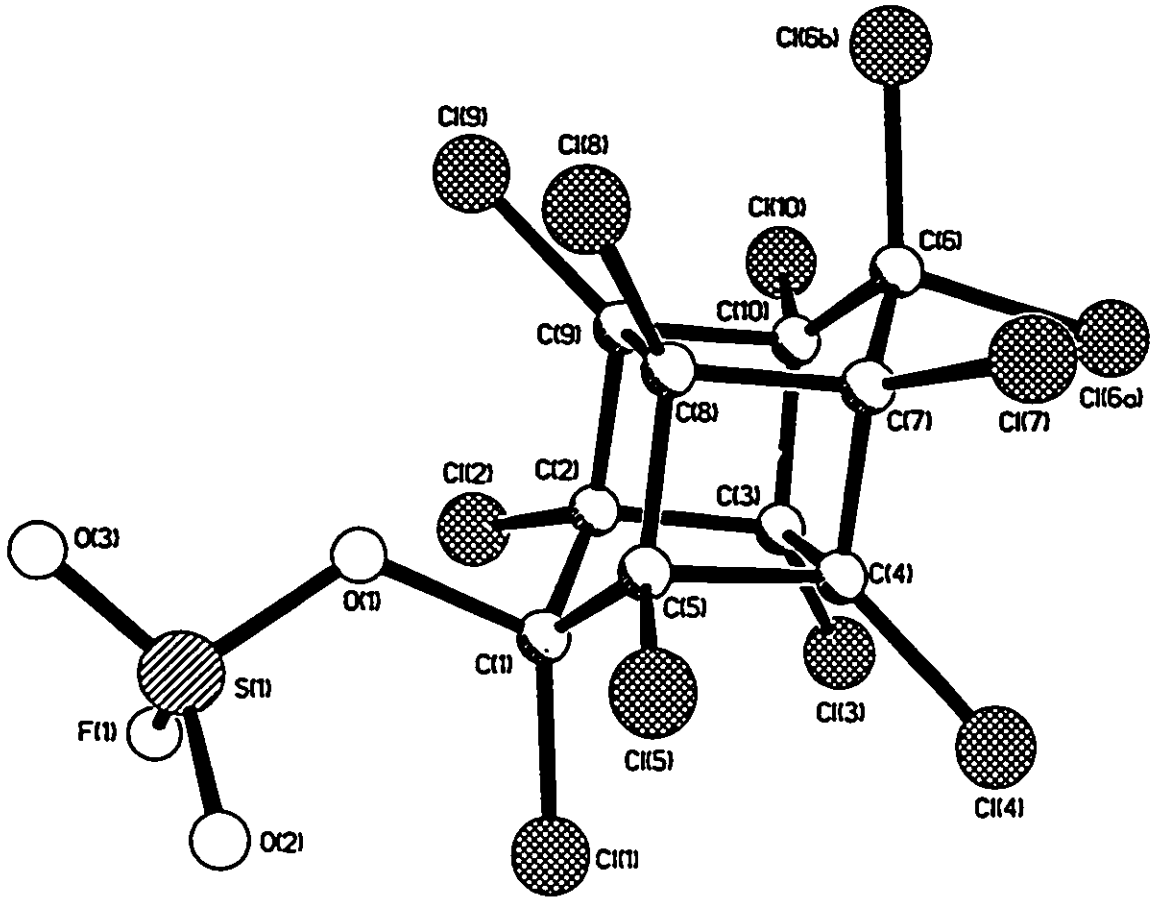

*Figure 35: X-ray crystal structure of $C_{10}Cl_{11}OSO_2F$, **91**.*

Another possible route to the $C_7Cl_4Ph_3H$ molecule has been investigated to circumvent the initial difficulties. Two of the chloro substituents of hexachlorocyclopentadiene, **89**, were first replaced with methoxy groups and the resulting product was treated with 1,2,3-triphenylcyclopropene. The Diels-Alder adduct, **92**, was characterized by NMR and mass spectrometry. The intent was to hydrolyze the ketal, **92**, to the ketone, **93**, and eliminate CO as had been done for C_7Ph_7H itself. However, it has thus far not been possible to hydrolyze the ketal to the ketone. There are literature precedents for the difficulty in hydrolyzing such ketals; for example, the Diels-Alder adduct from $C_5Cl_4(OMe)_2$ and acrylic acid can only be converted to the ketone after treatment in 90% H_2SO_4 [110]. Clearly, vigorous conditions will be required to hydrolyze **92**.

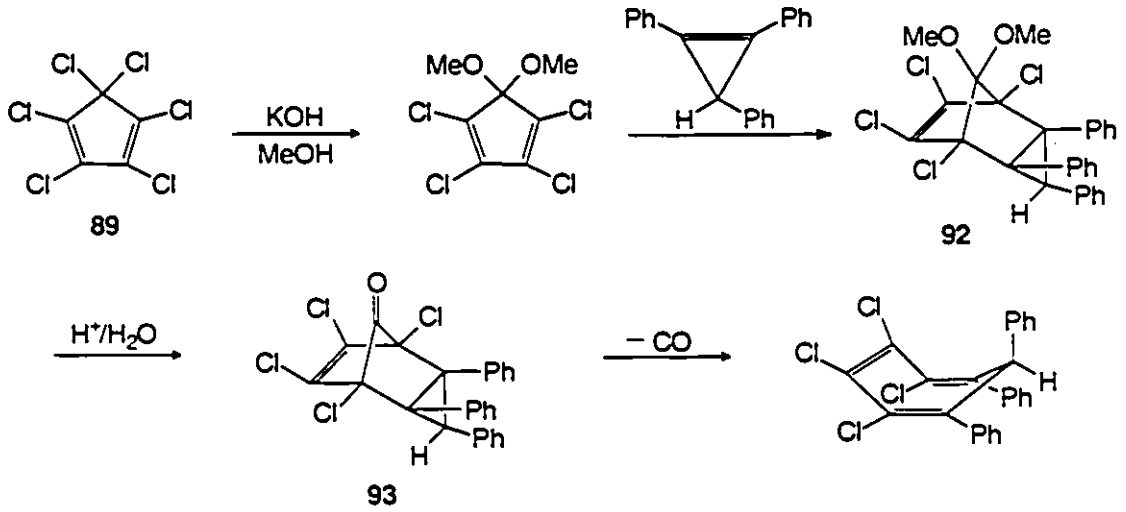

Alternatively, the dienophile in the Diels-Alder reaction may possess the chlorine groups. Tetrachlorocyclopropene, **94**, could be prepared [111] and subsequently treated with tetracyclone to give the tetrachlorotetraphenylcyclo-heptatriene molecule, $C_7Cl_4Ph_4$, **95**.

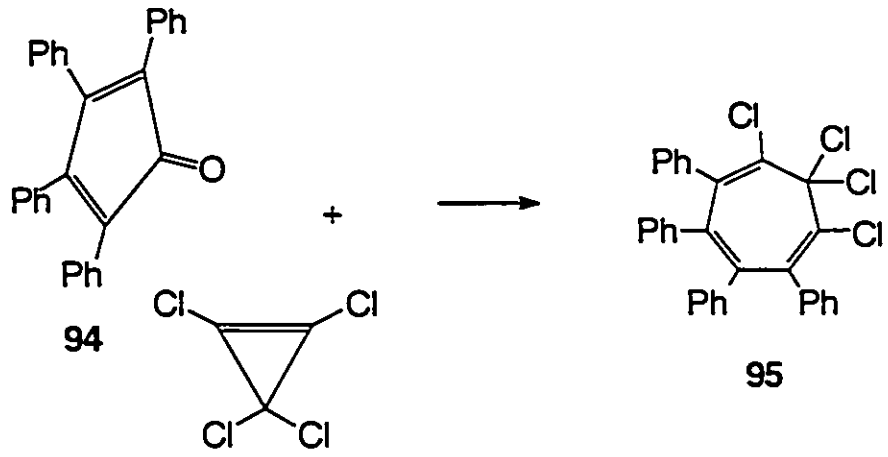

There is a reported synthesis of C_7Cl_8, **97**, via the $C_7Cl_7^+$ cation, **96** [112]. It would be interesting to treat both of these compounds, as analogues of cycloheptatriene and tropylium, with organometallic fragments.

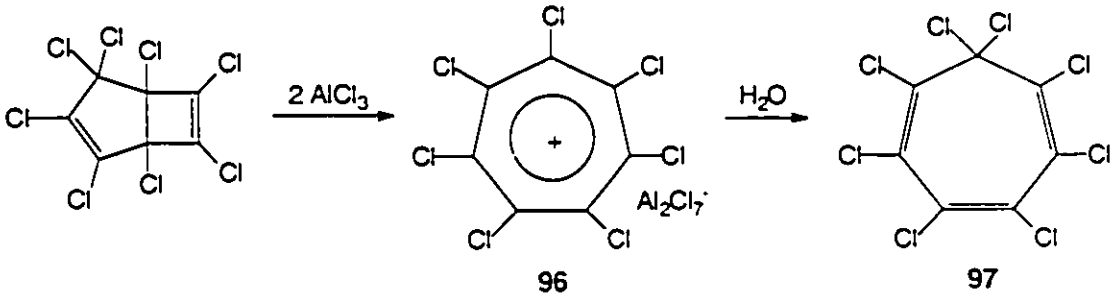

Initial studies on the reaction of the C_7Cl_8 ligand, **97**, with $RhCl(CO)(PPh_3)_2$ resulted in the formation of the *syn*-dimer, $C_{14}Cl_{12}$, **98**. This product may be a result of a metal carbene reaction. The *syn* and *anti* dimer have previously been prepared by reaction of octachlorocycloheptatriene and butyllithium [113].

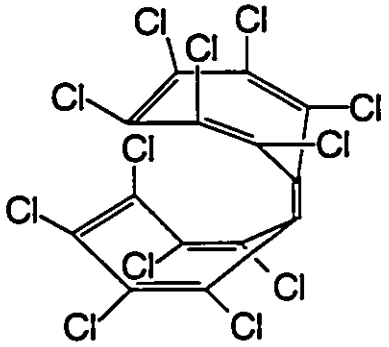

98

Other interesting products could result upon reaction of these chloro compounds with metal carbonyls, just as the novel multi-cluster system, **2**, was prepared via the reaction of hexachlorocyclopropane and dicobalt octacarbonyl [16].

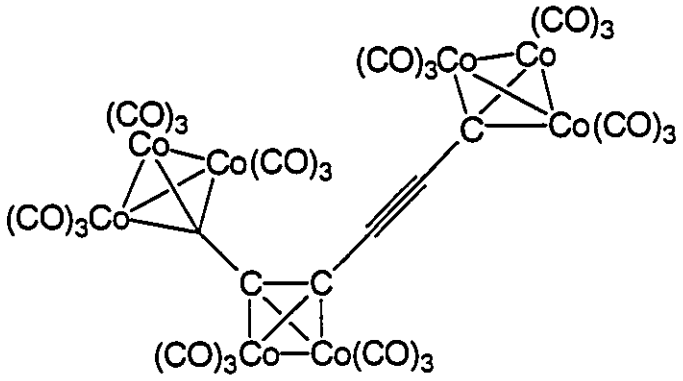

2

In these chloro derivatives, the chloro groups are not only smaller substituents, but also have the potential to undergo further reactions. For example, reaction of C_7Cl_8, **97**, with the trimethylsilylethynyl anion could result in replacement of at least one chloro group on the sp^3 carbon to give **99**. This, in

turn, could be treated with dicobalt octacarbonyl and subsequently allowed to react with aluminum trichloride to generate a cluster-complexed hexachloro-tropylium ion, **100**.

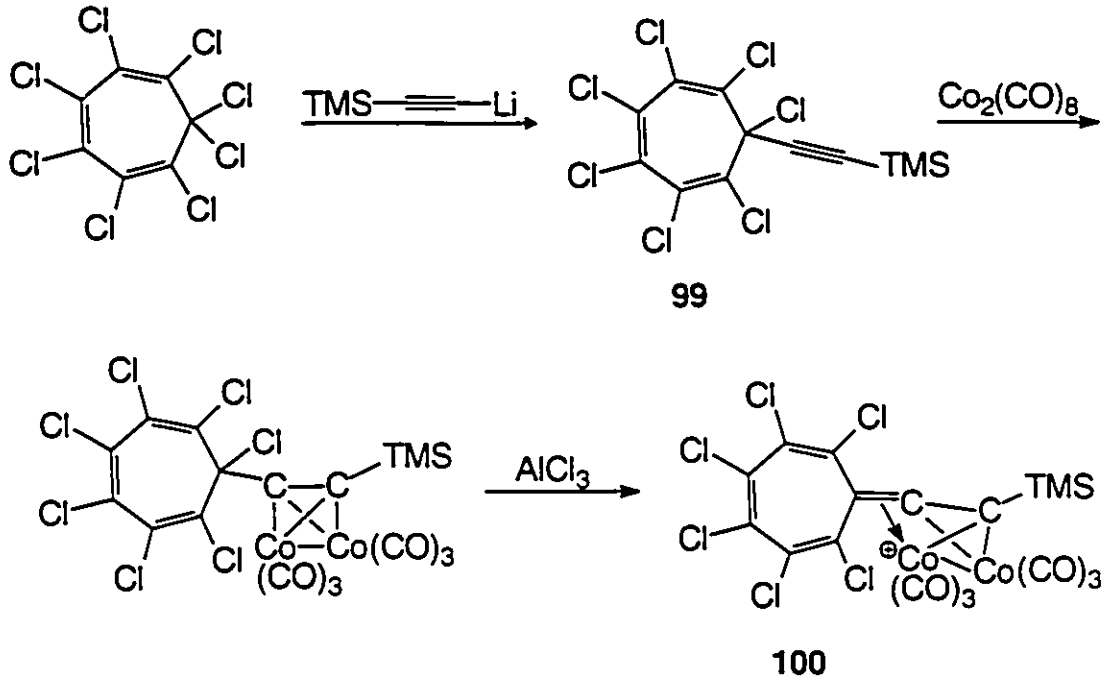

99

100

The stability of the tropylium ring may allow the isolation and an x-ray crystallographic study of **100** which would be the first $Co_2(CO)_6$ cluster cation to be structurally characterized.

CHAPTER NINE

EXPERIMENTAL SECTION

9.1 General Techniques

All reactions were carried out under an atmosphere of dry nitrogen employing conventional benchtop and glovebag techniques. All solvents were dried according to standard procedures before use [114]. Silica gel (particle size: 20-45 microns) was employed for flash column chromatography.

The 500 MHz ^{1}H and 125.7 MHz ^{13}C solution NMR spectra were recorded on a Bruker AM-500 spectrometer using a 5 mm dual frequency $^{1}H/^{13}C$ probe. The 300 MHz ^{1}H and 75.4 MHz ^{13}C NMR spectra were collected on a Bruker AC-300 spectrometer. The 200 MHz ^{1}H and 50.3 MHz ^{13}C NMR spectra were collected on a Bruker AC-200 spectrometer. ^{13}C CPMAS spectra were recorded on a Bruker MSL 100 instrument. All spectra were measured in CD_2Cl_2 or $CDCl_3$ and chemical shifts are reported relative to tetramethylsilane. NMR spectra were collected at ambient temperatures unless otherwise noted.

All direct electron impact (DEI), direct chemical ionization (DCI) ,and Fast Atom Bombardment (FAB) mass spectra were generated with a VG analytical ZAB-E double focusing mass spectrometer. Typical source conditions for DEI and

DCI include source temperature at 200°C, source pressure 2 X 10^{-6} mbar for DEI (4 X 10^{-5} mbar for DCI), mass resolution = 1000, electron energy = 70 eV, and an accelerating potential of 6kV. For FAB, 3-Nitrobenzyl alcohol was used as the sample matrix and xenon was the bombarding gas (8 keV). Electrospray (ESI) mass spectra were generated with a Fisons Platform quadrupole mass spectrometer with 50/50 CH_3CN/H_2O at 15 µl/min as mobile phase and for ESI^+, in some cases, a small amount of CF_3COOH is added.

Infrared spectra were recorded on a Perkin-Elmer 283, or a Bio-Rad FTS-40 instrument using NaCℓ plates. Melting points were determined on a Thomas Hoover capillary melting point apparatus and are uncorrected. Microanalytical data are from Guelph Chemical Laboratories, Guelph, Ontario.

9.2 Experimental Procedures

Preparation of p-$C_6H_4[O_2CCCℓ_3]_2$: $CℓCOCCℓ_3$ (10.13 mL, 90.8 mmol) was added dropwise over a period of 45 minutes to a solution of p-$C_6H_4(OH)_2$ (5.00 g, 45.4 mmol) and pyridine (7.34 mL, 90.8 mmol) in ether (80 mL). Pyridine was added until the mixture was no longer acidic. The reaction mixture was extracted with 150 mL of 1.2N HCℓ (four times), and the combined aqueous layers with 50 mL of ether (two times). The combined ether layers were dried over Na_2SO_4, and filtered. Evaporation of the solvent and recrystallization of the resultant solid from petroleum ether yielded p-$C_6H_4[O_2CCCℓ_3]_2$ as white platelets (10.28 g, 25.64

mmol, 57%). ^{1}H NMR ($CDC\ell_3$): δ 7.32 (s, 4H). ^{13}C NMR ($CDC\ell_3$): δ 160.28 (ester carbonyl), 148.66 (*C*1, *C4* of phenyl ring), 122.04 (*C*2, *C*3, *C*5, *C*6 of phenyl ring), and 114.41 (-*C*$C\ell_3$). IR ($CH_2C\ell_2$): $\nu_{c=o}$, 1785 cm^{-1}(s). Mass spectra (EI): m/z (%) 398 (18) $C_6H_4(O_2CCC\ell_3)_2$ [M^+]; 253 (20) [M - $COCC\ell_3$]$^+$; 237 (35) [M - $O_2CCC\ell_3$]$^+$. Peaks quoted are in each case the lowest mass in each envelope and correspond to $^{35}C\ell$.

Preparation of *p*-$C_6H_4[O_2CCCo_3(CO)_9]_2$, 15: A solution of $Co_2(CO)_8$ (9.21 g, 26.94 mmol) and *p*-$C_6H_4[O_2CCC\ell_3]_2$ (3.00 g, 7.48 mmol) in 110 mL of tetrahydrofuran (THF) under N_2 was stirred at room temperature for 1 hour and then at 40°C for 2 hours. After cooling to room temperature, the mixture was filtered and the solvent removed under vacuum. The sample was then redissolved in hexane, filtered, and the solvent removed under vacuum. This solid was placed onto a silica column and eluted with hexane/$CH_2C\ell_2$ (1:1) to obtain **15**, as a purple solid (0.372 g, 0.36 mmol, 4.8%). IR ($CH_2C\ell_2$): ν_{co} at 2105 (w), 2060 (vs), 2041 (s); $\nu_{c=o}$ at 1697 (w) cm^{-1}. Mass spectra (FAB$^+$): m/z (%) 626 (28) [M - 15CO]$^+$; 570 (25) [M - 17CO]$^+$; 542 (100) [M - 18CO]$^+$; 514 (42) [M - 19CO]$^+$, 486 (10) [M - $O_2CCCo_3(CO)_9$]$^+$.

Preparation of $C[CH_2O_2CCC\ell_3]_4$, 16: $C\ell COCC\ell_3$ (16.4 mL, 146.8 mmol) was added dropwise over a period of 1.5 hours to a solution of $C[CH_2OH]_4$ (5.00

g, 36.7 mmol) and pyridine (17.0 mL, 210.2 mmol) in ether (80 mL) and was then allowed to stir for 6 hours. Excess pyridine was added until the mixture was no longer acidic. The mixture was then extracted with 4 x 100mL of 1.2N HCℓ. The ether layer was dried with Na_2SO_4 and removed, leaving a white solid **16** which was further washed with petroleum ether (7.03 g, 9.79 mmol, 27%), m.p. 150-152°C. Recrystallization of **16** from diethyl ether/petroleum ether (50:50) gave X-ray quality crystals. ^{1}H NMR ($CDC\ell_3$): δ 4.53 (s). ^{13}C NMR ($CDC\ell_3$): δ 161.0 (ester carbonyl), 88.9 ($CC\ell_3$), 65.3 (CH_2), and 43.6 (tertiary *C*). IR ($CH_2C\ell_2$): $\nu_{C=O}$ 1770 (s) cm^{-1}. Mass spectrum (DCI): *m/z* (%) 730 (100) $[M + NH_3]^+$; 677 (7) $[M - C\ell]^+$; 551 (51) $[M - O_2CCC\ell_3]^+$; 390 (12) $[M - 2(O_2CCC\ell_3)]^+$; 244 (25) $[M - 4(CC\ell_3)]^+$; and 227 (8) $[M - 3(O_2CCC\ell_3)]^+$. Peaks quoted are in each case the lowest mass in each envelope and correspond to $^{35}C\ell$.

Reaction of 16 with $Co_2(CO)_8$: $Co_2(CO)_8$ (1.77 g, 5.12 mmol) and $C[CH_2O_2CCC\ell_3]_4$ (0.52 g, 0.72 mmol) in 20 mL of THF were heated at 40°C for 3.5 hours. After cooling, the mixture was filtered to remove cobalt salts, and the solvent was removed *in vacuo*. Flash chromatography using 100% $CH_2C\ell_2$ as eluant showed the presence of at least six different products. The first band to elute was $Co_4(CO)_{12}$, a purple-black solid (0.251 g, 0.439 mmol). The second band obtained was $C[CH_2O_2CCCo_3(CO)_9]_3(CH_2O_2CCC\ell_3)$, **17**, a purple oil (0.099 g, 0.059 mmol, 7%). IR ($CH_2C\ell_2$): ν_{CO} at 2111 (w), 2067 (vs), 2048 (s); $\nu_{C=O}$ at

1607 (m, broad) cm^{-1}. Mass spectrum: a) (FAB^+, MCA) *m/z* (%) 1208 (18) [M - 17CO]$^+$; 1180 (18) [M - 18CO]$^+$; 1095 (38) [M - 21CO]$^+$; 1068 (20) [M - 22CO]$^+$; 1039 (42) [M - 23CO]$^+$; 984 (15) [M - 25CO]$^+$; 956 (37) [M - 26CO]$^+$; and 927 (100) [M - 27CO]$^+$. b) (FAB^+) *m/z* (%) 1068 (24) [M - $CCo_3(CO)_9$ - $CH_2O_2CCC\ell_3$]$^+$; 1040 (68) [M - $CCo_3(CO)_9$ - $CH_2O_2CCC\ell_3$ - CO]$^+$; 958 (46) [M - $CCo_3(CO)_9$ - $CH_2O_2CCC\ell_3$ - 4CO]$^+$; 928 (100) [M - $CCo_3(CO)_9$ - $CH_2O_2CCC\ell_3$ - 5CO]$^+$; 844 (38) [M - $CCo_3(CO)_9$ - $CH_2O_2CCC\ell_3$ - 8CO]$^+$; and 760 (79) [M - $CCo_3(CO)_9$ - $CH_2O_2CCC\ell_3$ - 11CO]$^+$. The fourth band, a purple oil (0.033 g, 4.4%), was tentatively assigned as $C[CH_2O_2CCCo_3(CO)_9](CH_2O_2CCC\ell_3)_3$. IR ($CH_2C\ell_2$): ν_{CO} at 2103 (w), 2050 (vs), 2042 (s); $\nu_{C=O}$ at 1606 (w) cm^{-1}. Mass spectrum: (FAB^+, MCA) *m/z* (%) 1036 (7) [M$^+$]; 1007 (27) [M - CO]$^+$; 924 (20) [M - 4CO]$^+$. Peaks quoted are in each case the lowest mass in each envelope and correspond to $^{35}C\ell$.

Preparation of $C\ell_3CC(O)CH_2C(O)CH_3$, 23: According to the procedures of Coenen [58] and of Ringel [59], $C\ell_3CCN$ (35.0 g, 0.24 mol) and acetylacetone (25.0 g, 0.24 mol) were dissolved in 100 mL MeOH. While stirring, 50 mL of a saturated aqueous solution of sodium acetate was slowly added. The reaction mixture was stirred for 2 hours and was then slowly poured into 700 mL of cold H_2O, in which a white precipitate formed immediately. It was subsequently filtered and recrystallized from hexane to give $C\ell_3CC(NH_2)=CHC(O)CH_3$ (44.25 g, 0.22

mol, 90%). This product was then treated with 78.8 mL of conc. HCℓ. Heat was evolved and $NH_4C\ell$ and an oil separated out. After cooling the solution 63.0 mL of H_2O were added. The oily layer was then treated with 118 mL of ether, dried with Na_2SO_4, and filtered. Removal of the solvent gave a liquid, which was distilled at reduced pressure (bp_{18} 100-101°C) to yield **23** as a colorless liquid (31.68 g, 0.16 mol, 71%). ^{1}H NMR ($CDC\ell_3$): δ 6.10 (s, 1H, C*H* of enol), 4.05 (s, 2H, CH_2 of keto), 2.29 (s, 3H, CH_3 of keto), and 2.15 (s, 3H, CH_3 of enol). ^{13}C NMR ($CDC\ell_3$): δ 186.8, 185.3 (carbonyls), 94.7 ($CC\ell_3$), 92.9 (*C*H of enol), 48.9 (CH_2 of keto), 30.1 (CH_3 of keto), and 22.9 (CH_3 of enol). IR ($CH_2C\ell_2$): $\nu_{C=O}$ at 1595 (vs) cm^{-1}. Mass spectrum (EI): *m/z* (%) 202 (18) $C\ell_3CC(O)CH_2C(O)CH_3$ $[M]^+$; 187 (5) $[M - CH_3]^+$; 167 (36) $[M - C\ell]^+$; 152 (25) $[M - C\ell - CH_3]^+$; 139 (100) $[M - C\ell - CO]^+$; and 117 (27) $[M - C(O)CH_2C(O)CH_3]^+$. Peaks quoted are in each case the lowest mass in each envelope and correspond to $^{35}C\ell$.

Preparation of $A\ell[C\ell_3CC(O)CHC(O)CH_3]_3$, 25: Although **25** has been reported previously and characterized by mass spectrometry [60], no synthetic procedure nor NMR data are available. **23** (2.00 g, 9.83 mmol) was added to a solution of aluminum isopropoxide (0.669 g, 3.28 mmol) in 6.4 mL of benzene. After the solution was allowed to stand for 2 hours, benzene and the 2-propanol produced were removed by using a rotovap to yield a white solid, **25** (1.614 g, 2.54 mmol, 78%). ^{1}H NMR ($CDC\ell_3$): δ at 6.41 (s, 1H); 6.40 (s, 1H), 6.38 (s, 3H), 6.32 (s, 1H),

2.32 (s, 3H), 2.28 (s, 12H), and 2.23 (s, 3H). ^{13}C NMR ($CDC\ell_3$): δ at 201.0, 200.4, 199.9 ($C(O)CC\ell_3$); 179.3, 178.7, 178.1 ($C(O)CH_3$); 95.1, 94.7, 94.4 (*C*H); and 28.34 (CH_3). IR ($CH_2C\ell_2$): $\nu_{C=O}$ 1614 (s), $\nu_{C=C}$ 1513 (s) cm^{-1}. Mass spectrum (FAB^+): *m/z* (%) 429 (79) [M - tcac]$^+$; 394 (49) [M - tcac - Cℓ]$^+$; 359 (24) [M - tcac - 2Cℓ]$^+$; 347 (28) [M - tcac - $CC\ell_2$]$^+$; 312 (25) [M - tcac - $CC\ell_3$]$^+$; and 228 (55) [M - 2(tcac)]$^+$. Peaks quoted are in each case the lowest mass in each envelope and correspond to $^{35}C\ell$ and $^{27}A\ell$.

Preparation of $Cu[C\ell_3CC(O)CHC(O)CH_3]_2$, 27: Although **27** has been reported previously and characterized by mass spectrometry [60], no synthetic procedure is available. Copper nitrate trihydrate (2.969 g, 12.29 mmol) was dissolved in 27.5 mL of water and to this was added, with mixing, **23** (5.00 g, 24.58 mmol) and sodium acetate (2.015 g, 24.57 mmol) in 2.75 mL water. A solid precipitated out of solution and was filtered and dried. Recrystallization from methanol yielded a grey-green solid, **27**, (3.965 g, 8.46 mmol, 69%) with a melting point of 197-198°C. IR ($CH_2C\ell_2$): $\nu_{C=O}$ 1601 (s), $\nu_{C=C}$ 1507 (s) cm^{-1}. Mass spectrum (FAB^+) shows evidence for dimerization: *m/z* (%) 729 (9) [M - tcac]$^+$; 571 (20) [M - tcac - $CHC(O)CC\ell_3$]$^+$; 528 (12) [M - 2(tcac)]$^+$; 465 (51) [M - 2(tcac) - Cu]$^+$; 458 (28) [M - 2(tcac) - 2Cℓ]$^+$; 416 (100) [M - 2(tcac) - Cu - CH_2 - Cℓ]$^+$; 369 (66) [M - 2(tcac) - $CHC(O)CC\ell_3$]$^+$; and 348 (31) [M - 2(tcac) - $CC\ell_3$ - Cu]$^+$. Peaks quoted are in each case the lowest mass in each envelope and correspond to $^{35}C\ell$ and ^{63}Cu.

Preparation of Al$[Co_3(CO)_9CC(O)CHC(O)CH_3]_3$, 26: **25** (1.755 g, 2.77 mmol) and $Co_2(CO)_8$ (5.109 g, 14.94 mmol) in 50 mL of THF were stirred at room temperature for 1.5 hours and at 40°C for 1.5 hours. The resulting solution was filtered and the solvent removed *in vacuo.* Column chromatography, using eluant ether/hexanes (1:4), yielded $Co_4(CO)_{12}$ (1.51 g, 2.64 mmol) as the first band and **26**, a brown-black oil, as the second band (0.310 g, 0.19 mmol, 7%). ^{13}C NMR ($CDC\ell_3$): δ at 220.8 ($C(O)CCo_3(CO)_9$); 196.2 (Co-*C*O's); 187.6 ($C(O)CH_3$); 117.4 (*C*H); and 29.7 (CH_3). IR ($CH_2C\ell_2$): ν_{CO} at 2108 (w), 2063 (vs), 2045 (s); $\nu_{C=O}$ at 1723 (m), 1601 (w), and 1525 (w) cm^{-1}. Mass spectrum (FAB^+): *m/z* (%) 1574 (7) $[M - CO]^+$; 1518 (14) $[M - 3CO]^+$; 1378 (11) $[M - 8CO]^+$; 1294 (11) $[M - 11CO]^+$; 1238 (20) $[M - 13CO]^+$; 1210 (23) $[M - 14CO]^+$: 1182 (30) $[M - 15CO^+]$; 1154 (24) $[M - 16CO]^+$; 1126 (35) $[M - 17CO]^+$; 1077 (30) $[M - Co_3(CO)_9CC(O)CHC(O)CH_3]^+$; 1049 (25) $[M - Co_3(CO)_9CC(O)CHC(O)CH_3 - CO]$; 1014 (25) $[M - 21CO]^+$; 986 (23) $[M - 22CO]^+$; 958 (42) $[M - 23CO]^+$; 937 (50) $[M - Co_3(CO)_9CC(O)CHC(O)CH_3 - 5CO]$; 909 (68) $[M - Co_3(CO)_9CC(O)CHC(O)CH_3 - 6CO]^+$; 881 (100) $[M - Co_3(CO)_9CC(O)CHC(O)CH_3 - 7CO]^+$; 853 (70) $[M - Co_3(CO)_9CC(O)CHC(O)CH_3 - 8CO]^+$; 825 (60) $[M - Co_3(CO)_9CC(O)CHC(O)CH_3 - 9CO]^+$; and 797 (36) $[M - Co_3(CO)_9CC(O)CHC(O)CH_3 - 10CO]^+$.

Preparation of $Co[Co_3(CO)_9CC(O)CHC(O)CH_3]_2$, 28, and $Co[Co_3(CO)_9CC(O)CHC(O)CH_3]_3$, 29: **27** (0.76 g, 1.62 mmol) and $Co_2(CO)_8$

(2.00 g, 5.84 mmol) were dissolved in 30 mL of THF and stirred at room temperature for 1 hour and at 40°C for 1 hour. This mixture was allowed to cool, and filtration and solvent removal *in vacuo* yielded a crude solid that was purified by flash chromatography ($CH_2C\ell_2$/hexanes, 1:1). The first band was a brown-black oil, **28** (0.180 g, 0.162 mmol, 10%). IR of **28**, ($CH_2C\ell_2$): ν_{CO} at 2108 (m), 2063 (vs), 2045 (s); $\nu_{C=O}$ at 1722 (vw), and 1599 (w) cm^{-1}. Mass spectrum (FAB^+) of **28**: *m/z* (%) 1109 (20) $Co[Co_3(CO)_9CC(O)CHC(O)CH_3]_2$, $[M]^+$; 1082 (12) $[M - 1CO]^+$; 1024 (73) $[M - 3CO]^+$; 998 (32) $[M - 4CO]^+$; 941 (33) $[M - 6CO]^+$; 913 (100) $[M - 7CO]^+$; 885 (77) $[M - 8CO]^+$; 857 (58) $[M - 9CO]^+$; 829 (85) $[M - 10CO]^+$; and 800 (69) $[M - 11CO]^+$. The second band was a brown-black oil, **29** (0.126g, 0.077 mmol, 7%). IR of **29**, ($CH_2C\ell_2$): ν_{CO} at 2107 (m), 2063 (vs), 2044 (s); $\nu_{C=O}$ at 1723 (w), 1595 (m), and 1515 (m) cm^{-1}. Mass spectrum $(FAB)^+$ of **29**: *m/z* (%) 1521 (10) $[M - 4CO]^+$; 1353 (33) $[M - 10CO]^+$; 1297 (42) $[M - 12CO]^+$; 1157 (37) $[M - 17CO]^+$; 1129 (43) $[M - 18CO]^+$; 1024 (51) $[M - Co_3(CO)_9CC(O)CHC(O)CH_3 - 3CO]^+$; 997 (72) $[M - Co_3(CO)_9CC(O)CHC(O)CH_3 - 4CO]$; 913 (100) $[M - Co_3(CO)_9CC(O)CHC(O)CH_3 - 7CO]^+$; 885 (76) $[M - Co_3(CO)_9CC(O)CHC(O)CH_3 - 8CO$; 857 (77) $[M - Co_3(CO)_9CC(O)CHC(O)CH_3 - 9CO]$; 829 (96) $[M - Co_3(CO)_9CC(O)CHC(O)CH_3 - 10CO]^+$; and 801 (94) $[M - Co_3(CO)_9CC(O)CHC(O)CH_3 - 11CO]$. Repeated chromatography on **28** led to decomposition and yielded black crystals of **24**. Recrystallization from methylene chloride/ hexane (50:50) gave an X-ray quality sample of **24**.

Preparation of (benzoylacetone)$Cr(CO)_3$, 32: According to the literature procedure [62], (methylbenzoate)chromiumtricarbonyl (1.117 g, 4.104 mmol) and acetone (0.285 g, 4.907 mmol) in ether (20 mL) were treated with NaOEt (0.293 g, 4.309 mmol) over 1 hour under N_2 atmosphere. A bright yellow precipitate formed which was filtered and then dissolved in water. Bubbling CO_2(g) resulted in the formation of an orange-red precipitate, which was extracted with ether. The ether layer was dried over Na_2SO_4, filtered, and then removed, yielding a brick-red solid, **32** (0.653 g, 2.190 mmol, 54%), m.p. 119-121°C (Lit. 115-117°C [62]). ^1H NMR ($CDC\ell_3$): δ 5.99 (d, 2H, *ortho-H*), 5.84 (s, 1H, C*H* of enol), 5.56 (t, 1H, *para-H*), 5.28 (t, 2H, *meta-H*), 3.86 (s, 2H, CH_2 of keto). 2.31 (s, 3H, CH_3 of keto), and 2.15 (s, 3H, CH_3 of enol). ^{13}C NMR (acetone-d_6): δ 232.6 (Cr-*C*O of enol), 232.1 (Cr-*C*O of keto), 202.3, 192.9 (*C*O of keto), 191.3, 185.3 (*C*O of enol), 97.78 (*ipso-C* of enol), 97.2, 96.1 (*para-C*, *C*H of enol), 94.7, 92.1 (*meta-C*, *ortho-C*), 53.2 (CH_2 of keto), 24.4 (CH_3 of enol). ^{13}C CPMAS: δ 233.0 (Cr-*C*O of enol), 195.1, 183.0 (*C*O of enol), 97.3, 94.4 (*ipso-C*, *para-C*, *meta-C*, *ortho-C*, and *C*H of enol), and 26.6 (CH_3 of enol). IR ($CH_2C\ell_2$): $\nu_{C=O}$ at 1980 (s), and 1909 (s) cm^{-1}. Mass spectrum (DEI): *m/z* (%) 298 (5) $[M]^+$; 242 (8) $[M - 2CO]^+$; 214 (30) $[M - 3CO]^+$; 171 (10) $[M - 3CO - COCH_3]^+$; and 52 (100) $[Cr]^+$.

Preparation of C_7Ph_7H, 47: **47** was prepared from 2,3,4,5-tetraphenylcyclopentadienone and 1,2,3-triphenylcyclopropene according to the literature procedure [79]. Recrystallization from $CHCl_3$/ether gave a 72% yield of colourless crystals, m.p. 284-286 °C (Lit. 285-287.5 °C). ^1H and ^{13}C NMR data are listed in Table 3. Mass spectrum (DEI): *m/z* (%) 624(100) $[M]^+$; 546 (32) $[M-Ph-H]^+$; 469 (35) $[M-2Ph-H]^+$; 391 (17) $[M-3Ph-2H]^+$.

Preparation of C_7Ph_7HCO, 50: 2,3,4,5-Tetraphenylcyclopentadienone (2.341 g, 6 mmol) and 1,2,3-triphenylcyclopropene (0.806 g, 3 mmol) in benzene were stirred at room temperature for 6 days. **50** was purified by flash chromatography using 3:2 CH_2Cl_2/hexanes as the eluent. The first band gave **50** (1.568 g, 2.4 mmol, 80%), which recrystallized from CH_2Cl_2/hexane as colourless plates. ^1H NMR (200 MHz, CD_2Cl_2): δ 7.30-6.77 (m, 35H, phenyl protons), 3.60 (s, 1H, H7). ^{13}C NMR (50.288 MHz, CD_2Cl_2): δ 194.16 (C8), 142.97 (C3/C4), 137.04, 135.38, 135.10, 133.55, 133.41, 131.72, 130.01, 127.81, 127.37, 127.10, 126.98, 126.75, 126.39, 126.13 (phenyl carbons), 68.77 (C2/C5), 38.56 (C1/C6), 31.95 (C7). IR (CH_2Cl_2): ν_{CO} 1768 cm^{-1}. Mass spectrum (DEI): *m/z* (%) 652 (5) $[M]^+$; 624 (100) $[M-CO]^+$; 547 (5) $[M-CO-Ph]^+$.

Preparation of $C_7Ph_5Me_2H$, 51: 2,5-Dimethyl-3,4-diphenylcyclopentadienone dimer (1.30 g, 2.5 mmol) was heated in refluxing xylenes (25 mL) for 1 hour. Formation of the monomer, **53**, was indicated by a red colouration of the solution. 1,2,3-Triphenylcyclopropene (1.315 g, 4.9 mmol) was then added and the mixture heated under reflux for 4 days, after which time the xylenes were removed by distillation. The product was recrystallized from pentane to give

colourless crystals of **51** (0.80 g, 30%), m.p. 181-185 °C. ^{1}H and ^{13}C NMR data are listed in Table 3. Mass spectrum (DEI): *m/z* (%) 500 (100) $[M]^+$; 485 (10) $[M-CH_3]^+$; 407 (39) $[M-Ph-H]^+$.

Trace amounts of the ketone intermediate, $C_7Ph_5Me_2HCO$, a yellow solid, also recrystallized and were isolated. ^{1}H NMR (200 MHz, CD_2Cl_2): δ 7.28-6.23 (m, 25H, phenyl protons), 2.96 (s, 1H, H7), 1.15 (s, 6H, $2CH_3$), ^{13}C NMR (50.288 MHz, CD_2Cl_2): δ 197.13 (C8), 147.78 (C3/C4), 135.22, 133.53, 132.93, 131.17, 130.28, 128.24, 128.0, 127.73, 127.54, 126.71, 125.55 (phenyl carbons), 65.21 (C2/C5), 55.23 (C1/C6), 38.65 (C7), 9.82 (CH_3). IR (CH_2Cl_2) ν_{CO} 1752 cm^{-1}. Mass spectrum (DEI): *m/z* (%) 528 (32) $[M]^+$; 500 (100) $[M-CO]^+$; 485 (17) $[M-CO-CH_3]^+$; 407 (68) $[M-CO-CH_3-Ph-H]^+$.

Preparation of $C_7(p\text{-Tolyl})_2Ph_5H$, 52: **52** was prepared analogously to **47** from 2,5-diphenyl-3,4-ditolylcyclopentadienone (0.118 g, 0.29 mmol) and 1,2,3-triphenylcyclopropene (0.077 g, 0.29 mmol). The product was chromatographed over silica gel with eluent ether/pentane (2:98). The major band was separated and gave **52** as an oily yellow solid (0.123 g, 0.18 mmol, 65%), a mixture of isomers **52a** through **52d**. ^{1}H NMR (500 MHz, CD_2Cl_2): δ 7.97 (d, 10H, *ortho* of phenyl D), 7.85 (d, 4H, *ortho* of tolyl D), 7.49 (m, 10H, *meta* of phenyl D), 7.39 (d, 5H, *para* of phenyl D), 7.32 (d, 4H, *meta* of tolyl D), 7.16-6.14 (m, 198H, tolyl/phenyl protons), 5.31 (s, 5H, sp^3 H), 5.28 (s, 2H, sp^3 H), 2.44 (s, 1 CH_3), 2.22 (s, 2 CH_3's), 2.17 (s, 1 CH_3), 2.16 (s, 1 CH_3), 1.98 (s, 1 CH_3), and 1.97 (s, 1 CH_3). ^{13}C NMR (125.76 MHz, CD_2Cl_2): δ 144.19, 143.72, 143.54, 141.36, 141.20, 140.42, 139.72, 139.60, 138.04, 137.28, 136.86, 136.41, 136.03 (*ipso*

and ring carbons), 132.05, 131.84, 131.76, 131.55, 130.22, 130.08, 129.38, 128.79, 128.66, 128.28, 127.91, 127.51, 127.21, 127.17, 126.61, 126.35, 126.32, 125.34 (phenyl carbons), 58.27, 57.98 (sp^3 ring carbons), 21.24, and 20.92 (CH_3's). Mass spectrum (DEI): *m/z* (%) 652 (100) $[M]^+$; 561 (17) $[M\text{-}Tol]^+$; 483 (14) $[M\text{-}Tol\text{-}Ph\text{-}H]^+$.

Preparation of $C_7Ph_7^+Br^-$, 46a: The salt, **46a**, was prepared from C_7Ph_7H, **47**, and bromine in CCl_4 according to literature procedures [80]. The bright orange precipitate that forms after 5 days of stirring, was filtered and upon treatment with acetonitrile containing 6% acetone, turned to the orange-red compound, **46a**, (0.364 g, 0.52 mmol, 50%). ^1H NMR (200 MHz, CF_3COOH) δ 7.68 (s, phenyl protons). ^{13}C NMR (50.288 MHz, CF_3COOH) δ 142.28 (*ipso* or ring carbons), 131.36 (*ortho* carbons), 129.48 (*para* carbons), and 129.07 (*meta* carbons). Mass spectrum (ESI^+) *m/z* (%) 623 (30) $[M]^+$.

Preparation of $C_7Ph_7^+BF_4^-$, 46b: The salt, **46b**, was prepared from C_7Ph_7OH, **55**, and $HBF_4{\cdot}Et_2O$ in acetonitrile and acetic anhydride as reported in the literature [80]. Orange-yellow crystals of **46b** formed overnight (0.060 g, 0.08 mmol, 63%). ^1H NMR (200 MHz, CD_2Cl_2) δ 6.95 (d, 14H, *ortho* protons), and 6.79 (m, 21H, *meta* and *para* protons). ^{13}C NMR (50.288 MHz) δ 167.44 (ring carbons), 141.56 (*ipso* carbons), 130.03 (*ortho* carbons), and 126.99 (*meta* and *para* carbons). Mass spectrum (DEI) *m/z* (%) 623 (100) $[M]^+$; 545 (52) $[M\text{-}PhH]^+$; 467 (14) $[M\text{-}2PhH]^+$; 389 (10) $[M\text{-}3PhH]^+$. Mass spectrum (ESI^+) *m/z* (%) 623 (100) $[M]^+$.

Preparation of C_7(*m*-PhOMe)$_2$Ph$_5$H, 57: 0.936 g (3.49 mmol) of triphenylcyclopropene and 1.2 g (2.91 mmol) of 2,5-diphenyl-3,4-di-*m*-methoxyphenylcyclopentadienone, **58**, were refluxed in xylenes (25 mL) for 2 days. When the dark purple mixture became a light yellow solution, the xylenes was removed by distillation. The product was recrystallized from ether and hexane to give a white yellow solid, **57**, which comprised of a mixture of isomers. ^{1}H NMR (200 MHz, CD_2Cl_2) δ 7.97 (m, 10H, *ortho* of phenyl D), 7.50 - 5.87 (m, 228H, phenyl, *m*-methoxyphenyl and sp^3 protons), 3.85 (s, 6H, OCH_3), 3.61 (s, 12H, OCH_3), 3.49 (s, 3H, OCH_3), 3.47 (s, 6H, OCH_3), and 3.34 (s, 15H, OCH_3). ^{13}C NMR (50.288 MHz, CD_2Cl_2): δ 159.69, 158.61, 157.64 (*C*-OCH$_3$), 144.96, 144.76, 143.43, 143.04, 142.88, 142.01, 141.64, 141.51, 140.69, 140.35, 139.72 (*ipso* and ring carbons), 131.55, 131.27, 131.10, 129.81, 129.69, 129.53, 129.28, 128.37, 128.08, 127.54, 127.16, 126.76, 126.26, 126.00, 125.08 (phenyl carbons and *meta* carbons of *m*-methoxyphenyls), 122.22, 122.07, 119.44, 117.67, 117.49, 116.00, 114.91, 114.65, 113.23, 112.66, 112.20, 111.82, 111.55 (*ortho* and *para* carbons of *m*-methcxyphenyls), 57.67, 57.53, 55.17, and 54.98 (O*C*H$_3$'s). Mass spectrum (DEI) *m/z* (%) 684 (100) $[M]^+$; 606 (15) $[M\text{-}PhH]^+$.

Preparation of (C_7Ph_7H)Cr(CO)$_3$, 67: A mixture of C_7Ph_7H, **47** (0.413 g, 0.661 mmol) and Cr(CO)$_6$ (0.189 g, 0.859 mmol) in dry n-butyl-ether (15 mL) and dry THF (15 mL) was heated under reflux for 48 hours. The yellow solution was then cooled, and the solvent removed under reduced pressure. The residue was recrystallized from toluene and hexane to give **67**, a yellow solid (0.201 g, 0.263 mmol, 40%), ^{1}H NMR (300 MHz, $CDCl_3$) δ 7.07-6.19 (m, 30H, noncoordinated phenyls), 5.60-5.32 (m, 5H, coordinated phenyl). ^{13}C NMR (75.432 MHz,

$CDCl_3$) δ 143.58, 142.02, 140.03, 139.91, 138.27, 137.25 (*ipso* and ring carbons), 131.51, 131.30, 129.83, 127.75, 127.39, 127.14, 126.77, 126.41, 126.01, 125.58 (noncoordinated phenyl carbons), 93.18, 92.77, 92.03 (coordinated phenyl carbons), 55.82 (C7). IR (CH_2Cl_2) ν_{CO} 1968, 1894 cm^{-1}. Mass spectrum (DEI) *m/z* (%) 760 (5) $[M]^+$; 676 (100) $[M-3CO]^+$; 623 (70) $[M-Cr(CO)_3-H]^+$; 546 (30) $[M-Cr(CO)_3-Ph-H]^+$; 469 (25) $[M-Cr(CO)_3-2Ph-H]^+$. Anal. Calcd for $C_{52}H_{36}O_3Cr$: C, 82.10; H, 4.74. Found: C, 82.37; H, 4.52.

Preparation of $(C_7Ph_5Me_2H)Cr(CO)_3$, 68: To a mixture of $C_7Ph_5Me_2H$, **51**, (0.5 g, 1 mmol) and $Cr(CO)_6$ (0.22 g, 1 mmol), 5 mL of dry n-butyl-ether and 3 mL of dry THF were added and the reaction mixture was heated under reflux for 2 days. After cooling to room temperature, most of the solvent was removed and the remaining greenish yellow residue was chromatographed over silica gel with eluent hexane/CH_2Cl_2 (1:1). The yellow band was separated and concentrated under reduced pressure and kept for crystallization at -20 °C. The yellow amorphous solid (0.064 g, 0.1 mmol, 10%) of **68** precipitated and was filtered. ^1H NMR (200 MHz, CD_2Cl_2) δ 7.60-6.50 (m, 20H, noncoordinated phenyls), 5.83-5.28 (m, 5H, coordinated phenyl), 4.82 (s, 1H, H7), 1.89 (s, 3H, 1-Me), 1.17 (s, 3H, 4-Me). ^{13}C NMR (50.288 MHz, CD_2Cl_2) δ 144.05, 143.11, 141.84, 136.99 (ring carbons), 131.61, 130.70, 130.45, 130.28, 128.44, 128.20, 128.02, 127.90, 127.73, 127.34, 127.08, 126.77, 126.64, 126.42, 126.19, 125.94 (nonco-ordinated phenyl carbons), 92.78, 93.35, 93.53 (coordinated phenyl carbons), 56.87 (C7), 25.04 (1-Me), 20.44 (4-Me). IR (CH_2Cl_2) ν_{CO} 1966, 1889 cm^{-1}. Mass spectrum (DEI) *m/z* (%) 636 (12) $[M]^+$; 552 (55) $[M-3CO]^+$; 500

(100) [M-Cr(CO)$_3$]$^+$; 407 (85) [M-Cr(CO)$_3$-Ph-Me-H]$^+$. Mass spectrum (DCI, NH$_3^+$). *m/z* (%) 654 (15) [M+NH$_4$]$^+$.

Preparation of (C$_5$Ph$_4$OH)(C$_3$Ph$_3$H$_2$)Mo(CO)$_2$, 70: To a mixture of C$_7$Ph$_7$HCO, **50** (0.148 g, 0.23 mmol) and Mo(CO)$_6$ (0.068 g, 0.26 mmol), 20 mL of dry toluene was added. The reaction mixture was heated under reflux in the dark for 20 hours. After cooling, filtration under vacuum, and removal of solvent, the brown residue was flash-chromatographed on silica gel using 1:4 CH$_2$Cl$_2$/hexanes as the eluent. After removal of C$_7$Ph$_7$H and tetracyclone, a brown-red band gave **70** (0.057 g, 0.07 mmol, 31%). Recrystallization from CH$_2$Cl$_2$/hexanes yielded red-brown plates, m.p. 220-222 °C. ^{1}H NMR (500 MHz, CD$_2$Cl$_2$) δ 7.21-6.79 (m, 35H, phenyl protons), 5.04 (s, 1H, H3), 2.70 (s, 2H, H60a/H80a). ^{13}C NMR (125.721 MHz, CD$_2$Cl$_2$) δ 243.97, 240.54 (CO's), 140.94, 137.97, 133.83, 133.38, 133.21, 132.77, 131.02, 130.06, 129.52, 128.87, 128.70, 128.03, 127.99, 127.89, 127.69, 126.15 (phenyl carbons and ring *C*O), 114.61, 104.04, 97.26 (C20/C50, C30/C40, C70), 73.36 (C60/C80). IR (CH$_2$Cl$_2$) ν_{CO} 1945, 1874 cm^{-1}. Mass spectrum (DEI) *m/z* (%) 808 (39) [M$^+$]; 752 (98) [M-2CO]$^+$; 482 (84) [M-2CO-C$_3$Ph$_3$H$_2$-H]$^+$; 384 (100) [C$_5$Ph$_4$O]$^+$. Anal. Calcd for C$_{52}$H$_{38}$O$_3$Mo: C, 77.42; H, 4.71. Found: C, 77.31; H, 4.92.

Preparation of (C$_5$Ph$_2$Me$_2$OH)(C$_3$Ph$_3$H$_2$)Mo(CO)$_2$, 71: A mixture of 1,2,3-triphenyl-cyclopropene (0.268 g, 1 mmol) and 2,5-dimethyl-3,4-diphenylcyclopentadienone dimer (0.260 g, 0.5 mmol) and Mo(CO)$_6$ (0.264 g, 1 mmol) in dry n-butylether (12 mL) was refluxed under nitrogen for 18 hours. After cooling to room temperature, and filtration through Celite, the solvent was

removed by vacuum. The residue was chromatographed over silica gel using CH_2Cl_2/hexanes as eluent in a 1:4 ratio. The major band gave **71** (0.16 g, 0.234 mmol, 23%), a yellow powder. ^1H NMR (200 MHz, CD_2Cl_2) δ 7.51-6.92 (m, 25H, phenyl protons), 4.78 (s, 1H, O*H*), 2.66 (s, 2H, allyl 2C*H*), 1.85 (s, 6H, 2CH_3). ^{13}C NMR (50.288 MHz, CD_2Cl_2) δ 141.98, 138.63, 135.48, 133.58, 133.23, 131.95, 128.72, 128.53, 128.02, 127.97, 127.34, 125.86, (phenyl carbons and ring *C*O), 112.85, 102.70, 91.35 (ring and allyl *C*-Ph), 70.35 (allyl *C*H-Ph), 9.19 (2*C*H_3). IR (CH_2Cl_2) ν_{CO} 1947, 1876 cm^{-1}. Mass spectrum (DEI) *m/z* (%) 684 (3) $[M]^+$; 626 (5) $[M\text{-}2CO\text{-}2H]^+$; 366 (12) $[M\text{-}C_5Ph_2Me_2OH\text{-}2CO\text{-}1H]^+$; 260 (100) $[M\text{-}C_3Ph_3H_2\text{-}H\text{-}Mo(CO)_2]^+$.

Preparation of $C_7Ph_7SnMe_3$, 83: $C_7Ph_7^-K^+$, **48**, was prepared according to literature procedure by stirring $C_7Ph_7^+Br^-$, **46a**, (0.200 g, 0.284 mmol) over potassium metal (0.25 g, 6.25 mmol) in 20 mL diethyl ether for 17hrs [80]. The orange suspension became blue-black in colour. This solution was added via a cannula to $SnMe_3Cl$ (0.057, 0.284 mmol) in 5 mL of ether. The blue solution decolourized upon mixing with the $SnMe_3Cl$ solution, a white precipitate of KCl also formed. After filtration and removal of solvent, the light yellow product **83** was isolated (0.033 g, 0.043 mmol, 15%). Mass spectrum (DEI) *m/z* (%) 788 (30) $[M]^+$; 773 (100) $[M\text{-}CH_3]^+$; (DCI) *m/z* (%) 806 (22) $[M+NH_4]^+$; 773 (100) $[M\text{-}CH_3]^+$. Peaks quoted are in each case the highest mass in each envelope and correspond to ^{120}Sn.

Preparation of $C_7Ph_7SiMe_2H$, 84: $C_7Ph_7^-K^+$, **48**, was prepared according to literature by stirring 0.116 g (0.165 mmol) of $C_7Ph_7^+Br^-$, **46**, and 0.13 g (3.25

mmol) of potassium in 15 mL ether for 6 hours. The anion was added to neat $Si(CH_3)_2HCl$ (0.016 g, 0.165 mmol). The resulting light yellow suspension was filtered to remove salts and its solvent evaporated, leaving a light yellow solid, **84** (0.050 g, 0.070 mmol, 44%). ^1H NMR (200 MHz, CD_2Cl_2) δ 8.00 (d, 2H, *ortho* of phenyl D), 7.55-6.60 (m, 29H, phenyl protons), 6.29 (d, 4H, *ortho* of phenyl A), 4.72 (septet, 1H, Si*H*), 0.22 (d, 6H, Me's). ^{13}C NMR (50.288 MHz, CD_2Cl_2) δ 144.05, 143.71, 143.49, 141.19, 140.96, 139.67, 137.30 (ring and *ipso* carbons), 132.00, 131.67, 130.18, 128.80, 127.92, 127.52, 127.21, 126.87, 126.68, 126.39, 125.40 (phenyl carbons), 58.13 (sp^3 carbon), and 0.79 (Me's). IR (CH_2Cl_2) ν_{Si-H} 2126cm^{-1}. Mass spectrum (DEI) *m/z* (%) 668 (5) $[M-Me-H]^+$; 624 (100) $[M-Si-2Me]^+$.

Ring Current Induced Chemical Shift Calculation: These calculations were performed using the program LARC [115] and a list of induced chemical shifts can be found in Appendix Table A15.

Molecular orbital calculations were performed via the extended Hückel method using weighted H_{ij}'s [116]; orbital drawings were obtained by use of the program CACAO [117]. Orbital parameters were taken from reference [118].

X-ray Crystallography: X-ray crystallographic data for **16** were collected on a Rigaku AFC6R diffractometer with a rotating anode and graphite-monochromated Cu Kα radiation (λ = 1.54178Å). The X-ray crystallographic data for **24**, **32**, **47**,

50, and **70** were collected on a Siemens P4 diffractometer with a rotating anode and graphite-monochromated Mo Kα radiation (λ = 0.71073Å). The background measurements were obtained by using a stationary crystal and stationary counter at the beginning and end of the scan, each for 25% of the total scan time. The scan type used was θ-2θ. The scan rate, in ω, was 32.0°/min for **16**, while the scan speed was variable for **24** (1.50 - 60.00°/min), for **32**, **47**, **50** (5.00 - 60.00°/min), and for **70** (4.00 - 60.00°/min). In **16**, three standard reflections were measured after every 150 reflections. In **24**, **32**, **47**, **50**, and **70**, three standard reflections which were measured after every 97 reflections showed no instrument instability and only minor crystal decay. The molecules **16**, **47**, and **50** were solved by using Direct Methods, while for **24**, **32**, and **70**, the Patterson Method was used. Both of these procedures are contained in the SHELXTL-PLUS program library [119]. The method of refinement was full-matrix least-squares in each case. Crystal data collection parameters, atom coordinates, and selected bond lengths and angles are listed in the Appendix: **16** (Table A1,3,4), **24** (Table A1,5,6), **32** (Table A1,7,8), **47** (Table A2,9,10) **50** (Table A2,11,12), and **70** (Table A2,13,14).

REFERENCES

1. Cotton, F. A.; Wilkinson, G. *Advanced Inorganic Chemistry, 5th edition*; Wiley-Interscience: New York, 1988; p 1053.
2. Lukehart, C. M. *Fundamental Transition Metal Organometallic Chemistry;* Brooks/Cole Publishing: Monterey, California, 1985; Chapter 13.
3. Eisch, J. L. *J. Chem. Educ.* **1983**, *60*, 1009.
4. Powell, P. *Principle of Organometallic Chemistry, 2nd edition;* Chapman and Hall: New York, 1988; p 372.
5. Ryan, R. C.; Pittmann, Jr., C. U.; O'Connor, J. P. *J. Am. Chem. Soc.* **1977**, *99*, 1986.
6. Balavoine, G.; Collin, J.; Bonnet, J. J.; Lavigne, G. *J. Organomet. Chem.* **1985**, *280*, 429.
7. Osella, D.; Aime, S.; Boccardo, D.; Castiglioni, M. *Inorg. Chim. Acta.* **1985**, *100*, 97.
8. Stone, F. G. A. *Angew. Chem. Int. Ed. Engl.* **1984**, *23*, 89.
9. Green, M.; Jeffery, J. C.; Porter, S. J.; Razay, H.; Stone, F. G. A. *J. Chem. Soc. Dalton Trans.* **1982**, 2475.
10. Markby, R.; Wender, I.; Friedel, R. A.; Cotton, F. A.; Sternberg, H. W. *J. Am. Chem. Soc.* **1958**, *80*, 6529.
11. Seyferth, D. *Adv. Organmet. Chem.* **1976**, *14*, 97.
12. Sutton, P. W.; Dahl, L. F. *J. Am. Chem. Soc.* **1967**, *89*, 261.
13. Dent, W. T.; Duncanson, L. A.; Guy, R. G.; Reed, W. H. B.; Shaw, B. L. *Proc. Chem. Soc.* **1961**, 169.

14. Ercoli, R.; Santambrogio, E.; Tettamanti-Casagrande, G. *Chim. Ind. (Milano)*, **1962**, *44*, 1344.

15. Seyferth, D.; Hallgren, J. E.; Hung, P. L. K. *J. Organomet. Chem.* **1973**, *50*, 265.

16. Seyferth, D.; Spohn, R. J.; Churchill, M. R.; Gold, K.; Scholer, F. R. *J. Organomet. Chem.* **1970**, *23*, 237.

17. Seyferth, D.; Hallgren, J. E.; Esbach, C. S. *J. Am, Chem, Soc.*, **1974**, *96*, 1730.

18. a) Hammett, L. P.; Deyrup, A. J. *J. Am. Chem. Soc.* **1933**, *55*, 1900.
b) Treffers, H. P.; Hammett, L. P. *J. Am. Chem. Soc.* **1937**, *59*, 1708.

19. Seyferth, D.; Williams, G. H. *J. Organomet. Chem.* **1972**, *38*, C11.

20. Williams, G. H. *Ph.D. Thesis*, Mass. Inst. of Technol., **1973**.

21. Alich, A.; Nelson, N. J.; Shriver, D. F. *J. Chem. Soc., Chem. Commun.* **1971**, 254.

22. Seyferth, D.; Nestle, M. O.; Eschbach, C. S. *J. Am. Chem. Soc.* **1976** *98*, 6724.

23. Seyferth, D.; Nestle, M. O. *J. Am. Chem. Soc.* **1981**, *103*, 3320.

24. Gates, R. A.; D'Agostino, M. F.; Perrier, R. E.; Sayer, B. G.; McGlinchey, M. J. *Organometallics* **1987**, *6*, 1181.

25. Cotton, F. A.; Wilkinson, G. *Advanced Inorganic Chemistry, 5th edition*; Wiley-Interscience: New York, 1988; p 483.

26. Mehrotra, R. C.; Bohra, R. *Metal Carboxylates*; Academic Press: London, 1983.

27. (a) Di Donato, G. C.; Busch, K. L. *Inorg. Chem.* **1986**, *25*, 1551.
(b) Baikie, A. R. E.; Howes, A. J.; Hursthouse, M. B.; Quick, A. B.; Thornton, P. *J. Chem. Soc. Chem. Comm.* **1986**, 1587.

(c) Schauer, C. K.; Schriver, D. F. *Angew. Chem. Int. Ed. Eng.* **1987**, *26*, 255.

28. (a) Woehler, S. E.; Wittebort, R. J.; Oh, S. M.; Hendrickson, D. N.; Inniss, D.; Strouse, C.E. *J. Am. Chem. Soc.* **1986**, *108*, 2938.
(b) Summer Jr., C. E.; Steinmetz, G. R. *J. Am. Chem. Soc.* **1985**, *107*, 6124.

29. (a) Walsh, J. L.; Baumann, J. A.; Meyer, T. J. *Inorg. Chem.* **1980**, *19*, 2145. (b) Baumann, J. A.; Salmon, D. J.; Wilson, S. T.; Meyer, T. J. *Inorg. Chem.* **1979**, *18*, 2472.

30. Summer, Jr., C. E.; Steinmetz, G. R. *J. Am. Chem. Soc.* **1985**, *107*, 6124.

31. Cotton, F. A.; Walton, R. A. *Multiple Bonds Between Metal Atoms*; Wiley: New York, **1982**, Chapter 4.

32. Cotton, F. A.; Wang, W. *Nouv. J. Chim.* **1984**, *8*, 331

33. (a) Clark, R. J. H.; Hempleman, A. J.; Dawes, H. M.; Hursthouse, M. B.; Flint, C. D. *J. Chem. Soc. Dalton Trans.* **1985**, 1775.
(b) Piraino, P.; Bruno, G.; Tresoldi, G.; Schiavo, S.L..; Zanello, P. *Inorg. Chem.* **1987**, *26*, 91.

34. Fehlner, T. P. (ed). *Inorganometallic Chemistry*; Plenum: New York, 1992.

35. Cen, W.; Haller, K. J.; Fehlner, T. P. *Inorg. Chem.* **1991**, *30*, 3120.

36. Sturgeon, R. L.; Olmstead, M. M.; Schore, N. E. *Organometallics* **1991**, *10*, 1649.

37. Cen, W.; Haller, K. J.; Fehlner, T. P. *Inorg. Chem.* **1993**, *32*, 995.

38. Cen, W.; Fehlner, T. P. *J. Am. Chem. Soc.* **1992**, *114*, 5451.

39. Cen, W.; Haller, K. J.; Fehlner, T. P. *Organometallics* **1992**, *11*, 3499.

40. Quignard, F.; Choplin, A.; Basset, J. M. *J. Chem. Soc. Dalton Trans.* **1994**, *16*, 2411.

41. (a) Iroff, L. D.; Mislow, K. *J. Am. Chem. Soc.* **1978**, *100*, 2121; (b) Bartell, L. S.; Clippard, Jr., F. B.; Boates, T. L. *Inorg. Chem.* **1970**, *9*, 2436.

42. ALCHEMY is available from Tripos Associates. St. Louis, MO.

43. Sutton, P. W.; Dahl, L. F. *J. Am. Chem. Soc.* **1967**, *89*, 261.

44. Cotton, F. A.; Wilkinson, G. *Advanced Inorganic Chemistry, 5th edition*; Wiley-Interscience: New York, 1988; p 477.

45. Thompson, D. W.; Allred, A. L. *J. Phys. Chem.* **1971**, *75*, 433.

46. Kawaguchi, S. *Coord. Chem. Rev.* **1986**, *70*, 51.

47. Camerman, A.; Mastropaolo, D.; Camerman, N. *J. Am. Chem. Soc.* **1983**, *105*, 1584.

48. (a) Mostad, A.; Pederson, U.; Rasmussen, P.; Lawesson, S.-O. *Acta. Chem. Scand., Ser. B* **1983**, *37*, 901. (b) Etter, M. C.; Jahn, D. A.; Urbanczyk-Lipkowska, Z. *Acta Crystallogr., Sect. C.* **1987**, *43*, 260.

49. Jones, R. D. G. *Acta Crystallogr., Sect. B.* **1976**, *32*, 2133.

50. Tonnesen, H. J.; Karlsen, J.; Mostad, A.; Pederson, U.; Rasmussen, P. B.; Lawesson, S.-O. *Acta. Chem. Scand., Ser. B* **1983**, *37*, 179.

51. Jones, R. D. G. *Acta Crystallogr., Sect. B.* **1976**, *32*, 1224.

52. Siedle, A. R. *Comprehensive Coordination Chemistry, Vol. 2* Wilkinson, G.; Gillard, R. D.; McCleverty, J. A. (ed); Pergamon Press: Toronto, 987, p 365.

53. Bennett, M. J.; Cotton, F.A.; Eiss, R. *Acta Crystallogr., Sect. B.* **1968**, *24*, 904.

54 (a) Bullen, G. J.; Mason, R.; Pauling, P. *Inorg. Chem.* **1965**, *4*, 456. (b) Shibata, S.; Onuma, S.; Inoue, H. *Inorg. Chem.* **1985**, *24*, 1723.

55. Cotton, F. A.; Elder, R. C. *Inorg. Chem.* **1965**, *4*, 1145.

56. Cairns, C. J.; Busch, D. H. *Coord. Chem. Rev.* **1986**, *69*, 1.

57. Cotton, F. A.; Wise, J. L. *Inorg. Chem.* **1966**, *5*, 1200.

58. Coenen, M.; Faust, J.; Ringel, C.; Mayer, R. *J. Prak. Chem.* **1965**, *4*, 239.

59. Ringel, C.; Mayer, R. *J. Prak. Chem.* **1964**, *4*, 333.

60. Morris, M. L.; Koob, R. D. *Org. Mass. Spec.* **1982**, *17*, 503.

61. Bell, W.; Crayston, J. A.; Glidewell, C. *J. Organomet. Chem.* **1992**, *434*, 115.

62. Calderazzo, F.; Casagrande Tettamanti, G.; Ercoli, R. *Chim. Ind.* **1962**, *44*, 24.

63. Harris R. K., *Nuclear Magnetic Resonance Spectroscopy*, Pitman Books Limited, London: 1993.

64. Sanders, J. K. M.; Hunter, B. K. *Modern NMR Spectroscopy*; Oxford University Press: Oxford, 1987.

65. McGlinchey, M. J. *Adv. Organomet. Chem.* **1992**, *34*, 285, and references therein.

66. (a) Mailvaganam, B.; Frampton, C. S.; Sayer, B. G.; Top, S.; McGlinchey, M. J. *J. Am. Chem. Soc.* **1991**, *113*, 1177. (b) Iverson, D. J.; Hunter, G.; Blount, J. F.; Damewood, J. R. Jr.; Mislow, K. *J. Am. Chem. Soc.* **1981**, *103*, 6073. (c) Hunter, G.; Blount, J. F.; Damewood, J. R. Jr.; Iverson, D. J.; Mislow, K. *Organometallics* **1981**, *1*, 448.

67. Downton, P. A.; Mailvaganam, B.; Frampton, C. S.; Sayer, B. G.; McGlinchey, M. J. *J. Am. Chem. Soc.* **1990**, *111*, 27.

68. Kilway, K. V.; Siegel, J. S. *J. Am. Chem. Soc.* **1991**, *113*, 2332. Kilway, K. V.; Siegel, J. S. *J. Am. Chem. Soc.* **1992**, *114*, 255.

69. Li, L.; Decken, A.; Sayer, B. G.; McGlinchey, M. J.; Brégaint, P.; Thépot, J-Y.; Toupet, L.; Hamon, J-R.; Lapinte, C. *Organometallics*, **1994**, *13*, 682.

70. Mailvaganam, B.; Sayer, B. G.; McGlinchey, M. J. *J. Organomet. Chem.*, **1990**, *395*, 177.

71. Hunter, G.; Iverson, D. J.; Mislow, K.; Blount, J. F. *J. Am. Chem. Soc.* **1980**, *102*, 5942.

72. Gloaguen, B.; Astruc, D. *J. Am. Chem. Soc* **1990**, *112*, 4607.

73. (a) Keulen, E.; Jellinek, F. *J. Organomet. Chem.* **1966**, *5*, 490. (b) Gust, D.; Mislow, K. *J. Am. Chem. Soc.* **1973**, *95*, 1535. (c) Mislow, K. *Acc. Chem. Res.* **1976**, *9*, 26.

74. Boettcher, R. J.; Gust, D.; Mislow, K. *J. Am. Chem. Soc.* 1973, *95*, 7157.

75. Malisza, K. L.; Chao, L. F. C.; Britten, J. F.; Sayer, B. G.; Jaouen, G.; Top, S.; Decken, A.; McGlinchey, M. J. *Organometallics* **1993**, *12*, 2462.

76. Gust, D.; Patton, A. *J. Am. Chem. Soc.* **1978**, *100*, 8175.

77. Janiak, C.; Schumann, H. *Adv. Organomet. Chem.* **1991**, *33*, 291.

78. Bart, J. C. J. *Acta Crystallogr., Sect. B* **1968**, *24*, 1277.

79. Battiste, M. A. *J. Am. Chem. Soc.* **1961**, *83*, 4101.

80. (a) Breslow, R.; Chang, H. W. *J. Am. Chem. Soc.* **1965**, *87*, 2200. (b) Battiste, M. A. *J. Am. Chem. Soc.* **1962**, *84*, 3780.

81. Iwamura, H.; Mislow, K. *Acc. Chem. Res.* **1988**, *21*, 175.

82. For a very recent example of a molecular brake, see: Kelly, T. R.; Bowyer, M. C.; Bhaskar, K. V.; Bebbington, D.; Garcia, A.; Lang, F.; Kim, M. H.; Jette, M. P. *J. Am. Chem. Soc.* **1994**, *116*, 3657.

83. Battiste, M. A. *Chem. Ind.* **1961**, 550.

84. (a) Elschenbroich, Ch.; Salzer, A. *Organometallics - A Concise Introduction*, 2nd ed.; VCH Publishers: Weinheim, Germany, 1992, p. 358-361. (b) Bennett, M. J.; Pratt, J. L.; Simpson, K. A.; LiShingMan, L. K. K.; Takats, J. *J. Am. Chem. Soc.* **1976**, *98*, 4810. (c) Heinekey, D. M.; Graham. W. A. G. *J. Am. Chem. Soc.* **1979**, *101*, 6115. (d) Airoldi, M.; Deganello, G.; Gennaro, G.; Moret, M.; Sironi, A. *Organometallics* **1993**, *12*, 3694, and references therein.

85. Traetteberg, M. *J. Am. Chem. Soc.* **1964**, *86*, 4265.

86. Johnson, C. E., Jr.; Bovey, F. A. *J. Chem. Phys.* **1958**, *29*, 1012.

87. Waugh, J. S.; Fessenden, R. W. *J. Am. Chem. Soc.* **1957**, *79*, 846; **1958**, *80*, 6697.

88. Allen, C. F. H. *Chem. Rev.* **1962**, *62*, 653.

89. (a) Forsén, S.; Hoffman, R. A. *J. Chem. Phys.* **1963**, *39*, 2892. (b) Forsén, S.; Hoffman, R. A. *J. Chem. Phys.* **1964**, *40*, 1189. (c) Forsén, S.; Hoffman, R. A. *J. Chem. Phys.* **1966**, *45*, 2049. (d) Bain, A. D.; Cramer, J. A. *J. Magn. Reson.* **1993**, *A 103*, 217. (e) Bain, A. D.; Cramer, J. A. *J. Chem. Phys.* **1993**, *97*, 2884.

90. Nógrádi, M.; Ollis, W. D.; Sutherland, I. O. *Chem. Commun.* **1970**, 158.

91. It has been reported that, after 45 minutes at 300 °C, C_7Ph_7H shows evidence of [1,5] phenyl shifts. Harvey, J. A.; Ogliaruso, M. A. *J. Org. Chem.* **1976**, *41*, 3374.

92. (a) Anet, F. A. L. *J. Am. Chem. Soc.* **1964**, *86*, 458. (b) Anet, F. A. L.; Anet, R. In *Dynamic NMR Spectroscopy*; Jackman, L. M.; Cotton, F. A. eds., Academic Press: New York, 1975, pp 592-597. (c) Aonuma, S.; Komatsu, K.; Takeuchi, K. *Chem. Lett.* **1989**, 2107.

93. Coxon, J. M.; O'Connell, M. J.; Steel, P. J. *Aust. J. Chem.* **1985**, *38*, 1223.

94. Halton, B.; Battiste, M. A.; Rehberg, R.; Deyrup, C. L.; Brennan, M. E. *J. Am. Chem. Soc.* **1967**, *89*, 5964.

95. (a) Dunitz, J.; Pauling, P. *Helv. Chim. Acta.* **1960**, *43*, 2188. (b) Clark, G. R.; Palenik, G. J. *J. Organomet. Chem.* **1973**, *50*, 185.

96. Kruczynski, L; Takats, J. *Inorg. Chem.* **1976**, *15*, 3140.

97. Bennett, M. J.; Pratt, J. L.; Simpson, K. A.; Li Shing Man, L. K. K.; Takats, J. *J. Am. Chem. Soc.* **1976**, *98*, 4810.

98. Pauson, P. L.; Smith, G. H.; Valentine, J. H. *J. Chem. Soc. (C)* **1967**, 1061.

99. Roth, W. R.; Grimme, W. *Tetrahedron Lett.* **1966**, 2347.

100. Mays, M. J.; Morris, M. J.; Raithby, P. R.; Shvo, Y.; Czarkie, D. *Organometallics* **1989**, *8*, 1162.

101. Adams, H.; Bailey, N. A.; Hempstead, P. D.; Morris, M. J.; Riley, S.; Beddoes, R. L.; Cook, E. S. *J. Chem. Soc., Dalton Trans.* **1993**, 91.

102. (a) Mealli, C.; Midolloni, S.; Moneti, S.; Sacconi, L. *Angew. Chem. Int. Ed. Engl.* **1980**, *19*, 931. (b) McClure, M. D.; Weaver, D. L. *J. Organomet. Chem.* **1973**, *54*, C59. (c) Tuggle, R. M.; Weaver, D. L. *Inorg. Chem.* **1972**, *11*, 2237. (d) Keasey, A.; Maitlis, P. M. *J. Chem. Soc., Dalton Trans.* **1978**, 1830. (e) Frisch, P. D.; Khare, G. P. *Inorg. Chem.* **1979**, *18*, 781. (f) Kettle, S. F. A. *Inorg. Chem.* **1964**, *3*, 604. (g) Muskak, P.; Battiste, M. A. *J. Organomet. Chem.* **1969**, *17*, 46. (h) Mealli, C.; Midolloni, S.; Moneti, S.; Sacconi, L.; Silvestre, J.; Albright, T. A. *J. Am. Chem. Soc.* **1982**, *104*, 95. (i) Li, R. T.; Nguyen, S. T.; Grubbs, R. H.; Ziller, J. W. *J. Am. Chem. Soc.* **1994**, *116*, 10032.

103. Churchill, M. R.; Fettinger, J. C.; McCullough, L.; Schrock, R. R. *J. Am. Chem. Soc.* **1984**, *106*, 3356.

104. Ditchfield, R.; Hughes, R. P.; Tucker, D. S.; Bierwagen, E. P.; Robbins, J.; Robinson, D, J,; Zakutansky, J. A. *Organometallics* **1993**, *12*, 2258.

105. Larrabee, R. B. *J. Am. Chem. Soc.* **1971**, *93*, 1510.

106. (a) Whitesides, T. H.; Budnik, R. A. *Chem. Comm.* **1971**, 1514.
(b) Whitesides, T. H.; Budnik, R. A. *Inorg. Chem.* **1976**, *15*, 874.

107. Newcomber, J. S.; McBee, E. T. *J. Am. Chem. Soc.* **1949**, *71*, 946.

108. Pews, R. G. *Can. J. Chem.* **1969**, *47*, 1260.

109. Okaya, Y.; Bednowitz, A. *Acta Crystallogr.* **1967**, *22*, 111.

110. Ungnade, H. E.; McBee, E. T. *Chem. Rev.* **1958**, *58*, 249.

111. Tobey, S. W.; West, R. *Tet. Lett.* **1963**, *18*, 1179.

112. Kusada, K.; West, R.; Mallikarjuna Rao, V. N. *J. Am. Chem. Soc.* **1971**, *93*, 3627.

113. Hugel, H. M.; Horn, E.; Snow, M. R. *Aust. J. Chem.* **1985**, *38*, 383.

114. Perrin, D. D.; Armarego, W. L. F.; Perrin, D. R. *Purification of Laboratory Chemicals*; Pergamon Press: New York, 1980.

115. Agarwal, A.; Barnes, J. A.; Fletcher, J. L.; McGlinchey, M. J.; Sayer, B. G. *Can. J. Chem.* **1977**, *55*, 2575.

116. (a) Hoffmann. R. *J. Chem. Phys.* **1963**, *39*, 1397. (b) Hoffmann, R.; Lipscomb, W. N. *J. Chem. Phys.* **1962**, *36*, 2179. (c) Ammeter, J. H.; Bürgi, H. -B.; Thibeault, J. C.; Hoffmann. R. *J. Am. Chem.Soc.* **1978**, *100*, 3686.

117. Mealli, C.; Proserpio. D. M. *J. Chem. Ed.* **1990**, *67*, 3399.

118. Summerville, R. H.; Hoffmann. R. *J. Am. Chem. Soc.* **1976**, *98*, 7240.

119. SHELXTL-Plus; written by Sheldrick, G. M. Nicolet XRD, Madison, WI.

APPENDIX

Table A1: Structure determination summary

	16	24	32
empirical formula	$C_{13}H_8Cl_{12}O_8$	$C_{14}H_5Co_3O_{11}$	$C_{13}H_{10}CrO_5$
formula weight	717.6	526.0	298.21
crystal size mm	0.20 x 0.08x 0.25	0.30 x 0.30 x 0.33	0.25 x 0.25 x 0.25
colour, habit	colourless, plate	black, parallelepiped	red, parallelepiped
temperature K	296(2)	300(2)	293(2)
wavelength (Å)	1.54178	0.71073	0.71073
crystal system	triclinic	orthorhombic	tetragonal
space group	$P\bar{1}$	$Pna2_1$	$P4_32_12$
unit dimensions			
a (Å)	9.874(2)	16.226(2)	10.0840(10)
b (Å)	11.811(2)	11.6300(10)	10.0840(10)
c (Å)	12.858(3)	9.919(2)	25.387(5)
α (°)	114.35(3)	90.0	90.0
β (°)	95.63(3)	90.0	90.0
γ (°)	99.11(3)	90.0	90.0
volume ($Å^3$)	1326.5(5)	1871.7(4)	2581.5(6)
Z	2	4	8
density (calc) (Mg/m^3)	1.797	1.866	1.535
absorption coeff. (mm^{-1})	11.834	2.682	0.898
F(000)	708	1032	1216
theta range (°)	2.50-55.00	3.5-23.0	2.17-27.50
index ranges	$-10 \le h \le 10$, $0 \le k \le 12$, $-13 \le l \le 12$	$-1 \le h \le 13$, $-1 \le k \le 15$, $-1 \le l \le 21$	$-13 \le h \le 13$, $-13 \le k \le 13$, $-32 \le l \le 32$
no. reflections collected	3559	3279	6699
no. independent reflections	3349	2452	2972
no. of parameters	303	255	155
goodness of fit on F^2	2.50	0.890	1.039
final R indices [$I>2\sigma(I)$]	R1=0.0774, wR2=0.1106	R1=0.0303, wR2=0.0379	R1=0.0405, wR2=0.0954
R indices (all data)	R1=0.1039, wR2=0.1135	R1=0.0403, wR2=0.0410	R1=0.0542, wR2=0.1036
extinction coefficient	0.0006(8)	N/A	N/A
largest diff. peak ($Å^{-3}$)	1.06	0.36	0.349
largest diff. hole ($Å^{-3}$)	-0.59	-0.31	-0.232

Table A2: Structure determination summary

	47	50	70
empirical formula	$C_{49}H_{36}$	$C_{50}H_{36}O$	$C_{52}H_{38}MoO_3$
formula weight	624.78	652.79	806.76
crystal size mm	0.25 x 0.25x 0.25	0.1 x 0.1 x 0.05	0.2 x 0.2 x 0.1
colour, habit	colourless, parallellepiped	colourless, plate	red-brown, plate
temperature K	298(2)	300(2)	298(2)
wavelength (Å)	0.71073	0.71073	0.71073
crystal system	triclinic	monoclinic	triclinic
space group	P1	$P2_1/n$	P1
unit dimensions			
a (Å)	9.8320(10)	12.829(4)	13.265(3)
b (Å)	10.0260(10)	16.456(2)	13.561(3)
c (Å)	19.166(2)	18.226(3)	13.635(4)
α (°)	92.194(1)	90.0	71.84(2)
β (°)	90.57(1)	110.06(1)	65.04(2)
γ (°)	108.94(1)	90.0	61.20(1)
volume ($Å^3$)	1785.2(3)	3614.3(13)	1930.3(12)
Z	2	4	2
density (calc) (Mg/m^3)	1.162	1.200	1.388
absorption coeff. (mm^{-1})	0.066	0.070	0.385
F(000)	660	1376	832
theta range (°)	2.13-25.00	2.09-22.50	2.23-24.98
index ranges	$-1 \le h \le 11, -11 \le k \le 11, -22 \le l \le 22$	$-1 \le h \le 15, -1 \le k \le 19, -21 \le l \le 20$	$-1 \le h \le 12, -14 \le k \le 13, -15 \le l \le 14$
no. reflections collected	7480	6396	5717
no. independent reflections	6282	4666	4929
no. of parameters	446	461	513
goodness of fit on F^2	1.028	0.981	1.042
final R indices [$I>2\sigma(I)$]	R1=0.0527, wR2=0.1176	R1=0.0702, wR2=0.1238	R1=0.0658, wR2=0.1008
R indices (all data)	R1=0.0884, wR2=0.1398	R1=0.1602, wR2=0.1628	R1=0.1325, wR2=0.1231
extinction coefficient	0.0063(10)	N/A	0.0005(4)
largest diff. peak ($Å^{-3}$)	0.221	0.170	0.342
largest diff. hole ($Å^{-3}$)	-0.210	-0.180	-0.445

Table A3: Fractional atomic coordinates ($x10^4$) and equivalent isotropic displacement coefficients ($Å^2x10^3$) for $C(CH_2\text{-}O_2C\text{-}CCl_3)_4$, **16**. Equivalent isotropic U defined as one third of the trace of the orthogonalized U_{ij} tensor.

	x	y	z	U(eq)
Cl(11)	-2843(3)	9596(3)	7272(3)	96(2)
Cl(12)	-1030(3)	8241(3)	7943(3)	87(2)
Cl(13)	433(4)	10965(3)	9049(2)	96(2)
Cl(21)	4204(5)	12299(3)	10826(3)	131(2)
Cl(22)	5846(3)	12140(3)	9072(3)	128(2)
Cl(23)	3020(3)	12318(3)	8721(3)	109(2)
Cl(31)	8023(3)	7170(3)	3906(4)	120(2)
Cl(32)	5467(4)	5327(3)	2887(3)	131(2)
Cl(33)	6599(4)	6200(3)	5285(3)	123(2)
Cl(41)	-1240(3)	4035(3)	1274(3)	112(2)
Cl(42)	1695(3)	4438(3)	1393(3)	95(2)
Cl(43)	341(4)	6524(3)	1816(2)	90(2)
C(1)	2553(8)	8183(7)	5777(7)	44(4)
C(11)	1594(8)	9096(7)	5860(7)	45(4)
C(12)	242(9)	9731(9)	6838(7)	55(4)
C(13)	-1110(10)	9600(9)	7726(8)	64(5)
C(21)	3180(9)	8380(8)	6995(8)	56(4)
C(22)	3692(11)	10219(10)	8752(8)	65(5)
C(23)	4217(11)	11711(10)	9340(9)	78(5)
C(31)	3669(9)	8471(8)	5131(8)	52(4)
C(32)	5571(10)	7705(9)	4392(8)	57(4)
C(33)	6382(10)	6624(9)	4117(10	75(5)
C(41)	1739(9)	6809(7)	5169(6)	43(3)
C(42)	576(10)	5353(9)	3270(8)	54(4)
C(43)	351(10)	5133(9)	1987(8)	60(4)
O(11)	669(6)	8991(5)	6632(5)	52(3)
O(12)	-370(9)	10451(7)	6420(7)	93(5)
O(21)	3791(6)	9722(6)	7667(5)	59(3)
O(22)	3210(13)	9648(9)	9268(8)	131(6)
O(31)	4496(6)	7506(5)	4886(5)	52(3)
O(32)	5862(8)	8551(7)	4141(7)	86(4)
O(41)	1347(6)	6508(5)	3945(4)	49(3)
O(42)	119(10)	4582(7)	3553(6)	103(4)

Table A4: Selected bond lengths (Å) and bond angles (°) for $C(CH_2\text{-}O_2C\text{-}CCl_3)_4$, **16**.

C(1)-C(21)	1.534(13)	C(31)-C(1)-C(21)	111.9(7)
C(21)-O(21)	1.445(9)	C(41)-C(1)-C(21)	105.4(8)
O(21)-C(22)	1.293(11)	C(41)-C(1)-C(11)	110.9(6)
C(22)-C(23)	1.575(14)	C(1)-C(21)-O(21)	107.5(8)
O(22)-C(22)	1.205(17)	C(21)-O(21)-C(22)	117.0(8)
C(23)-Cl(21)	1.746(11)	O(21)-C(22)-O(22)	125.7(9)
C(23)-Cl(22)	1.720(11)	O(22)-C(22)-C(23)	122.4(9)
C(23)-Cl(23)	1.760(13)	Cl(23)-C(23)-Cl(21)	108.9(6)

Table A5: Fractional atomic coordinates ($x10^4$) and equivalent isotropic displacement coefficients ($Å^2x10^3$) for $CH_3C(O)CHC(OH)CCo_3(CO)_9$, **24**.

	x	y	z	U(eq)
Co(1)	1862(1)	7954(1)	3043	47(1)
Co(2)	1446(1)	8633(1)	5302(1)	48(1)
Co(3)	2691(1)	7436(1)	5035(1)	43(1)
C(1)	2430(3)	8887(4)	4308(5)	40(1)
C(2)	2858(3)	9978(4)	4135(5)	43(1)
C(3)	3669(3)	10160(4)	4514(6)	50(2)
C(4)	4040(4)	11247(5)	4358(6)	57(2)
C(5)	4927(4)	11430(5)	4756(9)	83(3)
C(10)	1327(4)	9003(6)	2057(7)	67(2)
C(11)	1191(4)	6698(5)	2954(7)	68(2)
C(12)	2633(4)	7634(5)	1799(7)	65(2)
C(20)	1691(4)	9241(5)	6912(8)	72(2)
C(21)	815(4)	9809(6)	4725(8)	74(2)
C(22)	692(3)	7541(5)	5790(8)	61(2)
C(30)	3152(4)	7798(5)	6624(7)	58(2)
C(31)	3629(4)	7081(5)	4175(8)	64(2)
C(32)	2230(3)	6028(4)	5382(7)	60(2)
O(2)	2421(2)	10809(3)	3602(5)	64(1)
O(4)	3641(3)	12088(3)	3874(6)	75(2)
O(10)	1017(4)	9674(5)	1412(7)	106(2)
O(11)	784(4)	5920(5)	2925(6)	106(2)
O(12)	3131(4)	7455(5)	1011(6)	98(2)
O(20)	1845(4)	9658(5)	7906(7)	116(3)
O(21)	426(3)	10543(5)	4362(8)	117(3)
O(22)	229(3)	6843(5)	6076(6)	91(2)
O(30)	3444(3)	8045(5)	7610(6)	92(2)
O(31)	4216(3)	6869(5)	3635(7)	98(2)
O(32)	1935(3)	5167(3)	5570(6)	88(2)

Table A6: Selected bond lengths (Å) and angles (°) for $CH_3C(O)CHC(OH)CCo_3(CO)_9$, **24**.

C(1)-C(2)	1.456(6)	C(1)-C(2)-C(3)	123.7(4)
C(2)-C(3)	1.385(7)	C(3)-C(2)-O(2)	120.7(4)
C(3)-C(4)	1.409(7)	C(2)-C(3)-C(4)	121.0(5)
C(4)-C(5)	1.507(9)	C(3)-C(4)-C(5)	120.5(5)
O(2)-C(2)	1.309(6)	C(5)-C(4)-O(4)	118.5(5)
O(4)-C(4)	1.268(7)	C(2)-O(2)-H(2)	119.8(3)
O(2)-H(2)	0.789	C(2)-C(1)-Co(2)	126.7(3)
Co(1)-C(1)	1.899(5)	C(2)-C(1)-Co(3)	136.0(4)
Co(2)-C(1)	1.900(5)	C(2)-C(1)-Co(1)	130.7(4)
Co(3)-C(1)	1.884(4)	Co(1)-Co(2)-Co(3)	59.9(1)
Co(1)-Co(2)	2.469(1)	Co(1)-Co(3)-Co(2)	60.1(1)
Co(2)-Co(3)	2.466(1)	Co(2)-Co(1)-Co(3)	60.0(1)
Co(1)-Co(3)	2.465(1)	Co(2)-C(1)-Co(3)	81.4(2)
Co(1)-C(11)	1.824(7)	Co(1)-C(1)-Co(3)	81.3(2)
Co(2)-C(22)	1.829(6)	Co(1)-C(1)-Co(2)	81.1(2)
Co(3)-C(32)	1.832(5)	C(10)-Co(1)-C(12)	96.0(3)
C(11)-O(11)	1.120(9)	C(20)-Co(2)-C(21)	96.2(3)
C(22)-O(22)	1.142(8)	C(30)-Co(3)-C(31)	96.8(3)
C(32)-O(32)	1.126(7)	C(11)-Co(1)-C(12)	102.5(3)
		C(20)-Co(2)-C(22)	100.8(3)
		C(30)-Co(3)-C(32)	102.4(3)
		Co(1)-C(11)-O(11)	178.6(7)
		Co(2)-C(22)-O(22)	178.5(6)
		Co(3)-C(32)-O(32)	178.3(6)

Table A7: Fractional atomic coordinates (x 10^4) and equivalent isotropic displacement parameters (Å^2 x 10^3) for (benzoylacetone)Cr(CO)$_3$, **32**. U(eq) is defined as one third of the trace of the orthogonalized U_{ij} tensor.

	x	y	z	U(eq)
Cr(1)	9503(1)	4156(1)	249(1)	37(1)
O(4)	8513(3)	7762(3)	-1533(1)	65(1)
O(2)	7533(3)	6141(3)	-897(1)	52(1)
O(13)	9132(4)	1637(3)	-362(1)	89(1)
O(12)	11462(3)	2736(4)	931(1)	91(1)
O(11)	11848(3)	4845(3)	-423(1)	88(1)
C(5)	10275(4)	9194(4)	-1312(2)	77(1)
C(4)	9331(3)	8117(4)	-1172(1)	54(1)
C(3)	9310(3)	7524(3)	-677(1)	49(1)
C(2)	8400(3)	6532(3)	-559(1)	40(1)
C(1)	8329(3)	5870(3)	-35(1)	38(1)
C(10)	7476(3)	4773(3)	31(1)	41(1)
C(9)	7402(3)	4096(4)	515(1)	50(1)
C(8)	8185(4)	4495(4)	938(1)	52(1)
C(7)	9025(3)	5604(3)	882(1)	49(1)
C(6)	9113(3)	6274(3)	404(1)	44(1)
C(13)	9280(4)	2609(4)	-132(1)	55(1)
C(12)	10699(4)	3276(4)	675(1)	57(1)
C(11)	10941(4)	4591(3)	-168(1)	52(1)

Table A8: Selected bond lengths (Å) and angles (°) for (benzoylacetone)$Cr(CO)_3$, **32**.

C(1)-C(2)	1.488(4)	O(4)-C(4)-C(3)	121.0(3)
C(2)-C(3)	1.390(5)	C(3)-C(4)-C(5)	122.7(4)
C(3)-C(4)	1.392(5)	C(2)-C(3)-C(4)	120.9(3)
C(4)-C(5)	1.488(6)	O(2)-C(2)-C(3)	121.7(3)
O(2)-C(2)	1.288(4)	C(1)-C(2)-C(3)	123.2(3)
O(4)-C(4)	1.285(5)	C(10)-C(1)-C(2)	119.2(3)
Cr(1)-centroid	1.714	C(1)-C(10)-C(9)	121.1(3)
Cr(1)-C(6)	2.207(3)	C(1)-C(6)-C(7)	120.5(3)
Cr(1)-C(10)	2.207(3)	C(10)-C(9)-C(8)	120.2(3)
Cr(1)-C(1)	2.216(3)	C(6)-C(7)-C(8)	120.7(3)
Cr(1)-C(8)	2.223(3)	C(7)-C(8)-C(9)	119.5(3)
Cr(1)-C(9)	2.225(3)	C(1)-Cr(1)-C(11)	92.74(13)
Cr(1)-C(7)	2.225(3)	C(1)-Cr(1)-C(13)	115.00(14)
Cr(1)-C(11)	1.847(4)	C(1)-Cr(1)-C(12)	156.07(14)
Cr(1)-C(12)	1.848(4)	C(8)-Cr(1)-C(12)	90.2(2)
Cr(1)-C(13)	1.850(4)	C(8)-Cr(1)-C(13)	117.9(2)
C(1)-C(10)	1.412(4)	C(8)-Cr(1)-C(11)	152.0(2)
C(1)-C(6)	1.426(4)	C(11)-Cr(1)-C(12)	86.4(2)
C(10)-C(9)	1.407(4)	C(11)-Cr(1)-C(13)	89.8(2)
C(9)-C(8)	1.392(5)	C(12)-Cr(1)-C(13)	88.9(2)
C(8)-C(7)	1.410(5)	Cr(1)-C(11)-O(11)	178.8(3)
C(7)-C(6)	1.393(4)	Cr(1)-C(12)-O(12)	178.4(3)
		Cr(1)-C(13)-O(13)	178.8(3)

Table A9: Fractional atomic coordinates (x 10^4) and equivalent isotropic displacement parameters ($Å^2$ x 10^3) for C_7Ph_7H, **47**. U(eq) is defined as one third of the trace of the orthogonalized U_{ij} tensor.

	x	y	z	U(eq)
C(1)	1177(2)	-142(2)	8347(1)	43(1)
C(11)	2156(2)	727(2)	8908(1)	43(1)
C(12)	1749(3)	1711(2)	9310(1)	59(1)
C(13)	2613(3)	2489(3)	9854(1)	70(1)
C(14)	3919(3)	2341(3)	9991(1)	69(1)
C(15)	4362(3)	1407(3)	9590(1)	66(1)
C(16)	3489(2)	601(2)	9057(1)	54(1)
C(2)	827(2)	-1561(2)	8281(1)	43(1)
C(21)	1308(2)	-2376(2)	8813(1)	46(1)
C(22)	945(3)	-2316(2)	9507(1)	57(1)
C(23)	1365(3)	-3076(3)	9996(1)	75(1)
C(24)	2143(3)	-3916(3)	9807(2)	80(1)
C(25)	2530(3)	-4009(3)	9127(2)	78(1)
C(26)	2111(3)	-3228(3)	8625(1)	64(1)
C(3)	-64(2)	-2417(2)	7696(1)	45(1)
C(31)	-1210(3)	-3760(2)	7884(1)	53(1)
C(32)	-2544(3)	-3717(3)	8015(2)	101(1)
C(33)	-3642(4)	-4925(5)	8211(2)	139(2)
C(34)	-3367(5)	-6164(5)	8257(2)	118(2)
C(35)	-2065(5)	-6234(4)	8111(2)	117(1)
C(36)	-982(4)	-5033(3)	7941(2)	92(1)
C(4)	101(2)	-2032(2)	7021(1)	46(1)
C(41)	-742(2)	-2984(2)	6435(1)	51(1)
C(42)	-1667(3)	-2573(3)	6028(2)	83(1)
C(43)	-2395(4)	-3387(4)	5458(2)	103(1)
C(44)	-2213(4)	-4629(4)	5291(2)	101(1)
C(45)	-1306(4)	-5079(4)	5688(2)	101(1)
C(46)	-569(3)	-4264(3)	6259(2)	79(1)
C(5)	1142(2)	-698(2)	6798(1)	44(1)
C(51)	1933(2)	-846(2)	6151(1)	49(1)
C(52)	1754(3)	-269(3)	5528(1)	68(1)
C(53)	2483(4)	-481(3)	4945(1)	88(1)
C(54)	3398(4)	-1252(3)	4973(2)	89(1)

Table A9: continued.

C(55)	3598(3)	-1821(3)	5584(2)	78(1)
C(56)	2858(3)	-1631(2)	6168(1)	62(1)
C(6)	1377(2)	561(2)	7143(1)	44(1)
C(61)	2430(2)	1910(2)	6923(1)	48(1)
C(62)	2009(3)	3094(3)	6872(1)	71(1)
C(63)	2956(4)	4358(3)	6669(2)	95(1)
C(64)	4342(4)	4469(3)	6522(2)	96(1)
C(65)	4792(3)	3321(3)	6582(2)	85(1)
C(66)	3843(3)	2046(3)	6779(1)	64(1)
C(7)	599(2)	657(2)	7820(1)	45(1)
C(71)	-1030(2)	273(2)	7768(1)	48(1)
C(72)	-1865(3)	-94(2)	8355(1)	56(1)
C(73)	-3326(3)	-336(3)	8328(1)	68(1)
C(74)	-3997(3)	-236(3)	7709(1)	78(1)
C(75)	-3190(3)	147(3)	7124(1)	79(1)
C(76)	-1725(3)	403(3)	7154(1)	62(1)

Table A10: Selected bond lengths (Å) and bond angles (°) for C_7Ph_7H, **47**.

C(1) - C(2)	1.352(3)	C(6) - C(5) - C(4)	123.6(2)
C(2) - C(3)	1.476(3)	C(1) - C(2) - C(3)	123.2(2)
C(3) - C(4)	1.360(3)	O(2) - C(1) - C(7)	120.4(2)
C(4) - C(5)	1.477(3)	C(5) - C(6) - C(7)	120.4(2)
C(5) - C(6)	1.351(3)		
C(6) - C(7)	1.529(3)		

Table A11: Fractional atomic coordinates (x 10^4) and equivalent isotropic displacement parameters ($Å^2$ x 10^3) for C_7Ph_7HCO, **50**. U(eq) is defined as one third of the trace of the orthogonalized Uij tensor.

	x	y	z	U(eq)
O(1)	1740(3)	540(2)	9509(2)	61(1)
C(1)	895(4)	1555(3)	7883(2)	40(1)
C(11)	1839(4)	1450(3)	7595(3)	46(1)
C(12)	2866(4)	1167(3)	8074(3)	57(2)
C(13)	3716(5)	1032(3)	7788(4)	73(2)
C(14)	3570(6)	1170(3)	7016(4)	84(2)
C(15)	2552(6)	1450(3)	6524(3)	73(2)
C(16)	1701(5)	1581(3)	6805(3)	57(2)
C(2)	422(4)	743(3)	8147(2)	41(1)
C(21)	655(4)	-65(3)	7845(3)	46(1)
C(22)	786(5)	-741(3)	8314(3)	60(2)
C(23)	938(5)	-1504(3)	8057(4)	81(2)
C(24)	938(5)	-1602(4)	7314(4)	87(2)
C(25)	773(6)	-956(4)	6819(4)	82(2)
C(26)	635(5)	-189(3)	7093(3)	68(2)
C(3)	-765(4)	863(3)	8129(3)	42(1)
C(31)	-1753(4)	457(3)	7562(2)	45(1)
C(32)	-2533(5)	72(3)	7792(3)	62(2)
C(33)	-3463(5)	-272(3)	7251(3)	75(2)
C(34)	-3609(5)	-229(3)	6469(3)	76(2)
C(35)	-2842(5)	152(4)	6232(3)	80(2)
C(36)	-1917(5)	500(3)	6767(3)	65(2)
C(4)	-771(4)	1410(3)	8687(2)	41(1)
C(41)	-1742(4)	1715(3)	8863(3)	46(1)
C(42)	-2072(5)	1367(4)	9435(3)	79(2)
C(43)	-2958(6)	1689(5)	9619(4)	101(2)
C(44)	-3502(6)	2355(5)	9223(4)	107(3)
C(45)	-3173(6)	2713(5)	8665(4)	99(2)
C(46)	-2304(5)	2402(4)	8484(3)	73(2)
C(5)	407(4)	1709(3)	9099(2)	42(1)
C(51)	593(4)	2092(3)	9887(2)	48(1)
C(52)	1072(4)	1667(3)	10576(3)	57(2)
C(53)	1190(5)	2044(4)	11288(3)	73(2)
C(54)	826(5)	2814(4)	11310(3)	79(2)
C(55)	321(5)	3235(4)	10626(3)	73(2)
C(56)	200(5)	2867(3)	9922(3)	61(2)

Table A11: continued.

C(6)	852(4)	2198(3)	8506(2)	37(1)
C(61)	1737(4)	2807(3)	8908(2)	46(1)
C(62)	2768(4)	2554(3)	9433(3)	57(2)
C(63)	3535(5)	3109(4)	9873(3)	71(2)
C(64)	3302(6)	3926(4)	9802(3)	74(2)
C(65)	2306(6)	4185(3)	9276(3)	70(2)
C(66)	1523(5)	3637(3)	8835(2)	54(2)
C(7)	109(4)	2275(3)	7656(2)	42(1)
C(71)	166(4)	2941(3)	7117(2)	41(1)
C(72)	1118(5)	3320(3)	7104(3)	53(1)
C(73)	1107(5)	3934(3)	6576(3)	64(2)
C(74)	92(6)	4166(4)	6041(3)	70(2)
C(75)	-866(5)	3819(3)	6030(3)	65(2)
C(76)	-832(5)	3197(3)	6565(2)	53(1)
C(8)	1007(4)	908(3)	9034(3)	45(1)

Table A12: Selected bond lengths (Å) and bond angles (°) for C_7Ph_7HCO, **50**.

C(1) - C(2)	1.607(6)	C(3) - C(2) - C(1)	111.1(4)
C(2) - C(3)	1.526(6)	C(4) - C(5) - C(6)	111.0(3)
C(3) - C(4)	1.353(6)	C(7) - C(6) - C(5)	118.9(4)
C(4) - C(5)	1.519(6)	C(7) - C(1) - C(2)	117.0(4)
C(5) - C(6)	1.600(6)	C(5) - C(8) - C(2)	98.1(4)
C(1) - C(6)	1.569(6)	C(7) - C(6) - C(1)	58.7(3)
C(5) - C(8)	1.548(6)	C(7) - C(1) - C(6)	59.2(3)
C(2) - C(8)	1.559(6)	C(1) - C(7) - C(6)	62.0(3)
C(8) - O(1)	1.194(5)		
C(1) - C(7)	1.518(6)		
C(6) - C(7)	1.525(6)		

Table A13: Fractional atomic coordinates (x 10^4) and equivalent isotropic displacement parameters ($Å^2$ x 10^3) for $(C_5Ph_4OH)(C_3Ph_3H_2)Mo(CO)_2$, **70**. U(eq) is defined as one third of the trace of the orthogonalized U_{ij} tensor.

	x	y	z	U(eq)
Mo(1)	1458(1)	1506(1)	2170(1)	29(1)
C(1)	740(8)	463(7)	2343(6)	34(2)
C(2)	721(7)	1231(6)	3769(7)	34(2)
C(10)	1788(7)	2929(6)	594(6)	30(2)
C(20)	1494(7)	3406(6)	1521(6)	30(2)
C(21)	2205(7)	3957(6)	1583(6)	27(2)
C(22)	3467(8)	3521(7)	1181(6)	38(2)
C(23)	4075(9)	4112(7)	1159(7)	49(3)
C(24)	3468(9)	5125(8)	1537(7)	48(3)
C(25)	2214(8)	5588(7)	1920(7)	43(2)
C(26)	1580(7)	5017(6)	1941(6)	34(2)
C(30)	300(7)	3458(6)	2208(6)	26(2)
C(31)	-434(7)	3987(6)	3240(6)	30(2)
C(32)	37(8)	3702(7)	4076(7)	39(2)
C(33)	-659(9)	4208(8)	5012(7)	49(3)
C(34)	-1827(10)	5043(8)	5137(8)	60(3)
C(35)	-2301(8)	5344(7)	4309(7)	49(3)
C(36)	-1606(8)	4815(6)	3375(6)	35(2)
C(40)	-134(7)	3038(6)	1689(6)	25(2)
C(41)	-1412(7)	3205(6)	1999(6)	28(2)
C(42)	-2055(8)	3905(7)	1294(7)	42(2)
C(43)	-3263(9)	4131(8)	1582(8)	53(3)
C(44)	-3868(9)	3691(8)	2578(8)	55(3)
C(45)	-3226(8)	2976(7)	3289(7)	44(2)
C(46)	-2007(7)	2734(7)	2989(6)	37(2)
C(50)	809(7)	2708(6)	665(6)	29(2)
C(51)	744(7)	2362(6)	-245(6)	30(2)
C(52)	1242(8)	2786(7)	-1307(6)	45(2)
C(53)	1181(8)	2495(8)	-2157(7)	52(3)
C(54)	655(9)	1762(7)	-1963(7)	54(3)
C(55)	163(8)	1348(7)	-909(7)	50(3)
C(56)	221(8)	1635(7)	-75(7)	45(2)
C(60)	3251(7)	238(7)	1141(7)	33(2)
C(61)	3295(7)	-415(7)	432(6)	36(2)
C(62)	3612(8)	-55(7)	-676(7)	41(2)

Table A13: continued.

C(63)	3589(9)	-531(8)	-1413(7)	57(3)
C(64)	3253(8)	-1422(8)	-1044(8)	54(3)
C(65)	2958(9)	-1829(8)	36(8)	57(3)
C(66)	2969(8)	-1336(8)	769(8)	57(3)
C(70)	3258(7)	-78(7)	2262(7)	33(2)
C(71)	3467(8)	-1256(6)	2844(7)	36(2)
C(72)	2577(8)	-1616(7)	3592(7)	44(2)
C(73)	2891(10)	-2755(8)	4047(7)	55(3)
C(74)	4076(10)	-3521(8)	3760(8)	64(3)
C(75)	4963(9)	-3173(8)	3040(8)	73(3)
C(76)	4669(9)	-2037(8)	2583(8)	62(3)
C(80)	3210(8)	818(7)	2636(7)	37(2)
C(81)	3255(7)	832(7)	3710(7)	38(2)
C(82)	2983(8)	134(8)	4671(7)	52(3)
C(83)	3062(9)	232(9)	5609(8)	66(3)
C(84)	3473(9)	985(9)	5592(8)	68(3)
C(85)	3774(9)	1678(8)	4645(9)	63(3)
C(86)	3660(8)	1604(7)	3729(8)	49(3)
O(1)	232(6)	-64(5)	2477(5)	59(2)
O(2)	235(6)	1098(5)	4680(5)	55(2)
O(3)	2829(5)	2785(4)	-290(4)	41(2)

Table A14: Selected bond lengths (Å) and bond angles (°) for $(C_5Ph_4OH)(C_3Ph_3H_2)Mo(CO)_2$, **70**.

C(10) - C(20)	1.421(10)	Mo(1) - C(80)	2.337(8)
C(20) - C(30)	1.440(10)	Mo(1) - C(70)	2.339(8)
C(30) - C(40)	1.437(10)	Mo(1) - C(1)	1.964(9)
C(40) - C(50)	1.446(10)	Mo(1) - C(2)	1.972(8)
C(10) - C(50)	1.427(11)	C(10) - C(20) - C(30)	105.9(7)
C(10) - O(3)	1.371(8)	C(40) - C(30) - C(20)	109.4(6)
C(60) - C(70)	1.456(11)	C(30) - C(40) - C(50)	107.3(7)
C(70) - C(80)	1.424(11)	C(10) - C(50) - C(40)	106.7(7)
C(1) - O(1)	1.131(8)	C(20) - C(10) - C(50)	110.8(7)
C(2) - O(2)	1.135(8)	C(2) - Mo(1) · C(1)	77.4(3)
Mo(1) - centroid	2.052	C(80) - C(70) - C(60)	111.2(7)
Mo(1) - C(60)	2.309(8)		

Table A15: Ring current effects in C_7Ph_7H, **47**, using the Johnson-Bovey Model[86].

H-centroid	H-centroid dist. Å	H-ring plane angle °	x	y	δ	$\delta_{tot.}$ ea. ortho	$\delta_{tot.}$ ortho pr
H32A-X1A	2.90	95.0	0.253	2.890	-1.940		
H32A-X1G	4.47	137.0	3.265	3.045	-0.128	-2.068	
H36A-X1A	6.34	119.8	3.170	5.490	-1.340		
H36A-X1B	3.45	115.4	1.480	3.110	-0.960		
H36A-X1G	4.68	120.7	2.389	4.024	-0.327	-1.421	0.647
H42A-X1A	3.66	103.8	0.870	3.550	-0.972		
H42A-X1F	4.35	133.6	3.414	3.585	-0.133	-1.105	
H46A-X1A	6.33	119.6	3.126	5.502	-0.136		
H46A-X1C	4.16	118.4	1.979	3.659	-0.503		
H46A-X1F	3.73	127.3	2.259	2.965	-0.497	-1.136	0.031
H22A-X1D	3.51	124.4	1.983	2.896	-0.688		
H22A-X1F	4.49	122.6	2.419	3.782	-0.345	-1.033	
H26A-X1D	5.19	136.0	3.733	3.605	-0.091		
H26A-X1F	4.35	138.1	3.238	2.905	-0.120	-0.211	0.822
H23A-X1D	4.83	102.0	1.004	4.724	-0.441		
H23A-X1F	5.55	105.5	1.483	5.348	-0.280	-0.721	
H25A-X1D	6.18	116.4	2.748	5.535	-0.162		
H25A-X1F	5.44	114.5	2.256	4.950	-0.250	-0.412	0.309
H52A-X1E	3.77	125.3	2.179	3.077	-0.528		
H52A-X1G	4.12	124.4	2.328	3.399	-0.417	-0.945	
H56A-X1E	5.13	137.9	3.806	3.439	-0.074		
H56A-X1G	4.56	129.2	2.882	3.534	-0.238	-0.312	0.633
H53A-X1E	5.13	105.7	1.388	4.939	-0.353		
H53A-X1G	5.11	101.6	1.028	5.006	-0.375	-0.728	
H55A-X1E	6.18	118.6	2.958	5.426	-0.152		
H55A-X1G	5.52	107.1	1.623	5.276	-0.278	-0.430	0.298
H16A-X1A	6.54	160.8	6.176	2.151	0.066		
H16A-X1B	3.32	124.3	1.871	2.743	-0.823		
H16A-X1E	5.31	130.3	3.434	4.050	-0.139	-0.896	
H12A-X1A	4.23	136.7	3.078	2.901	-0.158		
H12A-X1B	5.36	137.1	3.926	3.649	-0.072		
H12A-X1E	5.41	129.4	3.434	4.180	-0.139	-0.369	0.527
H66A-X1A	6.55	161.8	6.222	2.046	0.069		
H66A-X1C	3.26	123.0	1.776	2.734	-0.916		
H66A-X1D	5.20	128.9	3.265	4.047	-0.162	-1.009	
H62A-X1A	4.15	135.8	2.975	2.893	-0.187		
H62A-X1C	5.48	141.2	4.271	3.434	-0.031		
H62A-X1D	5.55	132.1	3.721	2.691	-0.011	-0.229	0.780
H72A-X1F	4.74	130.0	3.047	3.631	-0.200		
H72A-X1G	6.60	157.0	6.075	2.579	0.051	-0.150	
H76A-X1F	6.06	143.5	4.871	3.605	-0.008		
H76A-X1G	4.60	146.3	3.827	2.552	0.020	0.012	0.162

X1A - centroid of the D ring
X1B - centroid of the B ring
X1C - centroid of the B' ring
X1D - centroid of the C ring
X1E - centroid of the C' ring
X1F - centroid of the A ring
X1G - centroid of the A' ring